

Titre: Polymerization of N-butyl methacrylate in the presence of a surface
Title: active initiator

Auteur: Marjan Almassi
Author:

Date: 1996

Type: Mémoire ou thèse / Dissertation or Thesis

Référence: Almassi, M. (1996). Polymerization of N-butyl methacrylate in the presence of a
Citation: surface active initiator [Master's thesis, École Polytechnique de Montréal].
PolyPublie. <https://publications.polymtl.ca/31582/>

 **Document en libre accès dans PolyPublie**
Open Access document in PolyPublie

URL de PolyPublie: <https://publications.polymtl.ca/31582/>
PolyPublie URL:

**Directeurs de
recherche:** Pierre Bataille
Advisors:

Programme: Unspecified
Program:

UNIVERSITÉ DE MONTRÉAL

**POLYMERIZATION OF
N-BUTYL METHACRYLATE IN THE
PRESENCE OF A SURFACE ACTIVE INITIATOR**

MARJAN ALMASSI
DÉPARTEMENT DE GÉNIE CHIMIQUE
ÉCOLE POLYTECHNIQUE DE MONTRÉAL

MÉMOIRE PRÉSENTÉ EN VUE DE L'OBTENTION
DU DIPLÔME DE MAÎTRISE ÈS SCIENCE APPLIQUÉES
(GÉNIE CHIMIQUE)

AVRIL 1996

© Marjan Almassi, 1996.



National Library
of Canada

Acquisitions and
Bibliographic Services Branch

395 Wellington Street
Ottawa, Ontario
K1A 0N4

Bibliothèque nationale
du Canada

Direction des acquisitions et
des services bibliographiques

395, rue Wellington
Ottawa (Ontario)
K1A 0N4

Your file *Votre référence*

Our file *Notre référence*

The author has granted an irrevocable non-exclusive licence allowing the National Library of Canada to reproduce, loan, distribute or sell copies of his/her thesis by any means and in any form or format, making this thesis available to interested persons.

L'auteur a accordé une licence irrévocable et non exclusive permettant à la Bibliothèque nationale du Canada de reproduire, prêter, distribuer ou vendre des copies de sa thèse de quelque manière et sous quelque forme que ce soit pour mettre des exemplaires de cette thèse à la disposition des personnes intéressées.

The author retains ownership of the copyright in his/her thesis. Neither the thesis nor substantial extracts from it may be printed or otherwise reproduced without his/her permission.

L'auteur conserve la propriété du droit d'auteur qui protège sa thèse. Ni la thèse ni des extraits substantiels de celle-ci ne doivent être imprimés ou autrement reproduits sans son autorisation.

ISBN 0-612-17702-5

Name MARJAN ALMASSI

Dissertation Abstracts International is arranged by broad, general subject categories. Please select the one subject which most nearly describes the content of your dissertation. Enter the corresponding four-digit code in the spaces provided.

APPLIED SCIENCE, ENGINEERING, CHEMICAL

SUBJECT TERM

0542

SUBJECT CODE

U·M·I

Subject Categories

THE HUMANITIES AND SOCIAL SCIENCES

COMMUNICATIONS AND THE ARTS

Architecture 0729
 Art History 0377
 Cinema 0900
 Dance 0378
 Fine Arts 0357
 Information Science 0723
 Journalism 0391
 Library Science 0399
 Mass Communications 0708
 Music 0413
 Speech Communication 0459
 Theater 0465

EDUCATION

General 0515
 Administration 0514
 Adult and Continuing 0516
 Agricultural 0517
 Art 0273
 Bilingual and Multicultural 0282
 Business 0688
 Community College 0275
 Curriculum and Instruction 0727
 Early Childhood 0518
 Elementary 0524
 Finance 0277
 Guidance and Counseling 0519
 Health 0680
 Higher 0745
 History of 0520
 Home Economics 0278
 Industrial 0521
 Language and Literature 0279
 Mathematics 0280
 Music 0522
 Philosophy of 0998
 Physical 0523

Psychology 0525
 Reading 0535
 Religious 0527
 Sciences 0714
 Secondary 0533
 Social Sciences 0534
 Sociology of 0340
 Special 0529
 Teacher Training 0530
 Technology 0710
 Tests and Measurements 0288
 Vocational 0747

LANGUAGE, LITERATURE AND LINGUISTICS

Language
 General 0679
 Ancient 0289
 Linguistics 0290
 Modern 0291
 Literature
 General 0401
 Classical 0294
 Comparative 0295
 Medieval 0297
 Modern 0298
 African 0316
 American 0591
 Asian 0305
 Canadian (English) 0352
 Canadian (French) 0355
 English 0593
 Germanic 0311
 Latin American 0312
 Middle Eastern 0315
 Romance 0313
 Slavic and East European 0314

PHILOSOPHY, RELIGION AND THEOLOGY

Philosophy 0422
 Religion
 General 0318
 Biblical Studies 0321
 Clergy 0319
 History of 0320
 Philosophy of 0322
 Theology 0469

SOCIAL SCIENCES

American Studies 0323
 Anthropology
 Archaeology 0324
 Cultural 0326
 Physical 0327
 Business Administration
 General 0310
 Accounting 0272
 Banking 0770
 Management 0454
 Marketing 0338
 Canadian Studies 0385
 Economics
 General 0501
 Agricultural 0503
 Commerce-Business 0505
 Finance 0508
 History 0509
 Labor 0510
 Theory 0511
 Folklore 0358
 Geography 0366
 Gerontology 0351
 History
 General 0578

Ancient 0579
 Medieval 0581
 Modern 0582
 Black 0328
 African 0331
 Asia, Australia and Oceania 0332
 Canadian 0334
 European 0335
 Latin American 0336
 Middle Eastern 0333
 United States 0337
 History of Science 0585
 Law 0398
 Political Science
 General 0615
 International Law and Relations 0616
 Public Administration 0617
 Recreation 0814
 Social Work 0452
 Sociology
 General 0626
 Criminology and Penology 0627
 Demography 0938
 Ethnic and Racial Studies 0631
 Individual and Family Studies 0628
 Industrial and Labor Relations 0629
 Public and Social Welfare 0630
 Social Structure and Development 0700
 Theory and Methods 0344
 Transportation 0709
 Urban and Regional Planning 0999
 Women's Studies 0453

THE SCIENCES AND ENGINEERING

BIOLOGICAL SCIENCES

Agriculture
 General 0473
 Agronomy 0285
 Animal Culture and Nutrition 0475
 Animal Pathology 0476
 Food Science and Technology 0359
 Forestry and Wildlife 0478
 Plant Culture 0479
 Plant Pathology 0480
 Plant Physiology 0817
 Range Management 0777
 Wood Technology 0746
 Biology
 General 0306
 Anatomy 0287
 Biostatistics 0308
 Botany 0309
 Cell 0379
 Ecology 0329
 Entomology 0353
 Genetics 0369
 Limnology 0793
 Microbiology 0410
 Molecular 0307
 Neuroscience 0317
 Oceanography 0416
 Physiology 0433
 Radiation 0821
 Veterinary Science 0778
 Zoology 0472
 Biophysics
 General 0786
 Medical 0760

Geodesy 0370
 Geology 0372
 Geophysics 0373
 Hydrology 0388
 Mineralogy 0411
 Paleobotany 0345
 Paleocology 0426
 Paleontology 0418
 Paleozoology 0985
 Palynology 0427
 Physical Geography 0368
 Physical Oceanography 0415

HEALTH AND ENVIRONMENTAL SCIENCES

Environmental Sciences 0768
 Health Sciences
 General 0566
 Audiology 0300
 Chemotherapy 0992
 Dentistry 0567
 Education 0350
 Hospital Management 0769
 Human Development 0758
 Immunology 0982
 Medicine and Surgery 0564
 Mental Health 0347
 Nursing 0569
 Nutrition 0570
 Obstetrics and Gynecology 0380
 Occupational Health and Therapy 0354
 Ophthalmology 0381
 Pathology 0571
 Pharmacology 0419
 Pharmacy 0572
 Physical Therapy 0382
 Public Health 0573
 Radiology 0574
 Recreation 0575

Speech Pathology 0460
 Toxicology 0383
 Home Economics 0386

PHYSICAL SCIENCES

Pure Sciences

Chemistry
 General 0485
 Agricultural 0749
 Analytical 0486
 Biochemistry 0487
 Inorganic 0488
 Nuclear 0738
 Organic 0490
 Pharmaceutical 0491
 Physical 0494
 Polymer 0495
 Radiation 0754
 Mathematics 0405
 Physics
 General 0605
 Acoustics 0986
 Astronomy and Astrophysics 0606
 Atmospheric Science 0608
 Atomic 0748
 Electronics and Electricity 0607
 Elementary Particles and High Energy 0798
 Fluid and Plasma 0759
 Molecular 0609
 Nuclear 0610
 Optics 0752
 Radiation 0756
 Solid State 0611
 Statistics 0463

Applied Sciences

Applied Mechanics 0346
 Computer Science 0984

Engineering
 General 0537
 Aerospace 0538
 Agricultural 0539
 Automotive 0540
 Biomedical 0541
 Chemical 0542
 Civil 0543
 Electronics and Electrical 0544
 Heat and Thermodynamics 0348
 Hydraulic 0545
 Industrial 0546
 Marine 0547
 Materials Science 0794
 Mechanical 0548
 Metallurgy 0743
 Mining 0551
 Nuclear 0552
 Packaging 0549
 Petroleum 0765
 Sanitary and Municipal System Science 0554
 0790
 Geotechnology 0428
 Operations Research 0796
 Plastics Technology 0795
 Textile Technology 0994

PSYCHOLOGY

General 0621
 Behavioral 0384
 Clinical 0622
 Developmental 0620
 Experimental 0623
 Industrial 0624
 Personality 0625
 Physiological 0989
 Psychobiology 0349
 Psychometrics 0632
 Social 0451



Nom _____

Dissertation Abstracts International est organisé en catégories de sujets. Veuillez s.v.p. choisir le sujet qui décrit le mieux votre thèse et inscrivez le code numérique approprié dans l'espace réservé ci-dessous.



U.M.I.

SUJET

CODE DE SUJET

Catégories par sujets

HUMANITÉS ET SCIENCES SOCIALES

COMMUNICATIONS ET LES ARTS

Architecture	0729
Beaux-arts	0357
Bibliothéconomie	0399
Cinéma	0900
Communication verbale	0459
Communications	0708
Danse	0378
Histoire de l'art	0377
Journalisme	0391
Musique	0413
Sciences de l'information	0723
Théâtre	0465

ÉDUCATION

Généralités	515
Administration	0514
Art	0273
Collèges communautaires	0275
Commerce	0688
Économie domestique	0278
Éducation permanente	0516
Éducation préscolaire	0518
Éducation sanitaire	0680
Enseignement agricole	0517
Enseignement bilingue et multiculturel	0282
Enseignement industriel	0521
Enseignement primaire	0524
Enseignement professionnel	0747
Enseignement religieux	0527
Enseignement secondaire	0533
Enseignement spécial	0529
Enseignement supérieur	0745
Évaluation	0288
Finances	0277
Formation des enseignants	0530
Histoire de l'éducation	0520
Langues et littérature	0279

Lecture	0535
Mathématiques	0280
Musique	0522
Orientation et consultation	0519
Philosophie de l'éducation	0998
Physique	0523
Programmes d'études et enseignement	0727
Psychologie	0525
Sciences	0714
Sciences sociales	0534
Sociologie de l'éducation	0340
Technologie	0710

LANGUE, LITTÉRATURE ET LINGUISTIQUE

Langues	
Généralités	0679
Anciennes	0289
Linguistique	0290
Modernes	0291
Littérature	
Généralités	0401
Anciennes	0294
Comparée	0295
Médiévale	0297
Moderne	0298
Africaine	0316
Américaine	0591
Anglaise	0593
Asiatique	0305
Canadienne (Anglaise)	0352
Canadienne (Française)	0355
Germanique	0311
Latino-américaine	0312
Moyen-orientale	0315
Romane	0313
Slave et est-européenne	0314

PHILOSOPHIE, RELIGION ET

THEOLOGIE	
Philosophie	0422
Religion	
Généralités	0318
Clergé	0319
Études bibliques	0321
Histoire des religions	0320
Philosophie de la religion	0322
Théologie	0469

SCIENCES SOCIALES

Anthropologie	
Archéologie	0324
Culturelle	0326
Physique	0327
Droit	0398
Économie	
Généralités	0501
Commerce-Affaires	0505
Économie agricole	0503
Économie du travail	0510
Finances	0508
Histoire	0509
Théorie	0511
Études américaines	0323
Études canadiennes	0385
Études féministes	0453
Folklore	0358
Géographie	0366
Gérontologie	0351
Gestion des affaires	
Généralités	0310
Administration	0454
Banques	0770
Comptabilité	0272
Marketing	0338
Histoire	
Histoire générale	0578

Ancienne	0579
Médiévale	0581
Moderne	0582
Histoire des noirs	0328
Africaine	0331
Canadienne	0334
États-Unis	0337
Européenne	0335
Moyen-orientale	0333
Latino-américaine	0336
Asie, Australie et Océanie	0332
Histoire des sciences	0585
Loisirs	0814
Planification urbaine et régionale	0999
Science politique	
Généralités	0615
Administration publique	0617
Droit et relations internationales	0616
Sociologie	
Généralités	0626
Aide et bien-être social	0630
Criminologie et établissements pénitentiaires	0627
Démographie	0938
Études de l'individu et de la famille	0628
Études des relations interethniques et des relations raciales	0631
Structure et développement social	0700
Théorie et méthodes	0344
Travail et relations industrielles	0629
Transports	0709
Travail social	0452

SCIENCES ET INGÉNIERIE

SCIENCES BIOLOGIQUES

Agriculture	
Généralités	0473
Agronomie	0285
Alimentation et technologie alimentaire	0359
Culture	0479
Élevage et alimentation	0475
Exploitation des pâturages	0777
Pathologie animale	0476
Pathologie végétale	0480
Physiologie végétale	0817
Sylviculture et faune	0478
Technologie du bois	0746
Biologie	
Généralités	0306
Anatomie	0287
Biologie (Statistiques)	0308
Biologie moléculaire	0307
Botanique	0309
Cellule	0379
Écologie	0329
Entomologie	0353
Génétique	0369
Limnologie	0793
Microbiologie	0410
Neurologie	0317
Océanographie	0416
Physiologie	0433
Radiation	0821
Science vétérinaire	0778
Zoologie	0472
Biophysique	
Généralités	0786
Médicale	0760
SCIENCES DE LA TERRE	
Biogéochimie	0425
Géochimie	0996
Géodésie	0370
Géographie physique	0368

Géologie	0372
Géophysique	0373
Hydrologie	0388
Minéralogie	0411
Océanographie physique	0415
Paléobotanique	0345
Paléocécologie	0426
Paléontologie	0418
Paléozoologie	0985
Palynologie	0427

SCIENCES DE LA SANTÉ ET DE L'ENVIRONNEMENT

Économie domestique	0386
Sciences de l'environnement	0768
Sciences de la santé	
Généralités	0566
Administration des hôpitaux	0769
Alimentation et nutrition	0570
Audiologie	0300
Chimiothérapie	0992
Dentisterie	0567
Développement humain	0758
Enseignement	0350
Immunologie	0982
Loisirs	0575
Médecine du travail et thérapie	0354
Médecine et chirurgie	0564
Obstétrique et gynécologie	0380
Ophthalmologie	0381
Orthophonie	0460
Pathologie	0571
Pharmacie	0572
Pharmacologie	0419
Physiothérapie	0382
Radiologie	0574
Santé mentale	0347
Santé publique	0573
Soins infirmiers	0569
Toxicologie	0383

SCIENCES PHYSIQUES

Sciences Pures	
Chimie	
Généralités	0485
Biochimie	487
Chimie agricole	0749
Chimie analytique	0486
Chimie minérale	0488
Chimie nucléaire	0738
Chimie organique	0490
Chimie pharmaceutique	0491
Physique	0494
Polymères	0495
Radiation	0754
Mathématiques	0405
Physique	
Généralités	0605
Acoustique	0986
Astronomie et astrophysique	0606
Électronique et électricité	0607
Fluides et plasma	0759
Météorologie	0608
Optique	0752
Particules (Physique nucléaire)	0798
Physique atomique	0748
Physique de l'état solide	0611
Physique moléculaire	0609
Physique nucléaire	0610
Radiation	0756
Statistiques	0463
Sciences Appliquées Et Technologie	
Informatique	0984
Ingénierie	
Généralités	0537
Agricole	0539
Automobile	0540

Biomédicale	0541
Chaleur et thermodynamique	0348
Conditionnement (Emballage)	0549
Génie aérospatial	0538
Génie chimique	0542
Génie civil	0543
Génie électronique et électrique	0544
Génie industriel	0546
Génie mécanique	0548
Génie nucléaire	0552
Ingénierie des systèmes	0790
Mécanique navale	0547
Métallurgie	0743
Science des matériaux	0794
Technique du pétrole	0765
Technique minière	0551
Techniques sanitaires et municipales	0554
Technologie hydraulique	0545
Mécanique appliquée	0346
Géotechnologie	0428
Matières plastiques (Technologie)	0795
Recherche opérationnelle	0796
Textiles et tissus (Technologie)	0794

PSYCHOLOGIE

Généralités	0621
Personnalité	0625
Psychobiologie	0349
Psychologie clinique	0622
Psychologie du comportement	0384
Psychologie du développement	0620
Psychologie expérimentale	0623
Psychologie industrielle	0624
Psychologie physiologique	0989
Psychologie sociale	0451
Psychométrie	0632



UNIVERSITÉ DE MONTRÉAL

ÉCOLE POLYTECHNIQUE DE MONTRÉAL

Ce mémoire intitulé:

**POLYMERIZATION OF
N-BUTYL METHACRYLATE IN THE
PRESENCE OF A SURFACE ACTIVE INITIATOR**

présenté par: ALMASSI Marjan

en vue de l'obtention du diplôme de: Maîtrise ès sciences appliquées

a été dûment accepté par le jury d'examen constitué de:

M. LAFLEUR Pierre, Ph.D., président

M. BATAILLE Pierre, Ph.D., membre et directeur de recherche

M. INOUE Mitsuo, Ph.D., membre et codirecteur de recherche

M. VAN DE VEN Theo, Ph.D., membre

*To my parents for their full support during my life,
to my husband for his kindness, patience and encouragement,
and to my precious little angel, AmirAli.*

ACKNOWLEDGMENTS

I would like to thank my thesis supervisor, Dr. Pierre Bataille, for his great help and guidance throughout this work. I am sure that he knows how much I appreciate his help during the last two years.

I would like to extend my special thanks to my co-supervisor Dr. M. Inoue, from the Pulp and Paper Research Institute of Canada (PAPRICAN), for his valuable help during this work and his guidance with the pulp and paper research.

Finally, my special gratitude goes to Mr. A. Lachapelle, the laboratory assistant, and Mr. Alain Carignan, M. Sc. Candidate, McGill University, who helped with the use of the photon correlator spectrometer (PCS).

RÉSUMÉ

Les latex cationiques sont des produits actuellement utilisés dans l'industrie du papier. Les fibres cellulosiques ont une charge négative naturelle. Par l'utilisation d'un latex cationique, la répartition du latex sur la cellulose se fait plus facilement et de façon plus uniforme. Cependant, certains critères doivent être satisfaits: les particules de latex doivent présenter une certaine densité de charge afin de stabiliser les particules de polymère; les polymères obtenus doivent avoir une température de transition vitreuse spécifique, déterminée soit par le choix judicieux du monomère utilisé, soit par la plage de masse molaire d'un polymère donné ou encore une combinaison des deux. Finalement, les particules obtenues doivent être de faible taille afin qu'elles puissent pénétrer à l'intérieur du volume libre de la pulpe ou du réseau de la fibre.

Afin d'éliminer le problème de contamination dû à la présence des agents tensioactifs et d'augmenter la résistance du papier à l'eau, laquelle est réduite à cause de ces mêmes agents tensioactifs, les polymérisations sont effectuées en leurs absences.

La majorité des travaux de recherche effectués dans ce domaine, en absence d'agent tensioactifs, utilisait une concentration optimale de 10% en monomère. Le méthacrylate de butyle est utilisé dans ce projet à une concentration de 30%. Ce monomère est peu soluble dans l'eau (0.078% poids). La température de transition vitreuse de son polymère (39,81°C) se rapproche de la température à laquelle le papier

présente ses meilleures performances. Comme la faible solubilité du méthacrylate de butyle se rapproche de celle du styrène, l'étude de la cinétique de la polymérisation en émulsion sans agent tensioactif est faite en fonction des théories actuelles telles celles de la nucléation micellaire de Fitch et de Poehlein.

L'hydrochlorure de azobis -2,2' isobutyramidine est utilisé comme amorceur. Des charges positives sont créées sur le polymère en croissance avec la décomposition thermique de l'amorceur. Ces macromolécules se réarrangent dans la particule afin que ces charges se retrouvent à la surface de la particule.

Les résultats obtenus montrent que la vitesse d'agitation influence grandement la taille des particules. Avec une augmentation de la vitesse d'agitation, les particules produites sont petites, possèdent un potentiel zeta élevé et par conséquent profitent d'une plus grande stabilité. Cependant, une trop grande augmentation de la vitesse d'agitation produit un cisaillement élevé, entraînant une réduction de la diffusion normale du monomère dans la particule et par conséquent une augmentation du temps de réaction. Des vitesses d'agitation de 300, 400, 500 et 600 rpm ont été utilisées dans ce processus de polymérisation. Pour chaque vitesse de réaction, le rendement de la réaction, la masse molaire du polymère ainsi que la grosseur des particules et le potentiel zeta ont été mesurés.

La température influence aussi grandement la polymérisation. 4 différentes températures ont été vérifiées dans ce projet: 60, 70, 75 et 80°C.

Une valeur de 9.37 Kcal/mole a été obtenue comme énergie globale pour cette réaction. Les résultats montrent qu'à des températures élevées, la réaction s'effectue très

rapidement La quantité d'amorceur affecte aussi la vitesse de réaction, la masse molaire, la taille des particules ainsi que le potentiel zeta. En augmentant la quantité d'amorceur, de plus petites particules, possédant une masse molaire plus faible et un potentiel zeta plus élevé sont obtenues.

ABSTRACT

Cationic latices are products not commonly used in the paper industry. Cellulose fibers in their natural state have negative charge characteristics, thus an electrostatic attraction can be created between the fibers and the cationic latex polymer particles. This will help to distribute the particles uniformly on the pre-charged pulp surfaces and reinforce the produced papers. In order to reinforce the fibrous networks, the latex particles should have specific charge density in order to stabilize the polymer particles. As well, the particles should be as small as possible so they can penetrate into the free volume of the pulp or the fibrous network. While most polymerizations produce a low solids concentration (approximately 10%), an attempt was made to produce latices of high solids concentrations (about 30%) using n-butyl methacrylate (BMA). The advantage of BMA latices is the improvement in the polymer/paper interaction due to its glass transition temperature of 35.98⁰C. 2,2'-azobisisobutyramidine hydrochloride is used as the initiator in order to eliminate the detrimental effect of emulsifiers on the sizing performance of latices in paper. The positive charges are obtained from the thermal decomposition of this initiator and will locate on the surface of the polymer particles.

Since n-butyl methacrylate is similar to styrene in its solubility, kinetics of polymerization and particle growth have been analyzed by the theory of the emulsion polymerization of styrene without emulsifier, given by Song and Poehlein in 1989.

The agitator speed has been found to have a great influence on particle size and zeta potential. It has been suggested that for each speed there is a critical amount of initiator which can produce the most stable latex. In addition, because of the shearing effect of the speed on the diffusion of monomer molecules to the particles, an increase in the speed of agitation will increase the reaction time. In this work, four agitator speeds of 300, 400, 500 and 600rpm have been used in the polymerization process. At each speed, the reaction yield, molecular weight, zeta potential, and the particle size are measured.

Temperature also has a significant effect on the polymerization system. Four different temperatures of 60, 70, 75 and 80°C have been studied. As a result, an overall activation energy of reaction of $E_R = 9.37$ Kcal/mole has been obtained for the polymerization of this monomer in an emulsifier-free emulsion polymerization process. The results also show that at higher temperatures the reaction is very fast, and in less than an hour a high conversion with the same particle size having higher zeta potential and higher molecular weight is obtained. This is due to the effect of temperature on the thermal decomposition of the initiator.

The initiator affects the reaction rate, molecular weight, particle size, and zeta potential. By increasing the amount of initiator used in the polymerization, higher reaction rates with smaller particle size, higher zeta potential, and lower molecular weight are obtained.

CONDENSÉ EN FRANÇAIS

Les matériaux à base de latex cationiques ont différentes applications industrielles, dont l'une des plus importantes se trouve dans l'industrie du papier.

Les avantages suivants sont reliés à l'établissement de liaisons ioniques dans les réseaux de fibres:

- 1- les liaisons ioniques se forment rapidement en milieu aqueux, ne nécessitant aucun autre traitement thermique particulier;
- 2- les composés ioniques sont fréquemment solubles dans l'eau;
- 3- les liaisons ioniques sont réversibles;
- 4- la force d'attraction électrostatique a un rayon d'action plus grand que celui des liaisons covalentes;
- 5- les fibres de cellulose et de lignocellulose sont très soumises aux réactions ioniques à cause de leur caractère anionique naturel.

Les sites négatifs ne sont pas tous disponibles pour faire des liaisons dans les fibres parce que plusieurs se trouvent dans la région poreuse des fibres. Toutefois, les sites anioniques qui sont localisés à la surface des fibres peuvent agir comme agents de liaison en présence d'un polymère cationique.

Le caractère négatif des fibres de cellulose engendre une attraction physique entre les fibres et les particules de latex, laquelle aidera à la distribution uniforme des particules sur les surfaces des pulpes pré-chargées. Ainsi, il y aura un renforcement dans le papier produit par le cisaillement des liaisons fibre-fibre, remplacées par des liaisons fibre-polymère-fibre.

Ces types de latex peuvent être fabriqués par polymérisation en émulsion. Les produits contiennent alors des particules de taille supérieure à 500 nm, tandis que les espaces libres dans les réseaux fibreux sont en général plus petits que 100 nm. En plus, ces latex ont un grand pouvoir d'absorption d'eau de part leur nature émulsifiant. Pour réduire la contamination dans les émulsifiants, on a besoin de contrôler la taille des particules, et d'augmenter la répulsion entre elles dans l'eau, générée par les réseaux dans la polymérisation en émulsion; pour cette raison, une polymérisation en émulsion sans émulsifiant a été utilisée dans ce projet.

Le problème qui existe avec ce type de systèmes est qu'ils n'ont jamais été produits avec des concentrations de monomère plus hautes que 10%. Ce projet a été sélectionné avec comme objectif de produire des réseaux à concentrations de monomère supérieures à 30%. Pour vérifier ce type de systèmes, différentes conditions d'opération telles que la concentration de l'initiateur, la vitesse d'agitation et la température de polymérisation ont été employées. Pour chacune des différentes conditions, la conversion du monomère, la taille de particule, le potentiel zêta, et la masse moléculaire ont été déterminés, et les résultats sont présentés dans le chapitre 3.

Le monomère choisi est le n-butyle méthacrylate, insoluble dans l'eau, parce que ses homopolymères ont leurs température de transition vitreuse (T_v) presque égales à la température ambiante, à laquelle le papier devrait avoir des caractéristiques optimales. La T_v du polymère obtenu dans le présent travail est de 35.98°C.

En vue de produire des latex cationiques en l'absence d'émulsifiant, on suggère la génération de charge positives à partir de :

- (1) initiateurs ionisables,
- (2) polymères ou oligomères amphiliques,
- (3) comonomères hydrophiliques ou ioniques.

Le 2-2'azobis-isobutyramidine a été utilisé comme initiateur ionisable dans ce travail; ce matériau se décompose avec la chaleur et génère deux radicaux cationiques.

La solubilité du monomère dans l'eau a une grande influence sur la prédiction du mécanisme de la polymérisation en émulsion et de la polymérisation en émulsion sans émulsifiant. En général, pour les monomères relativement solubles dans l'eau, les particules sont nucléées suivant une nucléation homogène, alors que pour les monomères modérément solubles, comme c'est le cas avec le styrène et le n-butyle méthacrylate, le mécanisme se présentera comme une nucléation micellaire. La théorie de la polymérisation en émulsion est basée sur la théorie de nucléation micellaire développée par Fitch; dans le cas de la polymérisation en émulsion sans émulsifiant, on a appliqué les trois étapes d'initiation, de propagation, et de terminaison suggérées par Song et Poehlein [1989,1990]. Dans leur théorie, ils mentionnent que la polymérisation peut être initiée dans la phase aqueuse parce que l'initiateur utilisé dans le système est soluble dans l'eau.

La période de nucléation de la particule peut être divisée en deux étapes. L'étape 1, de courte durée (moins de 10 minutes), durant laquelle des noyaux de micelles sont produits en grand nombre à partir de grandes particules d'oligomères, leur stabilité étant due à la densité de charges à leur surface générée par les groupes finaux de l'initiateur. La faible solubilité du monomère dans la phase aqueuse et la vitesse de terminaison relativement élevée font que la concentration des petits oligomères augmente au point d'atteindre son CMC, occasionnant une diminution dans la longueur critique de la chaîne pour la micellisation in situ (n^*). Cette étape est connue comme l'étape n^* ou l'étape 1.

Le processus de polymérisation se poursuivant, le nombre et la taille des particules augmentent continuellement; la vitesse de capture des radicaux libres par les particules va jouer un rôle plus importante que la terminaison dans la phase aqueuse. Par conséquent, la concentration des oligomères dans la phase aqueuse ne va pas augmenter, et n^* sera pratiquement constant. Cette étape de nucléation de la particule est connue comme l'étape n^* constant ou l'étape 2.

Les micelles de particules d'oligomère produites durant l'étape 1 sont stables grâce à leur charge de surface créée par les groupes finaux de l'initiateur, mais elles ont légèrement tendance à coaguler. Lorsque les radicaux libres sont capturés par les particules de l'oligomère, la masse moléculaire du polymère augmente; ce résultat a été attesté par les courbes obtenues par GPC, où il est possible de distinguer deux pics localisés aux environs du poids moléculaire de 1000 et un autre pic dans la région de poids moléculaire élevé de 10^5 à 10^6 , lesquels pics sont reliés aux étapes de la réaction.

L'effet d'incorporer à de petites chaînes (plus petites que 5 nm) au polymère de masse moléculaire élevée a comme conséquence la réduction de la masse moléculaire des particules en croissance et de leur densité de charge surfacique. Donc, les micelles initiales de l'oligomère perdraient leur stabilité, provoquant une floculation et une coalescence très rapide durant l'étape de n^* constant.

Le coefficient de vitesse pour la coagulation de la particule a donc une valeur plus grande durant l'étape 2 que durant l'étape 1. Cette grande vitesse de coagulation va générer une rapide diminution du nombre de particules et sera accompagnée par une augmentation de la taille des particules. Cette augmentation causera un soudain accroissement du coefficient de vitesse de capture de radicaux par les particules. D'un autre côté, la diminution du nombre de particules provoquera une diminution de la vitesse de capture des radicaux par les particules. Ainsi, l'augmentation de la taille et du nombre de particules va réduire la vitesse de coagulation de la particule. Éventuellement, un remarquable équilibre va naître entre la nucléation de la particule à travers la micellisation in situ et la coagulation de la particule, et verra le nombre de particules tendre vers une valeur constante [Song, 1989].

On a choisi le type d'agitateur et sa vitesse parmi trois types d'agitateurs et trois vitesses. La méthode utilisée pour le choisir a été la décoloration, celle-ci consistant à mesurer le temps de décoloration pour chaque vitesse sélectionnée, le temps le plus petit étant le facteur sur lequel le type d'agitateurs est choisi. La vérification de la vitesse a été faite sur le milieu de la réaction de polymérisation, car le système est composé de deux phases formées par le monomère et par l'eau.

La méthode suivante a été utilisée pour toutes les réactions de polymérisation effectuée.

225 ml d'eau distillée sont incorporés dans un ballon. Un agitateur de téflon est placé au centre de l'ouverture du ballon, et relié à une tige d'acier, elle-même connectée à un moteur digital qui montre la vitesse de l'agitateur. Les précautions sont prise afin de s'assurer que la distance entre l'agitateur et le fond du ballon est la même pour chaque opération. Un condenseur de reflux refroidi à l'eau est posé sur une deuxième ouverture du ballon. La température à l'intérieur du réacteur est enregistrée à l'aide d'un thermocouple de type J relié à la troisième ouverture du ballon et connecté à un ordinateur. Le ballon est immergé dans un bain d'eau thermostatique à la température de 70 ± 0.5 °C. La réaction est faite sous une atmosphère d'azote, dont le débit est minime afin d'éviter au maximum l'évaporation du monomère. Pour prévenir la diffusion d'oxygène dans le système, le condensateur est connecté à un vase à sec avec de l'eau. Après avoir agité pendant 10 min sous atmosphère d'azote, 105 g de butyle méthacrylate est ajouté au réacteur. La température d'équilibre est obtenue après 20 min. L'initiateur est dilué dans 10 ml d'eau, pour ensuite être lavé dans 10 ml d'eau distillée. On a constaté qu'une durée de réaction de 90 à 120 min était suffisante pour la réaction, quoique cette durée dépende aussi de la température et de la vitesse d'agitation. Des échantillons ont été extraits à différents intervalles de temps pour chaque réaction. Une fois le temps de réaction achevé, le produit était recueilli dans des bouteilles de polyéthylène.

La quantité de monomère joue un rôle important dans le processus de la polymérisation. Avec des contenus élevés de monomère, il est très difficile de produire des réseaux stables sans la coagulation, et dans l'intervalle, lorsque la quantité du monomère est élevée, la conversion augmente accompagnée d'une réduction dans le temps de polymérisation, c.à.d. la concentration élevée du monomère va générer une augmentation de n^* (le nombre de molécules du monomère dans la chaîne primaire qui prendraient place après la nucléation). Donc on va produire de grandes particules dans une quantité minime, et voir diminuer la probabilité de diffusion du monomère dans les particules. Tant que la densité de charges positives n'est pas trop élevée par rapport à la taille des particules, il y aura plus de chances que la particule coagule avec une augmentation dans la probabilité de floculation du système avec la concentration élevée du monomère.

Comme prévu, la vitesse de polymérisation augmente avec un accroissement de la quantité d'initiateur. Dans les systèmes d'émulsion, l'augmentation du diamètre des particules est liée à l'augmentation de la conversion. Quand on utilise une basse concentration d'initiateur, le nombre de particules formées va diminuer, et les particules de latex ne peuvent plus absorber les noyaux d'autres particules dans la phase aqueuse. Dans ce cas, la vitesse de coagulation des particules sera comparable à l'hétérocoagulation des particules de latex. Donc les particules vont grandir à différentes vitesses.

À hautes concentrations d'initiateur, les particules seront petites qu'à basses concentrations d'initiateur, dans la même conversion, à cause d'une vitesse d'initiation

plus grande, ce qui augmente le nombre des particules à la même concentration du monomère. L'initiateur utilisé dans ce système de polymérisation est ionique, et le système est stabilisé par les groupes ioniques finaux de l'initiateur; donc, la diminution de la quantité d'initiateur cause une diminution des charges positives du milieu de polymérisation, et aussi des charges positives des particules du polymère. La coagulation des particules est plus prononcée et formée de particules larges. La taille des particules et le potentiel zêta ont une distribution aigue pour une quantité spécifique d'initiateur, lequel est de 3.7 à 3.8 à 600 rpm. Les données obtenues à différentes vitesses montrent qu'il y a un niveau spécifique de la quantité de l'initiateur, à laquelle la température enregistrée est stable et correspond à la température moyenne de la réaction.

Les conditions d'agitation ont une grande influence sur la dispersion des particules du monomère dans la phase continue, affectant la conversion, la taille de particule, et la distribution de taille des particules. Elles ont aussi un effet de cisaillement sur la diffusion des molécules du monomère sur les particules qui grandissent dans l'étape de propagation de la polymérisation. Donc, la polymérisation est faite à plus basses vitesses pour de hautes vitesses d'agitation.

Pour la polymérisation du styrène en émulsion sans émulsifiant, Song et Poehlein[1990] ont trouvé qu'à des vitesses plus hautes que 450 rpm, il y avait apparition de nouvelles particules après que les particules du polymère aient grandi jusqu'à un taille spécifique. La même conclusion peut être tirée pour le taille des particules de polybutyle-méthacrylate obtenue à 500 et 600 rpm, où il y a une diminution de taille de 800 à 900 nm. Cependant, il n'y a pas formation de particules à 400 rpm. Aux mêmes conditions

de conversion et de quantité d'initiateur, la taille de la particule augmente si on accroît la vitesse d'agitation lorsqu'elle est inférieure ou égale à 400 rpm; si la vitesse devient très élevée, la formation d'une nouvelle particule fait en sorte que la taille de la particule va diminuer.

Comme on a mentionné antérieurement, il existe un niveau particulier de la quantité d'initiateur à chaque vitesse d'agitation. L'accroissement de la vitesse d'agitation est l'unique solution pour prévenir la coagulation près de l'étape de conversion quand la quantité d'initiateur utilisée dans le réactant est plus grande que sa limite particulière. Ceci peut être relié à la diminution de la répulsion électrostatique due à l'augmentation de la vitesse de l'agitateur, et donc le temps nécessaire pour la coagulation pourrait être plus grand que le temps que met deux particules pour se rejoindre dans le système de polymérisation. De plus, la formation de nouvelles particules pendant la réaction de polymérisation va augmenter, et diminuera l'effet de la coagulation. Dans ce travail, quatre différentes vitesses d'agitation furent vérifiées : 300 rpm, 400 rpm, 500 rpm et 600 rpm. La vitesse d'agitation permet d'augmenter la quantité spécifique d'initiateur utilisée dans le système de polymérisation; par exemple, la quantité spécifique d'initiateur à 400 rpm est de 3.0 g et de 3.8 g à 600 rpm, basée sur les températures enregistrées, la diminution de la taille des particules et la distribution du potentiel zêta pour chaque vitesse. Puisque l'initiateur transporte la charge positive dans le système, les réseaux à hautes vitesses ont une meilleure stabilité. Si on veut obtenir de petites particules polymériques (plus petites que 150 nm), il est recommandé de travailler à des vitesses supérieures à 600 rpm.

L'effet de la vitesse d'agitation observé sur le système de polymérisation peut être décrit de la façon suivante : pour des quantités d'initiateurs plus faibles que leur niveau spécifique à chaque vitesse, les particules formées pendant l'étape de propagation grossissent jusqu'au point que la densité de charges à la surface ne suffisent plus à stabiliser les particules et elles commencent à coaguler. Cette coagulation apparaît encore quand la densité de la charge diminue à cause de la croissance des particules. Le produit sera alors composé de particules grandes (plus grandes que 2000 nm). Ce type de système a été observé durant la diminution de la température dans la réaction.

Si la quantité d'initiateur est plus grande que sa limite spéciale, dans la première étape de la polymérisation le nombre de radicaux libres dans le milieu de réaction sera élevé et les forces de cisaillement empêcheront les molécules du monomère d'entrer dans les particules du polymère, ce qui s'observe de part les petites particules, les basses vitesses de polymérisation, et les faibles valeurs du potentiel zêta. Puisqu'on emploie une grande quantité d'initiateur, on va produire plus de particules. Après les étapes 1 et 2, les particules vont grandir, perdre leur stabilité et précipiter, comme c'est le cas quand on diminue la température à la fin de la réaction. Si on additionne encore plus d'initiateur que le niveau spécial, la polymérisation est affectée aux limites de l'étape 1. Les particules perdent leur stabilité, se congloèrent et le matériel se change en un précipité complet. L'effet est confirmé par le soudain accroissement de la température de la réaction durant les étapes de la polymérisation.

Les enregistrements de température montrent qu'il y a une limite dans la quantité d'initiateur utilisée pour chaque vitesse d'agitation. De plus, à cette limite, la

température dans le réacteur reste constante durant toute la durée de la réaction, alors qu'à de plus basses concentrations d'initiateur la température augmente à la fin de la réaction, et qu'une plus grandes quantités d'initiateur que le limite cause une diminution sur la température de la réaction. Ce phénomène peut être mentionné comme témoignant de deux différents types de coagulation sur le système de polymérisation pour les petites et grandes particules [Chen & Lee, 1992]. Le premier survient durant la polymérisation quand de faibles quantités d'initiateur sont utilisées et résultant en la formation de grandes particules. D'un autre côté, quand de fortes quantités d'initiateur sont utilisées, les particules sont stables jusqu'aux conversions élevées, et quand la densité de la charge commence à diminuer à cause de la croissance des particules, la coagulation survient à la fin de la réaction. Si la quantité d'initiateur surpasse de 0.5 à 0.75 g le niveau spécial, de grandes quantités de particules sont formées au début de la réaction, et la vitesse de polymérisation est plus rapide. Dans cette étape, les particules en croissance vont perdre leur stabilité et le tout commencera à coaguler. Au même moment, la densité des particules est plus grande que dans les réactions préalables, et pendant que la coagulation commence elles se précipitent toutes et produisent un matériau solide à l'intérieur duquel des molécules de monomère sont piégées. La conversion final de ce solide est de 75%.

La température affecte la vitesse de décomposition de l'initiateur, sa vie moyenne, et diminue le temps de réaction. Les températures qui ont été vérifiées dans ce projet étaient de 60, 70, 75, et 80°C.

L'augmentation de la vitesse de polymérisation avec l'accroissement de la température est due à la décomposition thermique de l'initiateur. De plus grandes

particules sont produites à basses températures pour une même conversion, dû à la rapide décomposition de l'initiateur à hautes températures, résultant en une concentration plus élevée de particules. Dans ce cas, comme l'initiateur est cationique, les particules de latex seront stabilisées à hautes températures grâce au plus grand nombre de groupes finaux de l'initiateur. Ce même type de résultat a été rapporté par Song [1990] sur la polymérisation du styrène en émulsion sans émulsifiant. En raison de la vitesse élevée de polymérisation, une augmentation de la masse moléculaire suit une élévation de la température.

Les conclusions suivantes sont tirées à partir de la polymérisation en émulsion du n-butyle méthacrylate sans émulsifiant :

- la T_v obtenue pour le poly-n-butyle méthacrylate est de 35.98°C;
- à partir de cette valeur de T_v , on peut considérer que le polymère synthétisé est un des meilleurs pour une application qui touche le papier employé dans les imprimantes à jet d'encre; grâce à l'utilisation d'initiateur cationique dans la polymérisation, il y a un accroissement du nombre des liaisons fibre-polymère dans les réseaux fibreux;
- l'énergie d'activation (E_R) pour cette réaction de polymérisation est de 9.37 kcal/mol, laquelle montre que l'énergie consommée par la réaction est petite;
- la cinétique de réaction acceptée pour la polymérisation en émulsion sans émulsifiants du monomère utilisé dans le développement de cette recherche est celle suggérée par Song et Poehlein [1989,1990], basée sur la nucléation de micelles en trois étapes de polymérisation;

- la concentration de monomère a beaucoup d'effet sur la vitesse de polymérisation, comme c'est le cas lorsqu'on augmente la concentration de monomère et que la vitesse de polymérisation diminue;
- l'augmentation de la quantité d'initiateur va augmenter la vitesse de polymérisation et la densité de charge des particules du polymère, ainsi que diminuer la taille des particules; la masse moléculaire va diminuer si on augmente la concentration d'initiateur;
- la vitesse d'agitation affecte la polymérisation de la façon suivante :
 - en augmentant la vitesse, la vitesse de polymérisation diminue;
 - à partir de 400 rpm, de nouvelles particules sont créées durant la réaction lorsque la taille des particules atteint 800 - 900 nm;
 - la taille de la particule va diminuer quand la vitesse d'agitation est plus grande que 400 rpm;
 - le potentiel zêta diminue lorsque la vitesse passe de 400 à 500 rpm, mais il augmente lorsque celle-ci passe de 500 à 600 rpm;
- à partir de la concentration d'initiateur et de la vitesse d'agitation, il est possible de déterminer la quantité spécifique d'initiateur pour chaque vitesse.

Pour obtenir de meilleurs résultats, on recommande de travailler à des températures plus élevées que 70°C et à des vitesses d'agitation supérieures à 600 rpm.

La microémulsion peut être considérée comme un nouvelle branche de la science des polymères.

TABLE OF CONTENTS

ACKNOWLEDGMENTS	v
RÉSUMÉ	vi
ABSTRACT	ix
CONDENSÉ EN FRANÇAIS	xi
TABLE OF CONTENTS	xxiv
LIST OF TABLES	xxviii
LIST OF FIGURES	xxix
LIST OF APPENDIXES	xxxiii
NOMENCLATURE	xxxiv
INTRODUCTION	1
CHAPTER 1 - LITERATURE SURVEY	
1.1- INTRODUCTION.....	3
1.2- EMULSION POLYMERIZATION	5
1.2.1- EMULSION POLYMERIZATION THEORY.....	6
1.2.1.1- SMITH AND EWART THEORY(MICELLIZATION NUCLEATION).....	6
1.2.1.2- SMITH AND EWART KINETICS.....	8
1.2.1.3- FITCH'S THEORY(HOMOGENEOUS NUCLEATION).....	13
1.3- EMULSIFIER-FREE EMULSION POLYMERIZATION.....	16
1.3.1- EMULSIFIER-FREE POLYMERIZATION PROCESS.....	16

1.3.2- PARTICLE FORMATION.....	18
1.3.3- THEORY.....	20
1.3.3.1- CHANGING n^* STAGE (STAGE 1).....	20
1.3.3.2- CONSTANT n^* STAGE (STAGE 2).....	26
1.4- MICROEMULSION POLYMERIZATION.....	27
 CHAPTER 2 - EXPERIMENTAL PROCEDURE AND ANALYSIS	
2.1- INTRODUCTION.....	29
2.2- MIXING.....	29
2.3-POLYMERIZATION	30
2.3.1- MATERIALS.....	30
2.3.2- FORMULATION.....	30
2.3.3- POLYMERIZATION PROCEDURE	31
2.3.4- SAMPLING.....	32
2.4-POLYMER CHARACTERIZATION.....	33
2.4.1- YIELD.....	33
2.4.2-ZETA(ξ) POTENTIAL	34
2.4.3-PARTICLE SIZE.....	34
2.4.4-MOLECULAR WEIGHTS AND MOLECULAR WEIGHT DISTRIBUTION.....	35
2.4.5- GLASS TRANSITION TEMPERATURE, T_g	36

CHAPTER 3 - RESULTS

3.1- INTRODUCTION.....	38
3.2- MIXING.....	39
3.3- POLYMERIZATION RATE.....	39
3.4- PARTICLE SIZE.....	40
3.5- ZETA POTENTIAL	40
3.6- MOLECULAR WEIGHT.....	41
3.7- REACTION TIME.....	41
3.8- GLASS TRANSITION TEMPERATURE, T_g	42
3.9- OVERALL ACTIVATION ENERGY.....	42

CHAPTER 4 - DISCUSSION

4.1- INTRODUCTION.....	83
4.2- REACTION KINETICS AND MECHANISM.....	83
4.3- POLYMERIZATION RATE.....	87
4.4- PARTICLE SIZE.....	91
4.5- ZETA POTENTIAL	94
4.6- MOLECULAR WEIGHT.....	96
4.7- REACTION TIME.....	98
4.8- GLASS TRANSITION TEMPERATURE, T_g	98

4.8- GLASS TRANSITION TEMPERATURE, T_g	98
4.9- OVERALL ACTIVATION ENERGY	99
 CHAPTER 5 - CONCLUSION AND FUTURE WORK	
5.1- CONCLUSION.....	100
5.2- FUTURE WORK.....	101
REFERENCES.....	103
APPENDIXES.....	108

LIST OF TABLES

TABLE 2.3.1- The polymerization formulation.....	31
TABLE 3.2.1- The mixing time for different types of agitator at different speeds.....	39
TABLE B.1- Molecular weight determination from the obtained curves.....	116

LIST OF FIGURES

Figure 1.1.1 - Sketch of possible polymer locations in a fiber web.....	4
Figure 1.2.1- Emulsion polymerization procedure.....	7
Figure 1.2.2- Emulsion polymerization procedure.....	7
Figure 1.2.3- Emulsion polymerization procedure.....	7
Figure 1.2.4- Emulsion polymerization procedure.....	7
Figure 1.2.5- Emulsion polymerization procedure.....	7
Figure 1.2.6- Diffusion and homogeneous self-nucleation of a growing oligomeric radical.....	14
Figure 1.3.1 - Scheme of n^* changing with time.....	23
Figure 2.3.1 - The schematic of polymerization reactor.....	37
Figure 3.1.1 - Recorded temperature for different amounts of initiator at 400rpm and 70°C.....	43
Figure 3.1.2 - Recorded temperature for different amounts of initiator at 500rpm and 70°C.....	44
Figure 3.1.3 - Recorded temperature for different amounts of initiator at 600rpm and 70°C.....	45
Figure 3.2- Rate of polymerization for different monomer concentrations at 70°C, 400rpm and $[I] = 3.4g$	46
Figure 3.3- Effect of initiator concentration on the polymerization rate at 70°C and 400rpm.	47
Figure 3.4- Effect of speed on the rate of polymerization at 70°C and $[I] = 3.0g$	48
Figure 3.5- Effect of temperature on the rate of polymerization at 70°C and $[I] = 3.41g$	49

Figure 3.6.1- Effect of the amount of the initiator on the particle size at 70°C and 600rpm.....	50
Figure 3.6.2- Variation of particle size with conversion for different initiator concentrations at 70°C and 600rpm.....	51
Figure 3.7- Effect of agitator speed on the size of the polymer particles at constant conversion.....	52
Figure 3.8.1- Variation of particle size for agitation speeds greater than 400rpm at 70°C and [I]=3.8g.....	53
Figure 3.8.2- Variation of particle size for agitation speeds greater than 400rpm at 70°C and [I]=3.8g.....	54
Figure 3.9.1- Effect of speed on the particle size and the appearance of new particles for speeds greater than 400rpm at 70°C and [I]=3.0g.....	55
Figure 3.9.2- Effect of speed on the particle size and the appearance of new particles for speeds greater than 400rpm at 70°C and [I]=3.0g.....	56
Figure 3.10.1- Effect of agitator speed on particle size at 70°C and [I]=3.4g.....	57
Figure 3.10.2- Effect of agitator speed on particle size at 70°C and [I]=3.4g.....	58
Figure 3.11.1- Effect of temperature on polymer particle size at 400rpm and [I]=3.4g.....	59
Figure 3.11.2- Variation of particle size for different temperatures with respect to conversion at 400rpm and [I]=3.4g.....	60
Figure 3.12.1- Effect of initiator amount on the zeta potential at 600rpm and 70°C.....	61
Figure 3.12.2- Variation of zeta potential with conversion for different	

amounts of initiator at 600rpm and 70 ⁰ C.....	62
Figure 3.13.1- Effect of speed on the zeta potential at 70 ⁰ C and [I]=3.0g.....	63
Figure 3.13.2- Effect of speed on the zeta potential at 70 ⁰ C and [I]=3.0g.....	64
Figure 3.14.1- Effect of agitator speed on the zeta potential at 70 ⁰ C and [I]=3.8g.....	65
Figure 3.14.2- Effect of agitator speed on the zeta potential at 70 ⁰ C and [I]=3.8g.....	66
Figure 3.15.1- Effect of temperature variation on the zeta potential at 400rpm and [I]=3.41g.....	67
Figure 3.15.2- Effect of temperature variation on the zeta potential at 400rpm and [I]=3.41g.....	68
Figure 3.16- Variation of particle size with zeta potential at 400rpm and [I]=3.41g for different temperatures.....	69
Figure 3.17.1- Effect of amount of initiator on the molecular weight at 600rpm and 70 ⁰ C.....	70
Figure 3.17.2- Effect of amount of initiator on the molecular weight with respect to the conversion at 600rpm and 70 ⁰ C.....	71
Figure 3.18.1- Effect of speed on the molecular weight at 70 ⁰ C and [I]= 3.4g.....	72
Figure 3.18.2- Effect of speed on the molecular weight with respect to the polymerization conversion at 70 ⁰ C and [I]= 3.4g.....	73
Figure 3.19.1- Effect of temperature on the molecular weight at 400rpm and [I]= 3.4g.....	74

Figure 3.19.2- Effect of temperature on the molecular weight with respect to conversion at 400rpm and [I]= 3.4g.....	75
Figure 3.20- Typical GPC curves obtained from the emulsifier-free polymerization of n-butyl methacrylate at 600 rpm and [I] = 3.8g. in exp.L.....	76
Figure 3.21- Effect of agitator speed on the reaction time and temperature distribution at 70 ⁰ C for [I]=3.4g.....	77
Figure 3.22- Effect of temperature on the reaction time at 400rpm and [I]=3.4g.....	78
Figure 3.23- Frequency and temperature data from the DEA instrument for measurement of the T _g of poly-BMA.....	79
Figure 3.24- Graph of 1/T versus Ln(% conversion/ hr).....	80
Figure 3.25- The specified level for the initiator concentration at each speed.....	81
Figure 3.26- Effect of agitator speed on the particle size of the stable latexes.....	82
Figure 4.3.1- Thermal decomposition of ABAH ₂ ⁺⁺ 2Cl ⁻	90
Figure B.1- Calibration curve for the GPC.....	115

LIST OF APPENDIXES

APPENDIX A

A.1- DECOLORATION METHOD.....	108
A.2- SOLUTION PREPARATION.....	108
A.2.1- 2N IODINE-POTASSIUM IODIDE SOLUTION.....	108
A.2.2- 1N SODIUM THIOSULPHATE SOLUTION.....	109
A.2.3- STARCH INDICATOR	109
A.3- MIXING TEST PROCEDURE.....	109

APPENDIX B

B.1- REACTION YIELD DETERMINATION.....	111
B.2- ZETA POTENTIAL (ξ) DETERMINATION.....	112
B.3- MOLECULAR WEIGHT MEASUREMENTS.....	113
APPENDIX C.....	117

NOMENCLATURE

a	interfacial area	[m ²]
C_0	constant	[mol L ⁻¹]
C_{j^*}	water solubility of oligomer with chain length j	[mol L ⁻¹]
[CTAi]	chain transfer agent concentration	[mol L ⁻¹]
c_p	average concentration of the radicals in the particle	[L ⁻¹]
D_0	constant	
D_{ij}	diffusion coefficient	[cm ² s ⁻¹]
f	initiator efficiency	
j	chain length (number of carbons in the primary chains)	
K_c'	net rate coefficient for radical capture	
K_f	average rate coefficient for particle coagulation	[L mol ⁻¹ s ⁻¹]
k_0	specific rate constant	
k_p	propagation rate constant	[L mol ⁻¹ s ⁻¹]
k_t	termination rate constant	[L mol ⁻¹ s ⁻¹]
k_{tri}	chain transfer rate constant	
k_{tw}	termination rate constant for the radicals in the aqueous phase	[L mol ⁻¹ s ⁻¹]
L	average distance of the growing radical diffuses prior to self nucleation	[m]
[M]	monomer concentration inside the particle	[mol L ⁻¹]
[M _j]	concentration of oligomeric free radicals with chain length j	[mol L ⁻¹]
[M _{n*-1}]	concentration of oligomer radicals with the chain of n^*-1 in the aqueous phase	[mol L ⁻¹]
M_w	monomer concentration in the aqueous phase	[mol L ⁻¹]
m	number of oligomeric free radicals in association to form a micelle	

N	number of particles	[L ⁻¹]
N_A	Avogadro's number	[mol ⁻¹]
N_c	number of particles at the end of stage 1	
N_n	number of particles having n radicals ($n = 1,2,3,\dots$)	
N_s	particle number at steady state	[L ⁻¹]
n	number of free radicals	[L ⁻¹]
$n_{i\&j}$	respective particle concentrations	[L ⁻¹]
n_t	total number of particles	[L ⁻¹]
n^*	critical chain length for the insitu micellization	
[O_j]	concentration of oligomer with chain length j in the aqueous phase	[mol L ⁻¹]
[P]	particle concentration	[particles L ⁻¹]
Q	total electric charge on the particle	[C]
R	rate of radical generation	[L ⁻¹ s ⁻¹]
R_c	rate of radical capture	[L ⁻¹ s ⁻¹]
$R_{f,K}$	rate of flocculation for latex particles bearing charge of size i and j , where $K' = i + j$	[L ⁻¹ s ⁻¹]
R_i	effective rate of radical generation	[L ⁻¹ s ⁻¹]
R_{ij}	interaction radius of any two flocculating particles of i and j	[m]
[R_w]	concentration of the total free radicals in the aqueous phase	[mol L ⁻¹]
r_p	radius of the capturing particle	[m]
s	distance of the particle separation	[m]
T_g	glass transition temperature	[°C]
t	time	[sec]
t_s	time to reach the steady state	[sec]
V_A	Van-der-Waals-London attractive potential	[J]
V_{ij}	total interaction between the particles	[J]
V_p	total volume of the polymer particles in 1mL of aqueous phase	[m ³]
V_R	electrostatic repulsion	[J]

v	volume of particle	[m ³]
α	space charge shape parameters	
α_p	probability for free radicals to add a monomeric unit by propagation	
δ	space charge shape parameters	
ϵ	dielectric constant	[m ⁻² C ² N ⁻¹]
ρ'	overall rate of entrance	
ρ_i	free radical generation in the aqueous phase	[mol L ⁻¹ s ⁻¹]
τ	ratio of particle radius to double layer thickness	
τ_p	polymerization lifetime	[sec]
Ψ_0	surface electrical energy	[V]

INTRODUCTION

Throughout many centuries, man has produced paper and tried to improve its physical and mechanical properties. In 1960, the use of synthetic polymers to reinforce paper was discussed [Waterhouse,1983]. Polymers were incorporated into paper to enhance the interfiber bonding, improve the water resistance, or to modify the fiber surface. The latices were used as a polymer colloid to improve the tensile properties of paper. In order to facilitate the latex deposition, latex particles, bearing positive charge, are preferred due of their attraction to the negatively charged fibers. In 1976, a team of researchers the Pulp and Paper Research Institute of Canada published an article describing this process [Alince, 1976].

The purpose of the present work is to produce cationic latices with a high solids concentration, but with no emulsifier in the system. Cationic latexes produced by this procedure may improve not only the tensile strength, but also the sizing properties of the paper. Another important property for this type of lattice is their low polydispersity and smaller size compared with one obtained by conventional emulsion polymerization. The particle size significantly affects end-use performance of paper. Finer particles can cover a greater surface area of the pulp fiber, thus a lower amount of latex necessary. Another important factor in choosing the polymer latex as a reinforcing material is to have a proper glass transition temperature (T_g). Latexes with T_g closer to room temperature are

preferred because of easier film forming tendencies. Cationic latexes are also resistant to bacteria growth, thus they can be stored for very long times.

In this project, n-butyl methacrylate(BMA) has been used as the monomer in an emulsifier-free emulsion polymerization, because its glass transition temperature is close to room temperature. The objectives of this project are:

- (1) to produce a cationic BMA latex with a 30% solids content in an emulsifier-free form,
- (2) to optimize the polymerization reaction in terms of variables such as initiator concentration, reaction temperature, and mixing conditions, small particle size, high charge density and a T_g near the room temperature.

2,2'-azobis isobutyramidine dihydrochloride, abbreviated as $ABAH_2^{++} 2Cl^-$, was chosen as initiator. This is a water soluble initiator which produces positively charged radicals and starts the polymerization in the aqueous phase. These positive charges on the polymer particles will provide the colloidal stabilization without an emulsifier. In this work, the polymerizations were carried out at temperatures of 60, 70, 75, and 80°C to determine the overall activation energy of the reaction.

To investigate the effect of mixing conditions on the rate and particle size, four different speeds of 300, 400, 500, and 600rpm have been chosen. The experimental results were compared to a recent theory for the emulsifier-free emulsion polymerization suggested by Song [1989, 1990].

CHAPTER 1

LITERATURE SURVEY

1.1- INTRODUCTION

Interfiber bonding strength between natural or man made fibers can be reinforced using one or more types of polymers. These reinforcing polymers should provide properties such as dimensional stability, resistance to chemical and environmental degradation, ability to hold stitch, resistance to cracking, biological inertness, etc. Polymers added to the fibers can have different forms: (1) as a monomer which will be polymerized while it is mixed with fibers; (2) as low molecular weight polymer solutions which are then crosslinked; (3) as a nonaqueous solution; or (4) as a latex. These polymers can be added to the fibers before, during, or after the fiber networks have been formed. The polymer can be used as (1) a binder for coatings and fibers; (2) a protective agent against chemical and mechanical degradation; or (3) a retaining agent for fillers. The surface and aesthetic properties of the fibrous network, can also be improved by the polymer.

The polymers which presently being used in the paper industry are, Styrene/ Acrylic Ester copolymer (SAE) in a latex form and solution of a water soluble copolymer (Styrene/ Maleic Anhydride). SAE copolymer naturally has negative charges. They are deposited on the negative charged pulps by using a retention aid which is usually cationic starch.

In order to facilitate the adherent of the latex particles to the naturally negative charged pulp fibers, different researchers have studied cationic latexes which, they have the advantage of the physical charge attraction. The most extensive work has been carried out by Alince[1976, 1977, 1985]. However, the use of such latexes have not yet being commercialized.

Penetration of latex particles into the cracks and pores of the fibrous network is an important aspect. Possible locations for the particles in the fibrous network are shown in Figure 1.1.1. These locations include: (1) the interfiber bond, (2) within the cell wall of the fiber, (3) along the surface of the fiber, either as a film or agglomeration, and (4) bridge networks between fibers.

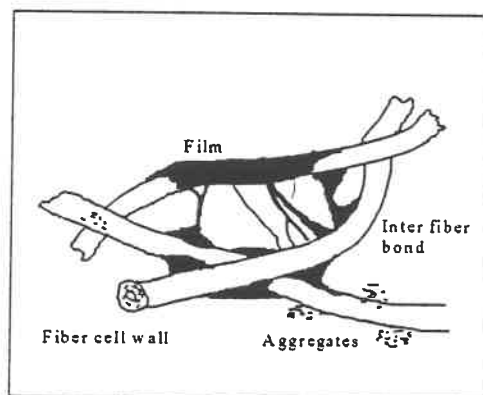


Figure 1.1.1 - Sketch of possible polymer locations in a fiber web.

If the effective diameter of a particle is quite large, it will be unable to penetrate into the pores and cracks in the surface. Thus the particle size of the latex can play an important role. In this work, more attention has been made on the particle size of the produced latices.

Glass transition temperature (T_g) of the latex is also an important aspect with respect to the adhesive properties of lignin and hemicellulose. The adhesion between the

latex and cellulose will increase at this temperature [Waterhouse, 1983]. A T_g of 40 to 55°C is recommended for the produced latexes. Higher than this T_g will make the treated paper more fragile and brittle. Although, lower T_g 's will have the film forming property on the pulps and the fibrous network but will increase the tackiness of the final product.

An emulsion polymerization system is used in this project for the production of a cationic latex. The utilized monomer in this project is n-butyl methacrylate. The water solubility of this material is very close to one for styrene, therefore, in this work, it has been suggested that the polymerization should follow the same mechanism as styrene, which is, a homogeneous polymerization, starting with a micellization nucleation procedure. These mechanisms will be mentioned in the foregoing sections.

1.2- EMULSION POLYMERIZATION

Emulsion polymerization is one of the most common methods used in the polymer industry. In general, an emulsion system consists of two liquid phases which are immiscible and where one of the phases is distributed in the form of droplets in the continuous phase by use of mechanical agitation. Typical emulsion polymerizations are made by the oil-in-water emulsion system, in which, minimally or partly soluble monomers are polymerized in water. In this system, monomers are emulsified in water by emulsifier which not only emulsifies the monomer droplets, but also stabilizes the final polymer particles in the water. Polymerization reaction starts by using a water-soluble initiator.

1.2.1- EMULSION POLYMERIZATION THEORY

The mechanism of emulsion polymerization in the presence of an emulsifier has been described by Harkins [1947], for which Smith and Ewart [1948] developed a mathematical model. The particle formation mechanism is based on micellization nucleation. Fitch [1973] extended the Smith and Ewart treatment and included the homogeneous nucleation mechanism, in which particles are nucleated by a growing oligomeric free radical that precipitates from the aqueous phase when it reaches a critical chain length, n^* .

1.2.1.1- SMITH AND EWART THEORY (MICELLIZATION NUCLEATION)

In this theory, the monomer will be dispersed in water in the form of fine droplets by mechanical agitation, which are then stabilized in the system by the surfactant, as shown in the Figure 1.2.1.

By adding the initiator to the polymerization system , the reaction starts inside the emulsified monomer droplets, as shown in Figure 1.2.2. After a conversion of about 10 to 20 percent, there are no more surfactant micelles in the system and the concentration of the emulsifier will drop below the CMC. All of the surface active agents are absorbed on the surface of the formed particles. From this point on, there is no more formation of new particles, and the number of the particles will remain constant. The polymerization proceeds only inside the particles. The particles receive their monomers from the monomer droplets by diffusion of the monomer inside the aqueous phase, shown in Figure 1.2.3, so that the reaction rate is constant. After about

40 percent polymerization, the monomer droplets disappear in the system (Figure 1.2.4). The polymerization stops when there are no further monomer molecules left inside the particles (Figure 1.2.5).

1.2.1.2- SMITH AND EWART KINETICS

In the kinetics of emulsion polymerization suggested by Smith and Ewart in 1948, they were concerned with the factors which govern the rate of polymerization in a single swollen particle, and mentioned the factors which determine the number of particles. They discussed three limiting cases in their kinetics in order to obtain the:

- rate of formation of free radicals;
- rate of escape of free radicals from reaction loci;
- rates of termination of free radicals in the reaction sites and water solubility.

A system was proposed, consisting of 1cm^3 of an external medium suspended in N isolated reaction locations (polymer particles), each having a volume, v , and an interfacial area, a . They assumed that the free radicals are initiated only in the external medium, and the rate of entrance of the free radicals into a single particle is expressed by the following Equation:

$$\frac{dn}{dt} = \frac{\rho'}{N} \quad (1.2.1)$$

where ρ' is the overall rate of entrance into all of the N polymerization sites.

When a free radical enters inside a monomer droplet, it causes polymerization which continues until the activity of the radical is destroyed or transferred out of the particle. The rate of radical transfer out of the particle is given by :

$$\frac{dn}{dt} = -k_o a \frac{n}{v} \quad (1.2.2)$$

where k_o is a specific rate constant for the event, (n/v) is the concentration of free radicals in the locus, and a is the interfacial area through which the transfer takes place. If the radical termination takes place only by combination of two radicals, the speed of termination in each particle is then given by:

$$\frac{dn}{dt} = -2k_t n \left[\frac{(n-1)}{v} \right] \quad (1.2.3)$$

the factor 2 is for the fact that two free radicals are destroyed at termination, k_t is the termination reaction rate constant, and $(n-1)/v$ is the concentration of the free radicals with which any of the n free radicals in a particle can react.

At steady-state, the rate of entrance into a particle is equal to the rate of leaving out of the particle plus the rate of termination. For reacting N particles, the following polymer chains can be obtained in each particle:

N_0	without radical
N_1	having one radical
N_2	having two radicals
N_n	having n radicals

For each entrance of one radical into a particle, the N_{n-1} becomes N_n , for each radical leaving the particle, the N_{n+1} becomes N_n , and for each termination inside the particle, a chain of N_{n+2} becomes N_n . Therefore, at the steady-state condition one can write:

$$\begin{aligned}
 & N_{n-1} \left(\frac{\rho'}{N} \right) + N_{n+1} k_o a \left(\frac{n+1}{v} \right) \\
 & + N_{n+2} k_t \left(\frac{(n+2)(n+1)}{v} \right) = N_n \left\{ \left(\frac{\rho'}{N} \right) + k_o a \left(\frac{n}{v} \right) + k_t n \frac{n-1}{v} \right\}
 \end{aligned} \tag{1.2.4}$$

The left side of this Equation is the rate of appearance of the particles and the right side shows the rate of particle disappearance.

Smith and Ewart solved this equation for three limiting cases:

- 1- Number of free radicals per particle much less than unity,
- 2- Number of free radicals per polymer particle approximately equal to 0.5,
- 3- Number of free radicals per polymer particle much greater than unity.

The case 2 explained all the results obtained with styrene and therefore, it will be the only case discussed here.

CASE 2; Number of free radicals per polymer particle approximately equal to 0.5

In this case, it is assumed that the rate of free radicals leaving the polymer particle is negligible compared to the rate of radicals entering into the particles. In addition, it has been assumed that the rate of termination reaction between a radical presently inside the particle and a radical which penetrates inside the particle is large enough so that the average time necessary for them to terminate is small compared to the average time interval between successive entrance of free radicals into a particle. With this condition, a very simple situation exists in which approximately half of the particles contain a single free radical and the other half contain no radicals. The requirements for this case can be expressed as:

$$k_o \left(\frac{a}{v} \right) \ll \rho' / N < k_t / v \tag{1.2.5}$$

By neglecting the terms involving k_o in Equation 1.2.4 one has:

$$N_{n-1} \left(\frac{\rho'}{N} \right) + N_{n+2} k_t \left[\frac{(n+2)(n+1)}{\nu} \right] = N_n \left\{ \left(\frac{\rho'}{N} \right) + k_t n \left(\frac{n-1}{\nu} \right) \right\} \quad (1.2.6)$$

In order to simplify Equation 1.2.6, a quantity called β is defined as:

$$\beta = \frac{k_t N}{\nu \rho'}$$

and Equation 1.2.6 is then written as:

$$N_{n-1} + N_{n+2} \beta (n+2)(n+1) = N_n [1 + \beta n(n-1)] \quad (1.2.7)$$

A satisfactory approximation for this Equation is that $\beta > 1$, thus Equation 1.2.7 will change as follows:

$$\frac{N_{n-1}}{N_n} = 1 + \beta n(n-1) \quad (1.2.8)$$

If $n = 0$;

$$N_2 = \frac{N_o}{2\beta}$$

and when $n = 1$;

$$N_1 = N_o + 6N_3\beta$$

N_3 can also be related to N_2 using Equation 1.2.8:

$$N_3 = \left[\frac{N_o}{2\beta(1 + 6\beta)} \right]$$

and,

$$N_1 = N_o \frac{1 + 6\beta}{1 + 6\beta}$$

This could be continued to obtain any degree of approximation desired. Since the rate of polymerization is considered, the important thing is the total number of particles, measured by:

$$n_t = 1N_1 + 2N_2 + 3N_3 + \dots + nN_n \dots$$

while the total number of particles is given by:

$$N = N_1 + N_2 + N_3 + \dots + N_n \dots$$

From these relations, the following Equation can be written:

$$n_t = \left[\frac{N}{2} \right] * \left[1 + \frac{1}{\beta} - \frac{1}{3\beta^2} + \dots \right]$$

Thus, when β is sufficiently large, the total number of free radicals present will be very close to one-half the number of polymer particles.

Under these conditions the rate of polymerization per cm^3 of water solution is expressed by a remarkably simple Equation:

$$-\frac{d[M]}{dt} = \frac{k_p [M] N}{2} \quad (1.2.9)$$

The mean polymerization lifetime, τ_p , will be $N/2\rho'$. If it is assumed that $\rho = \rho'$, then:

$$\tau_p = \frac{N}{2\rho} \quad (1.2.10)$$

The characteristic feature of emulsion polymerization can now be easily interpreted. It can be seen from Equation 1.2.8 that the number of polymerizing free

radicals will be nearly equal to half the number of particles. Since it is possible to have a large number of particles present, a fast rate of polymerization is naturally followed. Also, from Equation 1.2.10 it can be seen that the average lifetime of a free radical increases with an increase in number of particles. Therefore, it is possible to have high rates of polymerization and high molecular weights in emulsion polymerization [P. Bataille, 1994].

1.2.1.3-FITCH'S THEORY (HOMOGENEOUS NUCLEATION)

The Harkins-Smith-Ewart theory for micellization nucleation does not apply for systems involving partially water-soluble monomers. Fitch [1969, 1970] proposed a theory to predict the number of particles quantitatively, based on a homogeneous nucleation model. This model requires the knowledge of the rate of radical generation and the average distance that a primary oligomer radical can diffuse in solution before it self-nucleates. Polymerization starts in the aqueous phase and oligomeric chains appear. These chains grow by free radical propagation until a critical chain length, where the chains collapse upon themselves and a new polymer phase is formed. This is shown schematically in Figure 1.2.6 [Fitch, 1973]. The initiation point is Q, and the average distance the growing radical diffuses prior to self nucleation is L.

The rate of particle formation will thus be equal to the effective rate of radical generation, $R_i = fR$, where f is the initiator efficiency and R is rate of radical generation.

The soluble oligomers which are subsequently formed will then have a choice of forming more new particles by this process, or of being captured by pre-existing particles. Initially the rate of appearance of new particles, dN/dt , should thus be simply equal to the effective radical generation rate, R_i . As the capture of oligomeric radicals increases, the

rate of particle nucleation will be correspondingly reduced. Additionally, in real systems, flocculation is often a principal factor in determining the final number of particles, and in

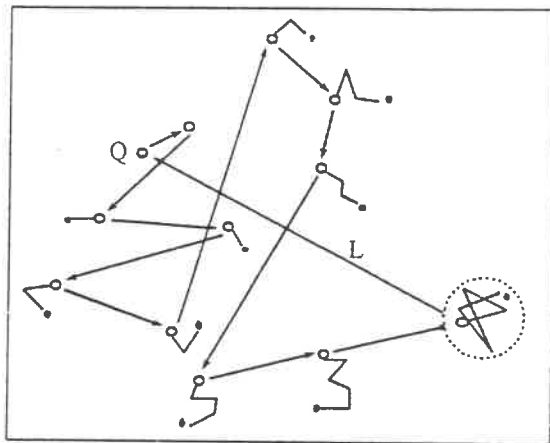


Figure 1.2.6- Diffusion and homogeneous self-nucleation of a growing oligomeric radical.

some systems the decrease in the number of particles is due solely to flocculation.

Therefore, the Equation for R_i should be modified to:

$$\frac{dN}{dt} = R_i - R_c - R_f \quad (1.2.11)$$

where R_f is the rate of flocculation. The rate of flocculation for latex particles bearing a charge is given by:

$$R_{fk'} = \frac{4\pi D_{ij} R_{ij} n_i n_j}{2 \int_2^{\infty} \exp\left(\frac{V_{ij}}{kT} \frac{ds}{s^2}\right)} \quad (1.2.12)$$

$$k' = i + j$$

$$V_{ij} = V_A + V_R$$

where D_{ij} is the diffusion coefficient, R_{ij} is approximately the sum of the radii, r_i and r_j , of any two flocculating particles, n_i and n_j are the respective particle concentrations, V_{ij} is

the potential energy barrier, which is comprised of two parts; V_A and V_R , the Van der waals-London attraction and the electrostatic repulsion, respectively, and s is a measure of the distance of the particle separation.

The overall rate of flocculation must be the sum of all the various rates, R_{f_k} , between the different sizes of particles:

$$R_f = \sum_{k=2}^{\infty} R_{f_k} \quad (1.2.13)$$

For small charged particles, stability by electrostatic repulsion, V , depends on the particle radii, r_i and r_j , and surface potential, Ψ_0 :

$$V(e)_{ij} = \frac{r_i r_j}{r_i + r_j} \left[\left(\frac{\epsilon \Psi_0^2 e^{-kH}}{s} \right) - \frac{A}{6} \left(\frac{2}{s^2 - 4} + \frac{2}{s^2} + \ln \frac{s^2 - 4}{s^2} \right) \right] \quad (1.2.14)$$

The surface potential depends upon the total electric charge, Q , fixed upon the particle surface due to the end groups:

$$\Psi_0 = \frac{Q \left[1 + \frac{e^{-\tau(s-2)}}{2s\tau} (1 - e^{-\tau^2}) (1 + \alpha) \right]}{\tau \epsilon (1 + \tau) (1 - \delta(1 + \alpha))} \quad (1.2.15)$$

The emulsifiers have a water absorbency characteristics. This property should be minimized for the papers used in ink jet printers. In this project in order to decrease the particle size and reduce the effect of emulsifiers in the produced latexes, an emulsifier-free emulsion polymerization has been used. The charge on the surface of the particles is maintained by using a cationic initiator, while stabilizing the polymer particles will replace the emulsifier.

1.3- EMULSIFIER- FREE EMULSION POLYMERIZATION

This method of polymerization has the distinct advantage of eliminating the emulsifier in the polymerization system. The produced latices in an emulsifier-free system are monodisperse with respect to their molecular weight and particle size, without removable surfactants. Therefore, they can be used as ideal model colloids for studying stability and other colloidal phenomena. Emulsifier-free emulsion polymerization has generated considerable interest since 1965 [Chiu,1991]. As an emulsion system, the continuous phase is water and monomer is dispersed by the use of mechanical agitation. The initiator is water soluble and it starts the polymerization in the aqueous phase. In such a system, polymer particles are stabilized by positive or negative charges. The charge on the particles could be obtained from (1) ionizable initiators, (2) amphiphilic polymers or oligomers, or (3) hydrophilic or ionic comonomers [Song,1989]. The kinetics of emulsifier-free emulsion polymerization have been described by Z.Song and G. W. Poehlein [1990], and will be discussed in the following sections.

1.3.1- EMULSIFIER- FREE POLYMERIZATION PROCESS

Homogeneous polymerization takes place in the aqueous phase in the beginning because a water-soluble initiator is used. As the polymerization proceeds, oligomers with different chain length are produced and their concentrations increase. For low water-soluble monomers, such as styrene, and due to its relatively high aqueous-phase termination rate, the products of the aqueous-phase polymerization are oligomers with average molecular weight of about 1000. These oligomers are surface active because of

the hydrophilic end group obtained from the initiator, and will undergo micellization and form the precursor particles.

Shinoda [1963] has shown that the CMC of surfactants decreases with increasing the chain length, j , according to the following Equation:

$$CMC = C_o e^{(-D_o j)} \quad (1.3.1)$$

where C_o and D_o are constants. Application of this model to the styrene emulsion polymerization system suggests that the longer oligomers will be the first to reach the CMC. The oligomeric radicals that grow to a sufficient length (the critical chain length for the in situ micellization, n^*) will then undergo micellization and oligomer micellar particles will be formed. The micellar particle nuclei are very small, and their number is also small at the beginning. Therefore, the rate of free radical capture by these particles is small compared to that of the aqueous-phase termination. The concentration of shorter oligomers will thus increase, because of the aqueous-phase termination or , possibly, chain transfer reactions, and in turn they will reach their CMCs. This will result in an decrease in n^* and an acceleration of particle nucleation. This early stage of particle nucleation will be called the variable n^* stage, or Stage 1.

As the polymerization proceeds, the particle number continues to increase and at the same time particles begin to grow through polymerization. The rate of free-radical capture by particles will then increase. The mechanism of radical capture by particles will eventually become much more significant than aqueous-phase termination. Consequently, the concentration of oligomers in the aqueous phase will no longer increase, and n^* will tend to remain constant. The remainder of the particle nucleation period will be called the constant n^* stage, or Stage 2.

Oligomer micellar particles produced during Stage 1 are stable because of the surface charge from the initiator end groups. Therefore, they will have little tendency to coagulate. However, as free radicals and monomer are captured by these oligomer micellar particles, high molecular weight polymer is formed inside. The effect of incorporating a high molecular weight chain into a small, probably less than 5nm, nucleus consisting mainly of low molecular weight material, results in particle growth and a rapid reduction in the surface charge density. Thus, the initial oligomer micellar particles lose the stability they had initially, and rapidly begin to flocculate and coalesce during the constant n^* stage.

The rate coefficient for particle coagulation is, therefore, much higher during Stage 2 than during Stage 1. The high rate of particle coagulation will result in a rapid decrease in particle number and a corresponding increase in particle size. The sharp rise in particle size, and in particle surface area, will in turn cause a sudden increase in the rate coefficient for radical capture by particles. The decrease in the particle number by agglomeration, on the other hand, will cause a decrease in the rate of radical capture by particles. However, the increase in particle size and decrease in particle number will also reduce the rate of particle coagulation. Eventually, an equilibrium will be established between particle nucleation through in situ micellization and particle coagulation. The number of particles will then tend to a constant value [Song, 1989].

1.3.2-PARTICLE FORMATION

Several particle nucleation mechanisms have been proposed for the emulsifier-free systems:

- (a) homogeneous nucleation, proposed by Fitch [1973], in which growing oligomeric free radicals precipitate from the aqueous phase when they reach a critical chain length n^* to form a primary particle;
- (b) growing free radicals which undergo termination followed by particle nucleation through coagulation of these dead species, suggested by Arai *et al* [1979];
- (c) growing free radicals which achieve a size and concentration at which they become surface active and undergo micellization, as proposed by Chen and Piirma [1980].

Munro *et al* [1979] suggested that, none of these alone can predict the particle nucleation for all of the monomers. The water solubility has a great influence on the mechanism prediction. In general, relatively water soluble monomer particles are nucleated by the homogeneous nucleation, while the sparingly water soluble monomers such as styrene the micellar nucleation mechanism occurs. The particle nucleation period can be divided into two stages. Stage 1 is short (less than 10 minutes), and a large amount of oligomer micelle particle nuclei are produced during this stage. The particles are stable due to the surface charge density generated by the initiator end groups. As the particle nuclei capture free radicals from the aqueous phase and produce internal high molecular weight polymers, the surface charge density decreases and particles lose their stability and begin to undergo coagulation. This is the beginning of stage 2, resulting in a rapid growth in particle size and a decrease in particle number. Goodall and Wilkinson [1980] observed micellar-like particles during the early stages of emulsifier free polymerization of styrene. Their GPC results on the early stage samples showed that the particles were composed of a significant fraction of material of approximately 1000 molecular weight and a high molecular weight fraction of 10^6 . The amount of the low

molecular weight fraction did not appear to increase as the reaction progressed, indicating that it was formed in quantity only during the early stage of the reaction. This suggests that a significant portion of the termination between the oligomeric free radicals occurs during the early stage of the reaction. The micelles produced through the micellization of the surface-active oligomer serve as a site for further polymerization, leading to the high molecular weight polymer.

The homogeneous nucleation theory was established by Fitch [1973], and was then developed by Hansen and Ugelstad [1978]. In these treatments, the critical chain length, n^* , was considered to be a constant for a given monomer system. This hypothesis is invalid for the early stage of particle nucleation in emulsifier-free systems.

1.3.3- THEORY

1.3.3.1- Changing n^* Stage (Stage 1)

The homogeneous nucleation theory is based on the precipitation of the oligomeric radicals to form particle nuclei when they reach a critical chain length n^* . This holds only when the aqueous phase is saturated with the oligomer species of the chain length n^* . Every species of oligomer has a finite solubility in the aqueous phase. The water solubility of oligomer with chain length j , C_j^* , decreases as the chain length j in the aqueous phase, $[O_j]$, increases, due to the termination reaction and chain transfer reactions. The increase in $[O_j]$ is particularly significant at the beginning of the polymerization, when no particles are formed. Thus, the value of the critical chain length n^* will vary with reaction time as the concentration of oligomer of shorter length reaches its saturated concentration, C_j^* .

As mentioned previously, n^* is assumed to be constant, when the emulsifier is employed at concentrations higher than CMC for a given monomer. However, in an emulsifier-free system, a constant value for n^* is valid only during the latter stage of the particle nucleation period when the concentration of particles is high enough to absorb most of the free radicals generated in the aqueous phase. Thus, the concentrations of the oligomers with chain length less than n^* will not increase beyond their solubilities in the aqueous solution.

The micellization nucleation theory is based on the formation of oligomeric micelle particles when the growing oligomeric free radicals achieve a size and concentration at which they become surface active and undergo micellization. As with the solubility of the oligomers in water, the CMC of the surface-active oligomers decreases with increase in the chain length j .

One can argue that micellization nucleation and homogeneous nucleation are very similar, with only a difference in the size of the particles formed: a precursor particle formed in homogeneous nucleation consists of only a few oligomer chains, while an oligomer micelle particle generated from the micellization nucleation is composed of up to a hundred oligomeric chains.

Precursor particles generated from homogeneous nucleation are unstable because of their small size and lack of surface charge density. These precursor particles will undergo coagulation to form larger polymer particles with sufficient surface charge to be stable. Therefore, particles from homogeneous nucleation are more likely to grow through coagulation than through polymerization.

Oligomer micelle particles from micellization nucleation, on the other hand, are stable because of sufficient charges on their surface. This is confirmed by the emulsifier-free emulsion polymerization of styrene, investigated by Goodall and Wilkinson [1980]. Therefore, the formation of stable latex particles from homogeneous nucleation and micellization nucleation are different only in the rate of coagulation among oligomer micelle particles consisting of short oligomers in micellization nucleation, and among precursor particles consisting of longer oligomers in homogeneous nucleation.

Shinoda [1963] has shown that the CMC of surfactant decreases with increasing the chain length, j , according to the following Equation:

$$CMC = C_o e^{(-D_o j)} \quad (1.3.1)$$

Particles are nucleated from oligomeric free radicals with chain length n^* , when the concentration of oligomers with chain length above n^* are all at their corresponding limit of water solubilities or CMCs. As soon as the oligomeric free radicals precipitate from their aqueous solution, m of these radicals associate to form an oligomer micelle in the case of micellization nucleation, or to form a precursor particle in the case of homogeneous nucleation. The value of m will be much greater for micellization nucleation than for homogeneous nucleation. Thus, the particle nucleation rate can be written as:

$$\frac{d[P]}{dt} = \frac{k_p M_w [M_{n^*-1}]}{m} - K_f [P]^2 \quad (1.3.2)$$

where t is the time, $[P]$ is the particle concentration, M_w is monomer concentration in the aqueous phase, $[M_{n^*-1}]$ is the concentration of free radicals with chain length n^*-1 in the aqueous phase, k_p is the propagation rate constant, and K_f is the average rate coefficient

for particle coagulation. $\frac{d[P]}{dt}$ represents the rate of particle nucleation through homogeneous precipitation and/or in-situ micellization of oligomer radicals with chain length n^* . The term $(K_p M_w [M]^{n^*-1})$ is the production rate of oligomer radicals with chain length n^* . Assuming the termination of radicals in the aqueous phase is solely by disproportionation, the increase in inactive oligomer j can then be expressed as:

$$\frac{d[O_j]}{dt} = k_{tw}[R_w][M_j] + \sum_i k_{tri}[M_j][CTA_i] \quad (1.3.3)$$

where $[O_j]$ is the concentration of oligomer with chain length j in the aqueous phase, $[M_j]$ is the concentration of oligomeric free radicals with chain length j , $[R_w]$ is the concentration of the total free radicals in the aqueous phase, k_{tw} is the termination rate constant for the radicals in the aqueous phase; and $[CTA_i]$ and k_{tri} are the concentration and chain transfer rate constant, respectively, of the chain transfer agent (CTA)_i (i can

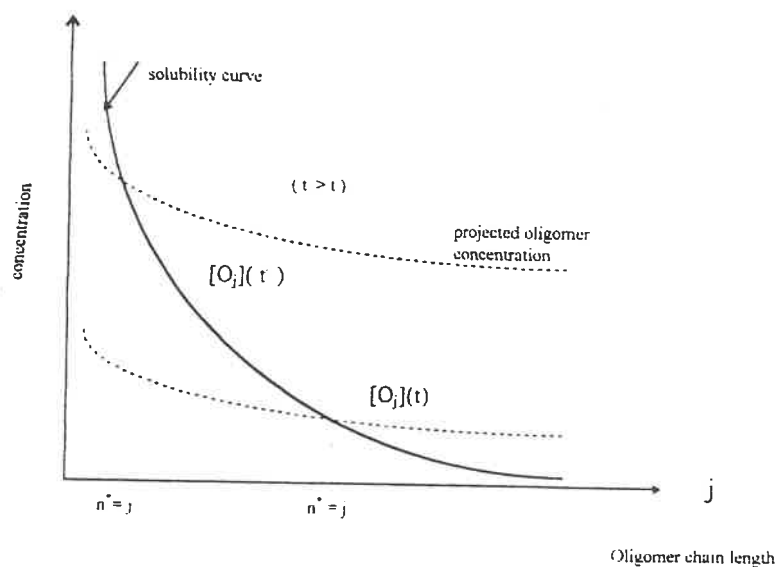


Figure 1.3.1- Scheme of n^* changing with time.

represent monomer, initiator, solvent, etc.). If a steady-state concentration of free radicals is assumed and $[CTA_i]$ is constant, ($[CTA_m]$ is the monomer concentration in the aqueous phase, M_w , for chain transfer to monomer), the right side of the Equation 1.3.3 can be considered constant, and the following Equation is obtained by integration:

$$[O_j] = \left\{ k_{tw}[R_w] + \sum_i k_{tri}[CTA_i] \right\} [M_j]t \quad (1.3.4)$$

By solving the balance Equations for free radicals in the aqueous phase with the assumption of steady state free radical concentration, the following relationships can be derived:

$$[M_j] = [\rho / (k_p M_w)] \alpha_p^j \quad (1.3.5)$$

$$(j = 1, 2, 3, \dots)$$

$$[R_w] = [\rho / (k_p M_w)] * \left[\alpha_p (1 - \alpha_p^{n^*-1}) / (1 - \alpha_p) \right] \quad (1.3.6)$$

where;

$$\rho = \sum_i k_{ri} [R_w] [CTA_i] + \rho_i \quad (1.3.7)$$

$$\alpha_p = k_p M_w / \left\{ k_p M_w + k_{tw} [R_w] + K'_c [P] + \sum_i k_{tri} [CTA_i] \right\} \quad (1.3.8)$$

where ρ_i is the free radical generation rate in the aqueous phase, K'_c is the net rate coefficient for radical capture which includes the effect of the free radical desorption from particles, n^* is the critical chain length of oligomers for homogeneous nucleation or in-situ micellization, and α_p can be considered as the probability of free radicals adding a monomeric unit by propagation.

In principle, $[R_w]$ will change with time since n^* changes with time. However, because n^* is large at the beginning, as seen in Figure 1.3.1, $[R_w]$ is not significantly influenced since $\alpha_p < 1$. Therefore, $[R_w]$ can be assumed to be constant. This justifies the derivation of Equation 1.3.4 from Equation 1.3.3. Substituting Equation 1.3.5 into Equation 1.3.4 gives:

$$[O_j] = \left\{ k_{tw}[R_w] + \sum_i k_{tri}[CTA_i] \right\} * \left[\rho / (k_p M_w) \right] \alpha_p^j t \quad (1.3.9)$$

When the concentration of oligomer with chain length j equals the water solubility (in the homogeneous nucleation) or the CMC (in the micellization nucleation) of the same oligomer species C_j^* , the j will become the critical chain length n^* . Thus,

$$[O_j] = \left\{ k_{tw}[R_w] + \sum_i k_{tri}[CTA_i] \right\} * \left[\rho / (k_p M_w) \right] \alpha_p^{n^*} t = C_j^* \quad (1.3.10)$$

The water solubility or the CMC of the oligomers, C_j^* , is assumed to decrease with length j according to the Equation 1.3.1, i.e.,

$$C_j^* = C_o e^{(-D_o j)} \quad (1.3.11)$$

Substituting Equation 1.3.11 into Equation 1.3.10 and solving for n^* gives:

$$n^* = \left[\ln(E_1 / t) \right] / E_2 \quad (1.3.12)$$

where

$$E_1 = \frac{C_o k_p M_w}{\rho \left(k_{tw}[R_w] + \sum_i k_{tri}[CTA_i] \right)} \quad (1.3.13)$$

$$E_2 = \ln(\alpha_p e^{D_o}) = D_o + \ln \alpha_p \quad (1.3.14)$$

Substituting Equations 1.3.5 and 1.3.12 into Equation 1.3.2 yields:

$$\frac{d[P]}{dt} = \left(\frac{\rho}{\alpha_p m} \right) \left(\frac{t}{E_i} \right)^{d_o} - K_f [P]^2 \quad (1.3.15)$$

where

$$d_o = \frac{-(\ln \alpha_p)}{(D_o + \ln \alpha_p)} \quad (1.3.16)$$

$$N = Ft^{d_o+1} \quad (1.3.17)$$

where

$$F = N_A \rho / \{m(d_o + 1)\alpha_p E_i^{d_o}\} \quad (1.3.18)$$

and N_A is Avogadro's number.

1.3.3.2- Constant n^* Stage (Stage 2)

The derivation of the equations for determining particle concentration is much simpler when n^* is constant. The production rate of particles for the in-situ micellization can be written as:

$$\frac{d[P]}{dt} = \frac{k_p M_w [M_{n^*-1}]}{m} - K_f [P]^2 \quad (1.3.2)$$

where $[M_{n^*-1}]$ is the concentration of oligomer radicals with the chain length n^*-1 and can be expressed as:

$$[M_{n^*-1}] = \frac{\rho_i \alpha_p^{n^*-1}}{k_p M_w} \quad (1.3.19)$$

Thus the Equation 1.3.2 becomes:

$$\frac{d[P]}{dt} = \frac{\rho_i \alpha_p^{n^*-1}}{m} - K_f [P]^2 \quad (1.3.20)$$

Equation 1.3.20 is then solved to give:

$$N = [P]N_A = N_s \frac{(1 + A_1) - (1 - A_1)e^{-t/\tau}}{(1 + A_1) + (1 - A_1)e^{-t/\tau}} \quad (1.3.21)$$

where N_A is Avogadro's number, and N_s is the particle number at steady state calculated from the equation below:

$$N_s = N_A \sqrt{\frac{\rho_i \alpha_p^{n^*-1}}{mK_f}} \quad (1.3.22)$$

τ is defined by

$$\tau = \frac{N_A}{2K_f N_s} \quad (1.3.23)$$

and A_1 is the ratio of particle number, N_c , at $t = t_c$ (the end of Stage 1), to the particle number N_s at $t = \infty$. That is, $A_1 = N_c/N_s$.

1.4- MICROEMULSION POLYMERIZATION

Microemulsion polymerization is a very simple polymerization process first reported by Stoffer and Bone[1980]. Monomer is dispersed in water by use of a surfactant, and the polymerization is initiated by use of a lipophilic radical. A cosurfactant, such as alcohol, can be used in these systems. Microemulsions are usually formed spontaneously by mixing the components, and there is no need for high shear conditions. The polymerization reaction is very fast and reaches conversions of greater than 80% in less than an hour, with small particle sizes(<130 nm)[Candau,1990]. The

obtained latices from these systems are thermodynamically stable, transparent, and nonbirefringent with low viscosity and high molecular weights (10^6). The particle size in these systems is controlled by the ratio of the monomer to surfactant, and the amount of the initiator. The ultimate characteristics of these latices depend on the nature of the surfactant.

In 1990, Puig and Kaler and their coworkers [Pérez-Luna *et al*, 1990] described the ternary microemulsion polymerization system (monomer-water-initiator) for styrene. Another report was published on the kinetics of the ternary microemulsion polymerization for methyl methacrylate [Rodriguez-Guadarrama *et al*, 1993], where high molecular weight polymers (10^6) with small particle sizes (<70 nm) were obtained. It was also mentioned that the activation energy for the system was lower than in a bulk polymerization.

CHAPTER 2

EXPERIMENTAL PROCEDURE AND ANALYSIS

2.1-INTRODUCTION

The effect of experimental variables such as temperature, the speed and type of agitator, and the amount of initiator on the polymerization rate, particle size, zeta potential, and molecular weight are examined.

2.2-MIXING

A decoloration method was used to evaluate the mixing efficiency[Yap,1976] of three types of agitators: propeller, turbine, and anchor. Each of these agitators was tested at three different speeds and the mixing time was measured with a chronometer (precision of 0.1 sec). The decoloration method and the materials used are described completely in appendix A.

2.3-POLYMERIZATION

2.3.1-MATERIALS

Distilled water and concentrated hydrochloric acid were used in all of the polymerization reactions.

N-butyl methacrylate, the monomer, was obtained from Omega Chemical Company (Quebec, Canada) as 99% pure, with a molecular weight of 142.19 and a density of 0.889g/cm³. Other physical properties of this monomer are B.P.(boiling point)=163.5-170.5°C; flash point=66°C; inhibitor 10ppm of methylethylhydroquinone. In order to purify the monomer from the inhibitor, it was washed three times with 5M sodium hydroxide solution at a volume ratio of 5:1, monomer to caustic, respectively. The washed monomer was chilled to -4°C to freeze out the residual caustic soda. The frozen caustic was then filtered out and stored at 4°C in a dark bottle until required. The purified monomer was used within one month.

The initiator used in this project was 2,2'-azobisisobutyramidine dihydrochloride, and was supplied by Wako Chemicals Company USA incorporation (VA, U.S.A.) as V-50. It was kept at 4°C until use. The initiator was used without further purification.

2.3.2-FORMULATION

The formulation used throughout this project is given in Table 2.3.1.

Table 2.3.1- The polymerization formulation

- n-butyl methacrylate	105g
- distilled water	245g
- concentrated hydrochloric acid	20 drops
- initiator	2.5-4g (As indicated in appendix B)
- temperature	70°C or as indicated
- speed	As indicated for each experiment

2.3.3-POLYMERIZATION PROCEDURE

A schematic of the polymerization set up is given in Figure 2.3.1. The polymerization reactions were carried out in a 1 liter round bottomed flask with a four necked flanged top. A total reactant mass of 350g was normally used. A typical preparation is as follows:

225ml of distilled water was added to the flask. A teflon stirrer of half-moon shape was connected to a stainless steel shaft fitted with a teflon guide, and added to the central outlet of the flask cover. The shaft was connected to a digital motor which indicated the agitator speed. Care was taken to ensure that the stirrer was at uniform distance from the bottom of the flask in each experiment. The water-cooled reflux condenser was added to the second outlet of the flask. A J-type thermocouple, connected to a computer, was placed in the third outlet in order to record the temperature inside the

reactor. The flask was immersed in a thermostat water bath and a thermometer was placed in the water bath ($70 \pm 0.5^{\circ}\text{C}$). A nitrogen gas blanket was maintained over the reacting medium throughout the reaction. The flow rate was maintained at a low level to minimize monomer evaporation. To prevent the back diffusion of oxygen into the system, the condenser was connected to the atmosphere via a beaker filled with water. After stirring for 10 minutes under nitrogen atmosphere, 105g of butyl methacrylate was added to the vessel. The system was then left for 20 minutes to attain temperature equilibrium. The initiator was dissolved in 10ml of water and was washed with another 10ml of distilled water. A reaction time of 90 to 120 minutes was found to be adequate, although this depends to some extent on temperature and agitator speed. Samples were taken at different time intervals for each reaction. At the end of the reaction time, the vessel was removed from the thermostat bath and allowed to stand for a few minutes; the product was then stored in polyethylene bottles.

2.3.4-SAMPLING

A glass tube with an internal diameter of 6mm was used for sampling. The samples were poured into covered testing tubes. 1ml of inhibitor (hydroquinone 0.1% gHQ/ml solution) was then added in order to stop the polymerization reaction. The samples were left standing for 24hours. The unreacted monomer separated out from the top layer and was removed, as it may have dissolved the polymer, thereby affecting the particle size and the charge density of polymer particles.

2.4-POLYMER CHARACTERIZATION

The following properties were determined:

- yield
- zeta potential
- particle size
- molecular weight and molecular weight distribution
- glass transition temperature, T_g .

2.4.1-YIELD

The polymer conversion was followed gravimetrically at different time intervals during the reaction. Weighing bottles were weighed on a balance with 0.0001g precision. Approximately 1g of 0.1% hydroquinone solution was added to the bottles and weighed with the same precision. Samples were taken from the reaction medium using a glass tube, and poured in the weighing bottles. The bottles were weighed and put under infrared light for an hour, to evaporate the water and the unreacted monomer. The bottles were then placed in a Fisher Scientific isothermperature vacuum oven (model 282A) and left at 45°C overnight. The bottles were weighed several times until a relative constant weight was obtained. The equations used to measure the percentage of the yield are given in Appendix B-1.

2.4.2-ZETA(ζ) POTENTIAL

The zeta potential was determined from electrophoretic mobility and measured using an MK-II Rank Brothers Microelectrophoresis instrument. The instrument was calibrated for the rectangular cell before use and the location of the stationary layers were measured.

A very dilute suspension of a sample was made (1 drop in 100ml of distilled water). The suspension was poured into the rectangular thermostat water bath (25°C), two electrodes were placed in their positions and a constant voltage of 50 volts was adjusted between the two electrodes. Using a television screen and a chronometer with a precision of 0.01sec, the displacement of one particle from one point to another point of premeasured distance was measured. The zeta potential for each sample was determined according to the procedure given in Appendix B-2.

2.4.3-PARTICLE SIZE

A laser light scattering goniometer from Brookhaven Instruments Corporation was used to determine the particle size of the latices. Twice distilled deionized water was passed through a 2-micron filter and poured to clean and dust-free sampling tubes. A very small amount of the latex (1 drop in 100ml of the afore-mentioned water) was added to this sampling tube, which was then shaken to form a uniform, light opaque suspension. The samples were placed in a paraffin bath at 25°C. The laser light was sent through two narrow adjustable windows to the sample and the scattered beams were collected,

identified, and counted by a laser detector(type TFL) adjusted on 90° from the main beam. The signals obtained from the detector were sent to a primary computer to measure and calculate particle size. The data were sent to a BI-2030AT Digital Corrolator where they were compared and correlated, and then saved in a second computer. Care was taken not to have overflows of the laser light through the detector. The average of three saved particle sizes was accepted as the particle size of each sample.

2.4.4-MOLECULAR WEIGHTS AND MOLECULAR WEIGHT DISTRIBUTION

The molecular weight of the latices was determined by passing the samples through two GPC columns in series, from Waters Association. The first column was an ultrastyrigel-type which has a linear pore size with an effective molecular weight of 2,000 to more than 10,000,000. The second column was also an ultrastyrigel-type with a pore size of 500\AA and an effective fractionation of molecular weight of 100 to 10,000.

The samples obtained from the experiments were dried in a vacuum oven at 45°C . A 0.2% solution of dried sample was made in the THF (HPLC grade solvent, obtained from Caledon Laboratories, Ontario, Canada). In order to obtain a complete solution, the sample solutions were left to stand overnight. The solutions were passed through a 0.5 m filter, type FH (from Millipore Corporation). The obtained curves were analyzed and the molecular weight and its distribution were measured by the Equations given in Appendix B-3.

2.4.5- GLASS TRANSITION TEMPERATURE, T_g

The glass transition temperature of the latex was determined via a Dielectric Analyzer, DEA 2970. The polymer was pre-dried in an aluminum foil dish and was kept in a vacuum desiccator until placed in the two parallel plates of DEA apparatus. A minimum spacing of 0.5mm was chosen between the two parallel plates, along with a ram maximum force of 250.00N. 10 different frequencies were chosen between 0.1 and 3000Hz for temperatures of -40 to 75°C and a speed of 1 °C/min. These temperature and frequency intervals let the polymer chains become rubber-like, and the movements can be verified and thus the polymer glass transition is determined.

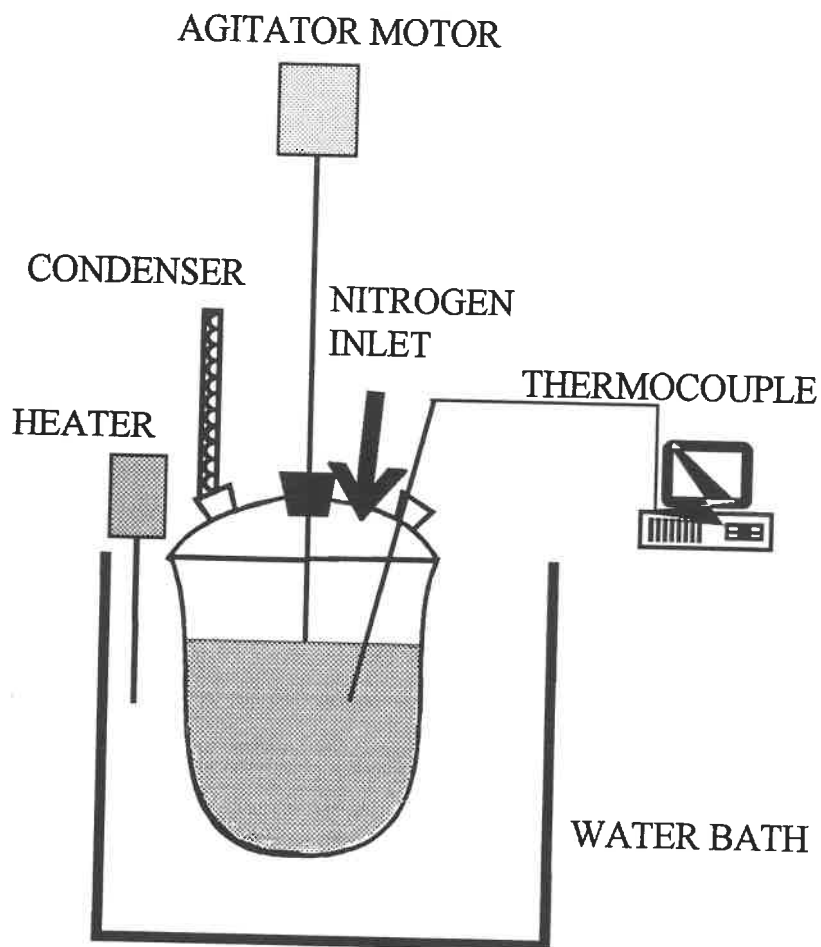


Figure 2.3.1 - The schematic of polymerization reactor.

CHAPTER 3

RESULTS

3.1-INTRODUCTION

The results of the experimental work discussed in Chapter 2 will be given in this Chapter. The effect of temperature, amount of initiator, and the speed of agitation on the characteristics of the polymer particles is investigated. The formulation and the polymerization conditions used for each experiment are shown in Appendix C. A discussion of the results will be made in the following Chapter.

The temperature inside the polymerization medium was not always constant during the reaction. This temperature was measured every 10 seconds and the results were recorded on a computer, and are shown in Figures 3.1.1-3 for speeds of 400, 500, and 600rpm. As a result, it can be suggested that there is a specific level in the amount of initiator where the steady reaction temperature is maintained.

3.2-MIXING

The decoloration method was used to find the optimum agitator type and agitation speed. The following results were obtained for three types of agitators (propeller, turbine and anchor):

Table 3.2.1- The mixing time for different types of agitators at different speeds.

	100 rpm	200 rpm	300 rpm
propeller	45 sec	20 sec	10 sec
turbine	56 sec	14.3 sec	12.2 sec
anchor	15.7 sec	11.2 sec	4.3 sec

3.3-POLYMERIZATION RATE

The polymerization rate was affected by the following variables thusly:

- decreasing the monomer concentration increased the polymerization rate, Figure 3.2,
- an increase in the amount of initiator increased the polymerization rate, Figure 3.3,
- increasing the agitation speed decreased the polymerization rate, Figure 3.4,
- an increase in the reaction temperature increased the polymerization rate, Figure 3.5.

3.4-PARTICLE SIZE

The following variables affect the particle size in the emulsifier-free emulsion polymerization of BMA thusly:

- the particle size decreased with an increase in the amount of initiator, Figure 3.6.1-2, also it can be seen that, there is a limit in the amount of initiator added to the polymerization system, where, there is a rapid increase in the particle size, at the early stages of the reaction, Figure 3.6.2,
- the effect of agitation speed on the particle size can be divided into two identical groups of:
 - * below 400rpm, the particle size increased with an increase in the agitation speed, Figure 3.7
 - * higher than 400rpm, the particle size decreased with an increase in the agitation speed, Figure 3.8.1-2, Figure 3.9.1-2, Figure 3.10.1-2,
- increasing the temperature decreased the particle size at the same conversion and the polydispersity of the latex particles, Figure 3.11.1-2.

3.5-ZETA POTENTIAL

The afore-mentioned polymerization variables had the following affects on the particles zeta potential:

- increasing the initiator concentration increased the zeta potential of the BMA particles at the same conversion, Figure 3.12.1-2,

- increasing the agitation speed increased the zeta potential and delayed the coagulation to higher conversions, Figure 3.13.1-2, Figure 3.14.1-2,
- at the same conversion, increasing the temperature increased the zeta potential and the zeta potential has a sharper distribution, Figure 3.15.1-2.

3.6-MOLECULAR WEIGHT

- The effect of initiator concentration on the molecular weight can be divided into:
 - * concentrations lower than a specific level, where an increase in the amount of initiator decreased the molecular weight, Figure 3.17.1-2,
 - * concentrations higher than the specific level, where an increase in the initiator concentration increased the molecular weight, Figure 3.17.1-2,
- the molecular weight increased with an increase in the agitation speed, Figure 3.18.1-2,
- the molecular weight increased with an increase in the temperature, Figure 3.19.1-2,
- the GPC diagrams were reviewed and the micellization nucleation kinetics is suggested for the polymerization of BMA, Figure 3.20.

3.7-REACTION TIME

The examined parameters affected the reaction time as follows:

- increasing the amount of initiator decreased the polymerization time, Figure 3.3,
- the reaction time was increased with an increase in the agitation speed, Figure 3.21,

-increasing the reaction temperature decreased the polymerization time, Figure 3.22.

3.8-GLASS TRANSITION TEMPERATURE, T_g

The glass transition temperature was found to be 35.98°C for one sample using the DEA by extrapolating the obtained line from frequency versus temperature (Figure 3.23).

3.9-OVERALL ACTIVATION ENERGY, E_R

The kinetics of polymerization were also studied at four different temperatures of $60, 70, 75,$ and 80°C . The slope of the linear portion of the time vs. conversion graph plotted as $(1/T)$ versus $\text{Ln}(\text{conversion \%}/\text{time})$, Figure 3.24. The overall activation energy of the reaction was found to be $E_R = 9.37 \text{ Kcal/mole}$.

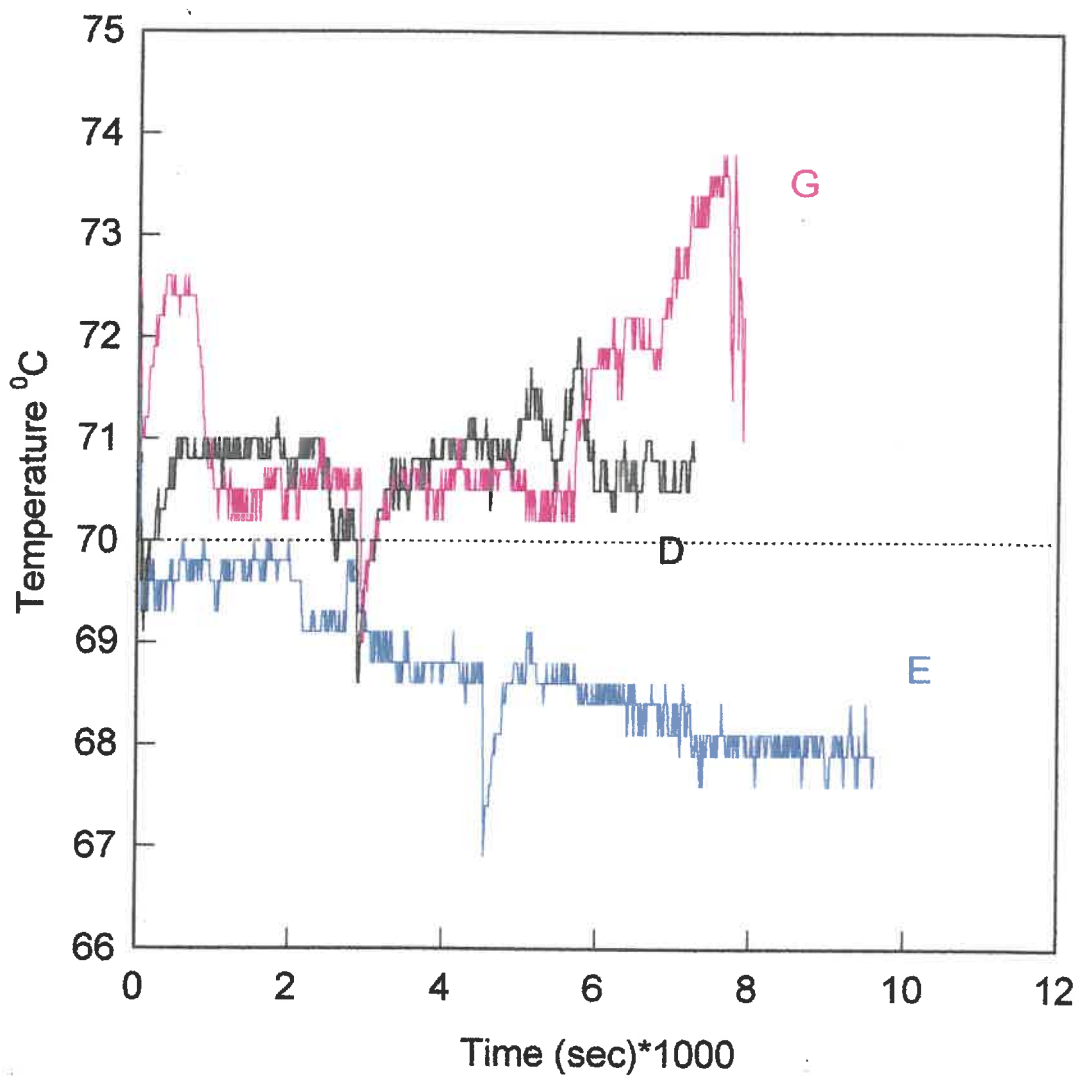


Figure 3.1.1 - Recorded temperature in different amounts of initiator at 400 rpm and 70°C.

— exp. E - [I] = 2.7g.

— exp. D - [I] = 3.0g.

— exp. G - [I] = 3.7g.

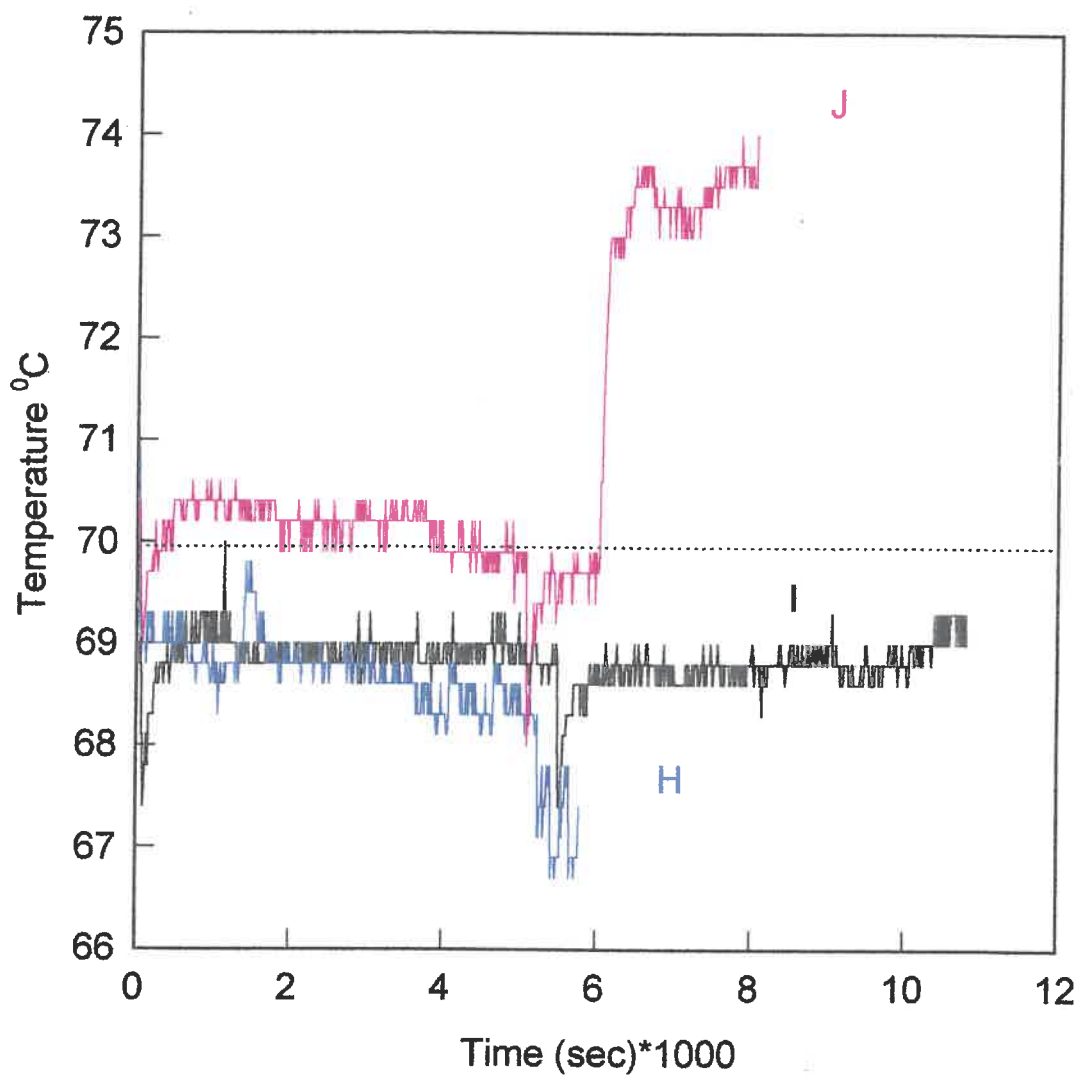


Figure 3.1.2 - Recorded temperature in different amounts of

initiator at 500rpm and 70°C.

— exp. H - [I] = 3.0g.

— exp. I - [I] = 3.4g.

— exp. J - [I] = 3.8g.

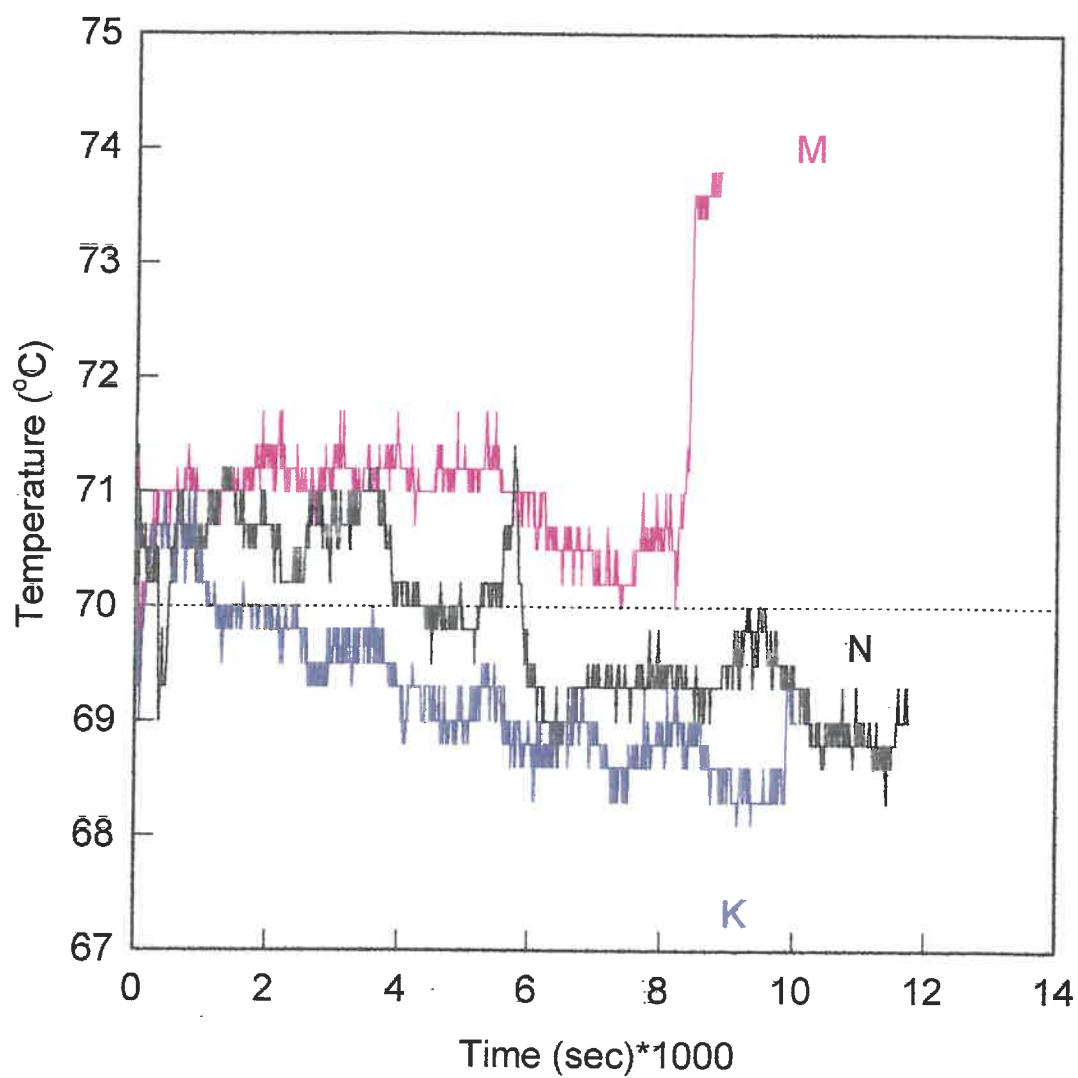


Figure 3.1.3 - Recorded temperature in different amounts of initiator at 600 rpm and 70°C.

- exp. K - [I] = 3.5 g.
- exp. N - [I] = 3.7 g.;
- exp. M - [I] = 4.0 g.;

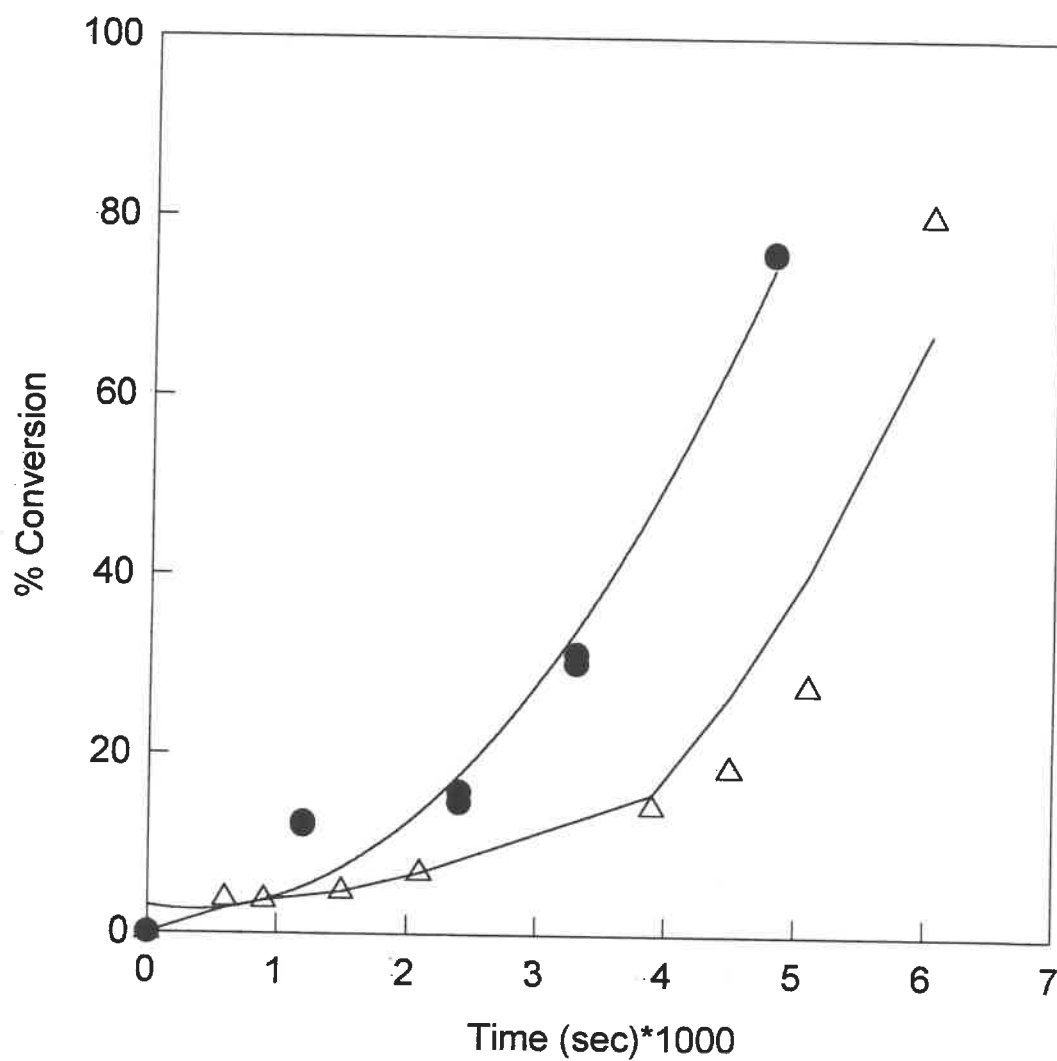


Figure 3.2 - Rate of polymerization for different monomer concentrations at 70°C, 400rpm and $[I]=3.4g$.

- exp. 23 - 0.21 g of monomer/g of the total material added to the reactor;
- △ exp. I - 0.30 g of monomer/g of the total material added to the reactor.

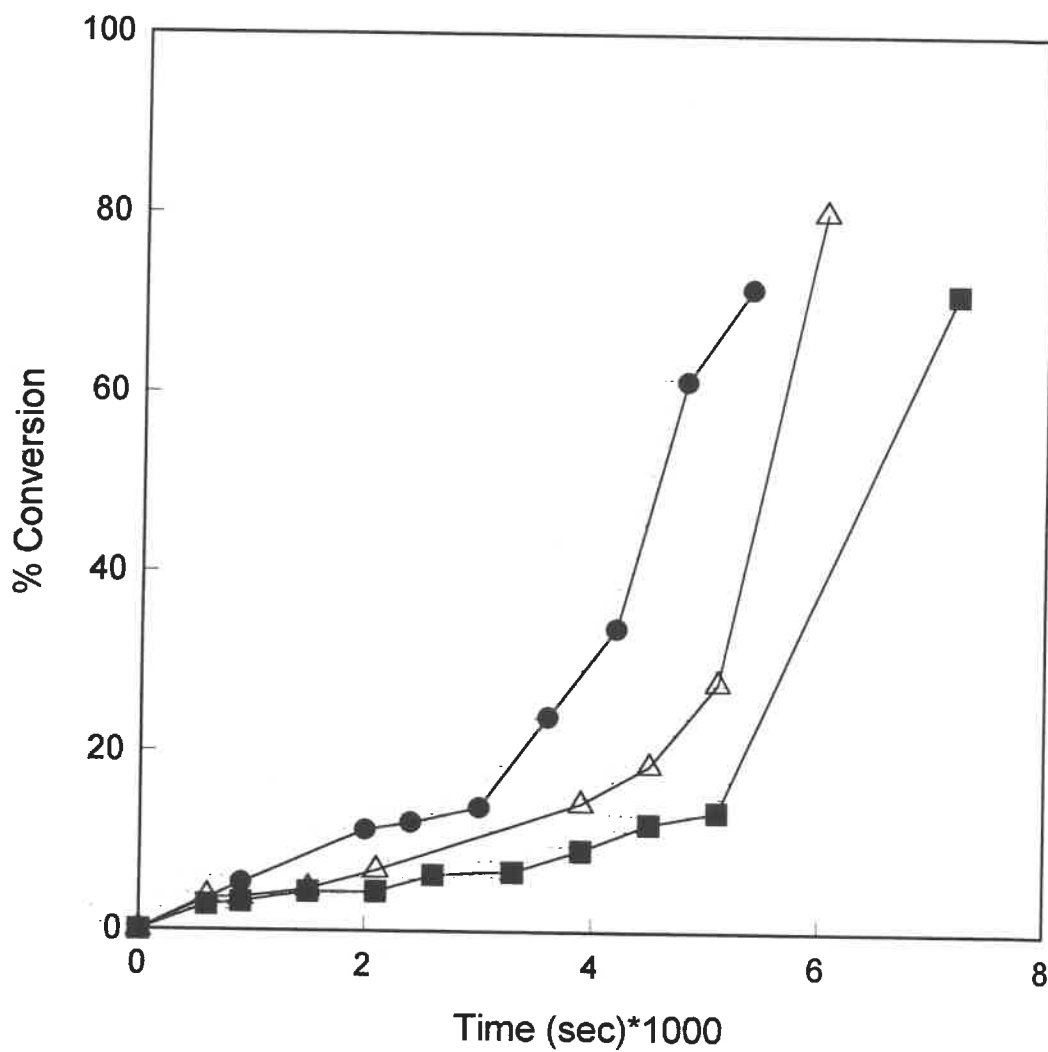


Figure 3.3 - Effect of initiator concentration on the polymerization rate at 70⁰ C and 400 rpm.

- exp. D - [I] = 3.00 g. ;
- △ exp. A - [I] = 3.41 g. ;
- exp. F - [I] = 3.70 g.

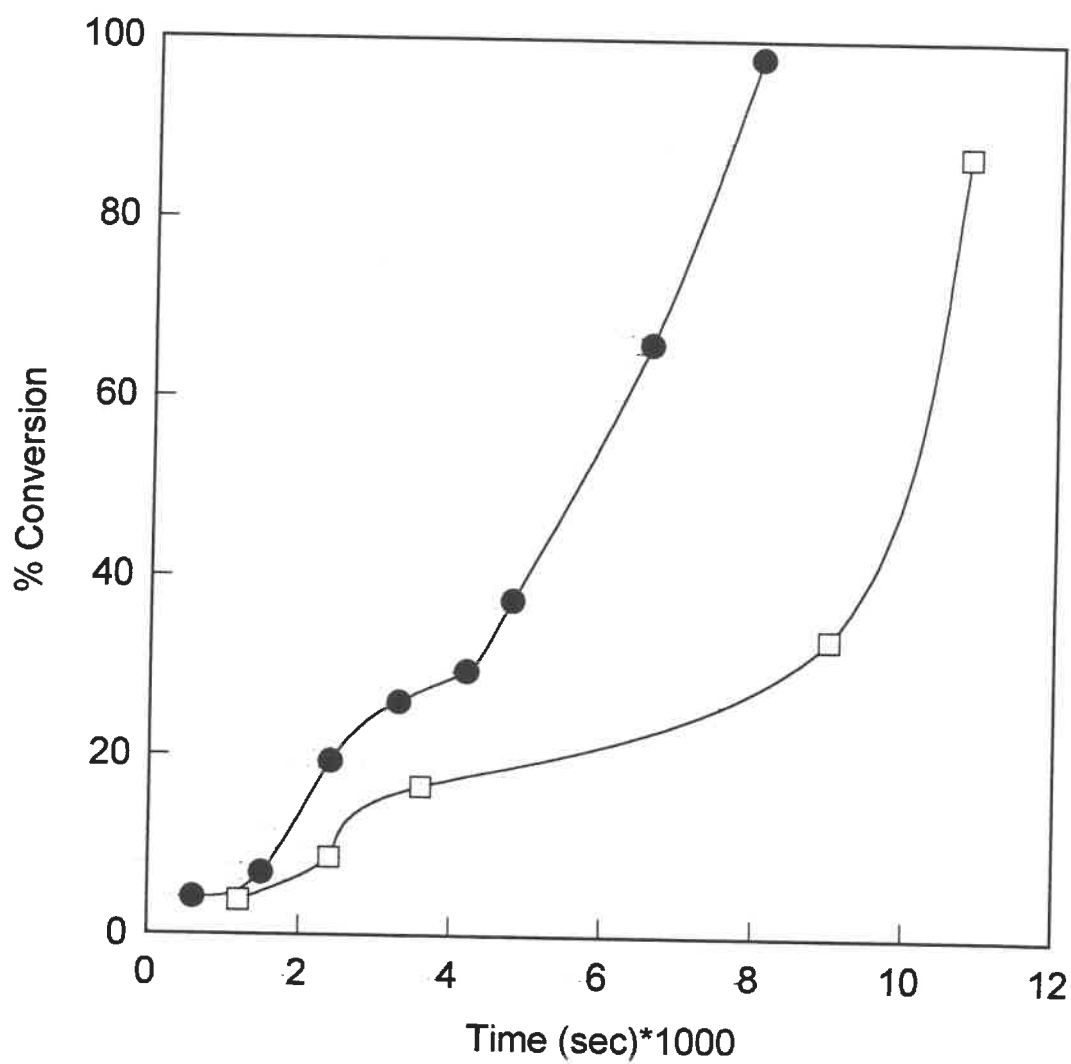


Figure 3.4 - Effect of speed on the rate of polymerization at 70°C and [I] = 3.0g.

- exp. D - 400rpm
- exp. H - 500rpm

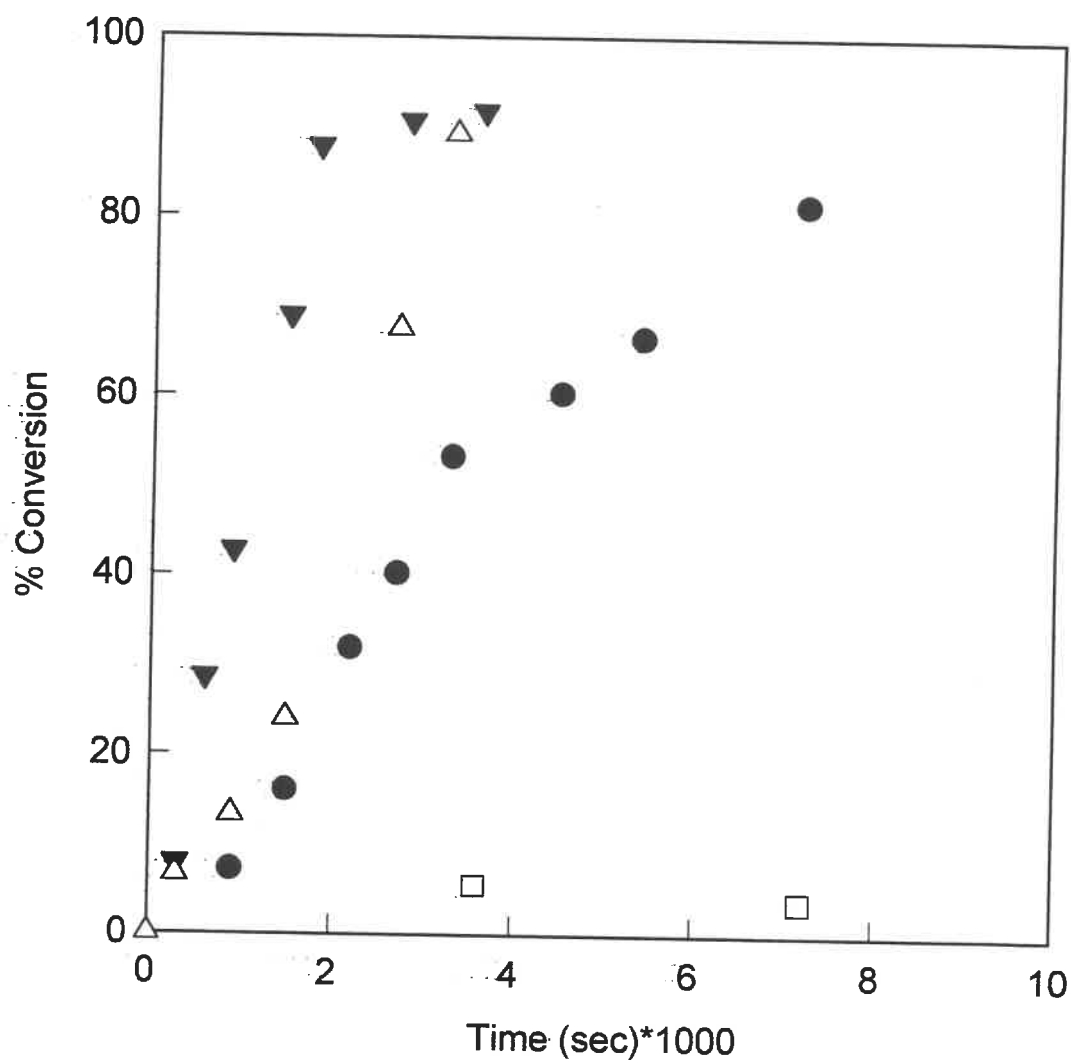


Figure 3.5- Effect of temperature on the rate of polymerization at 400rpm and $[I]=3.41g$.

- exp. C - 60°C
- exp. A - 70°C
- △ exp. O - 75°C
- ▼ exp. B - 80°C

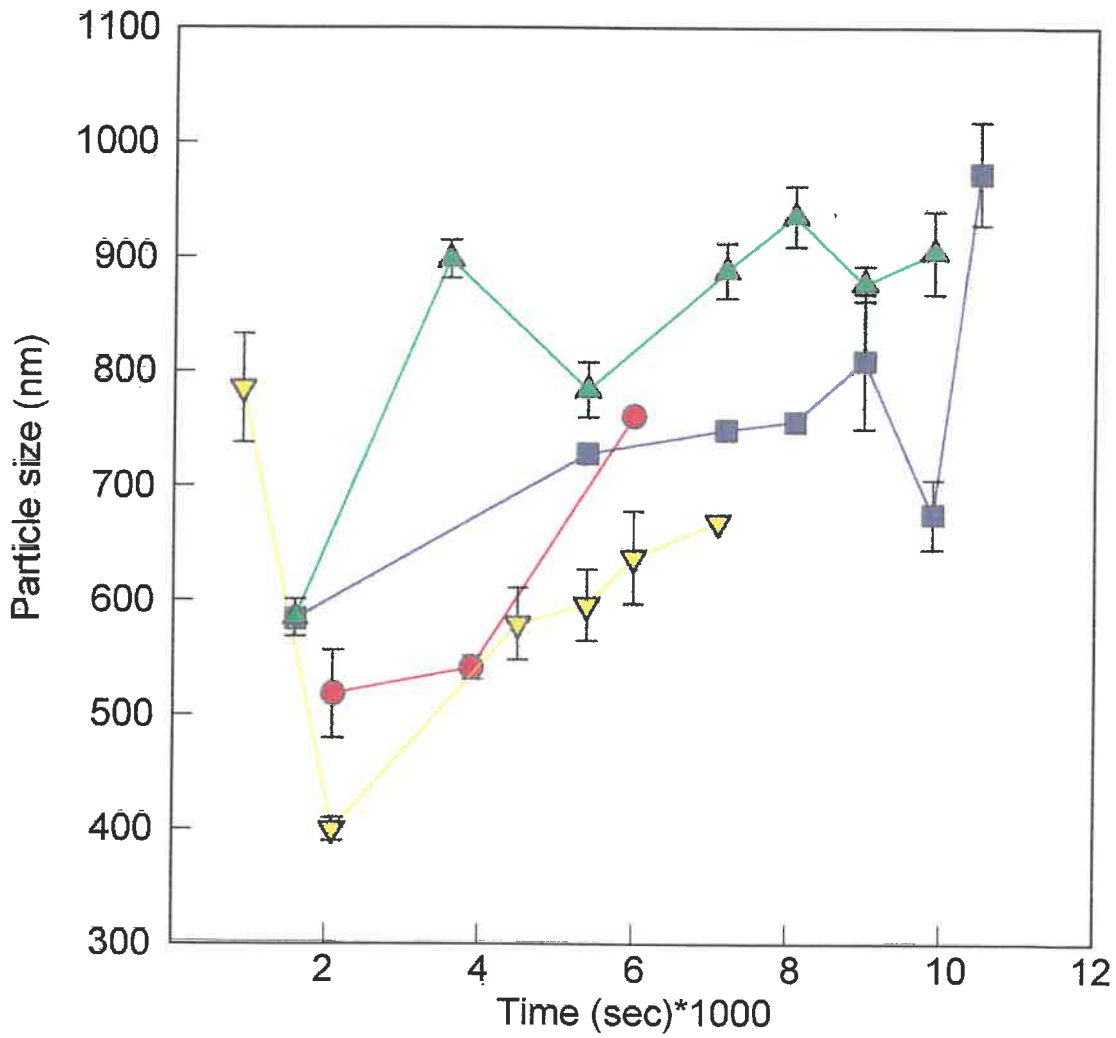


Figure 3.6.1 - Effect of the amount of the initiator on the particle size at 600 rpm and 70⁰C.

- exp. K - [I] = 3.5 g.;
- ▲ exp. N - [I] = 3.7 g.;
- exp. L - [I] = 3.8 g.;
- ▼ exp. M - [I] = 4.0 g.

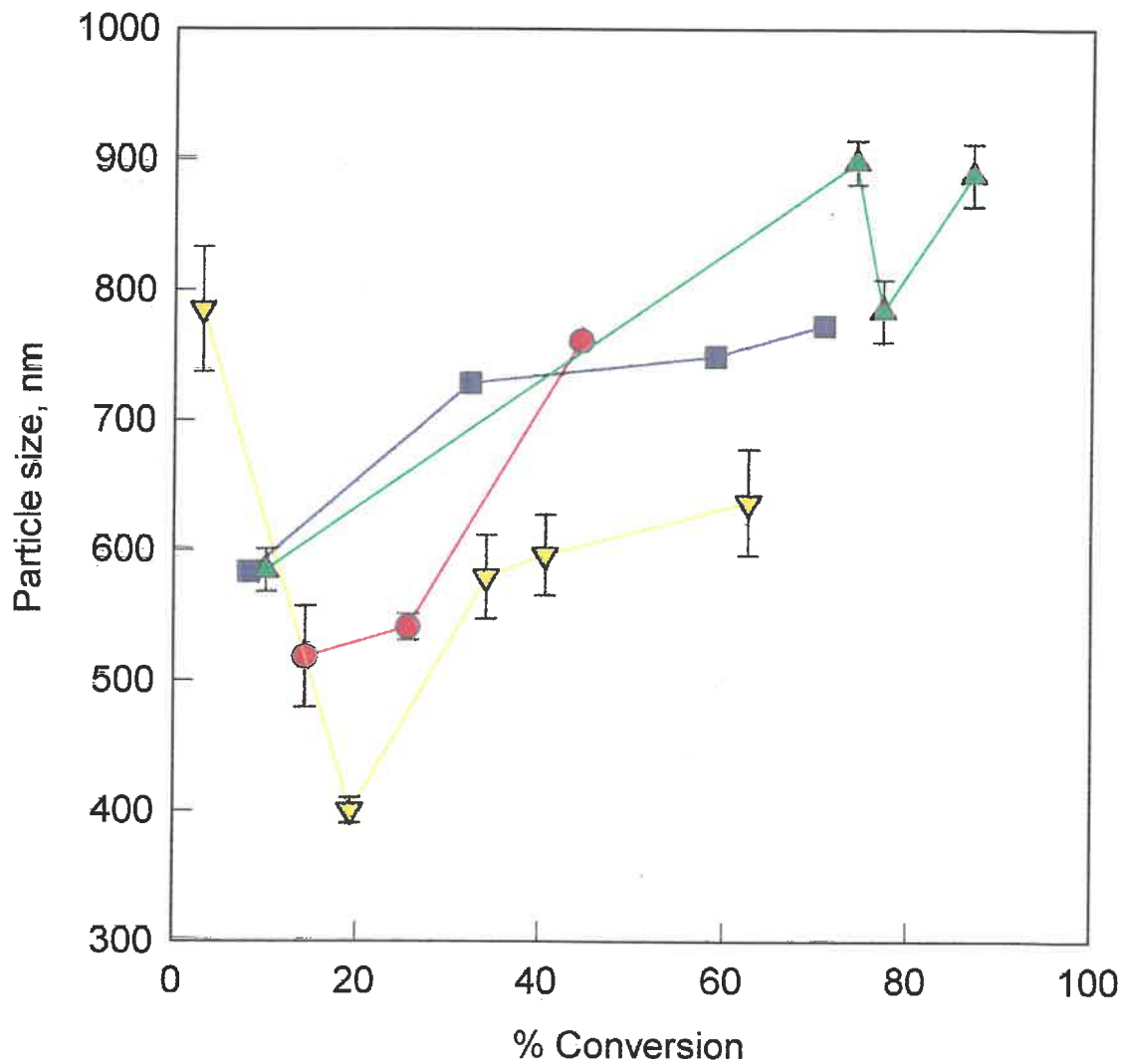


Figure 3.6.2 - Variation of particle size with conversion for different initiator concentrations at 600 rpm and 70⁰ C.

- exp. K - [I] = 3.5 g.;
- ▲ exp. N - [I] = 3.7 g.;
- exp. L - [I] = 3.8 g.;
- ▼ exp. M - [I] = 4.0 g.

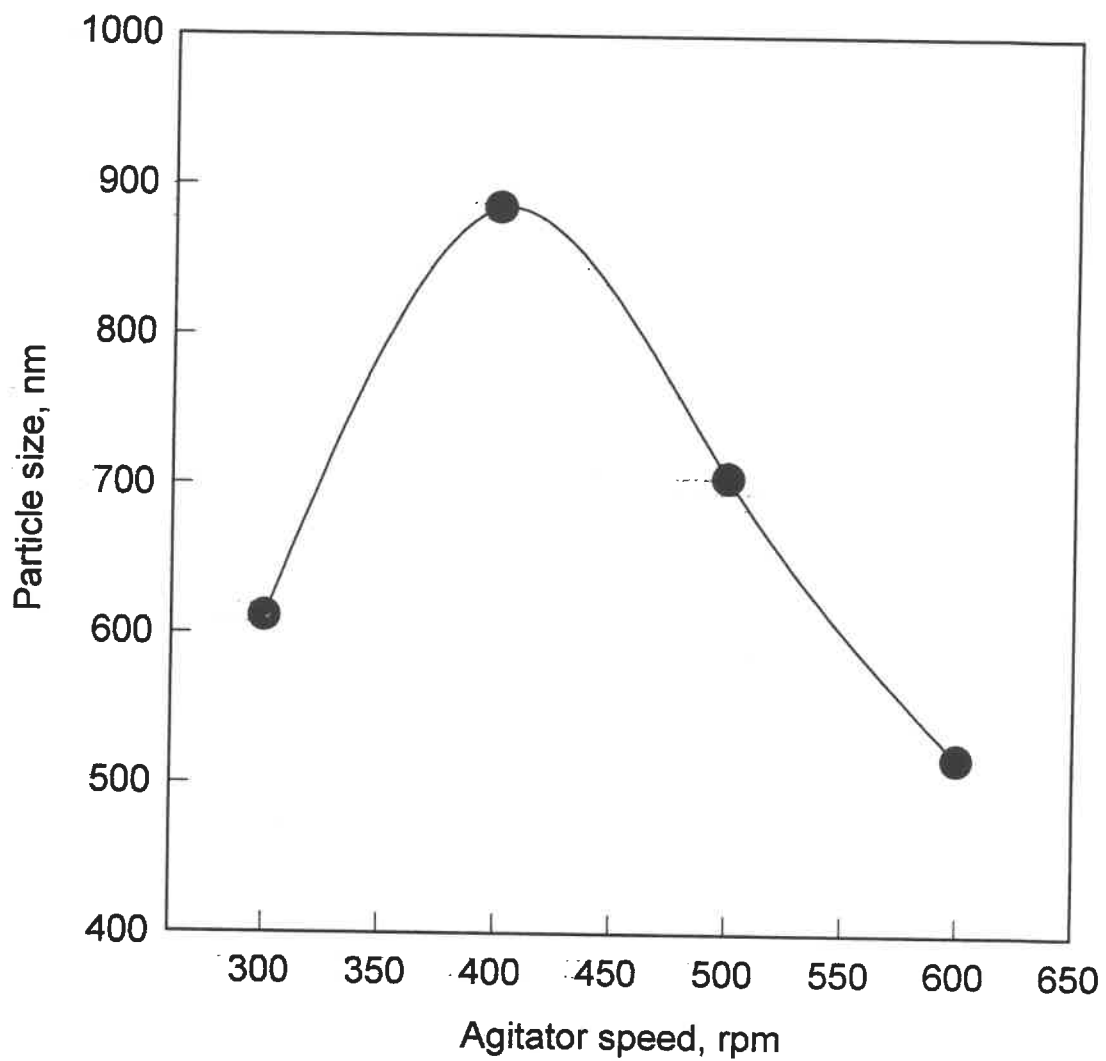


Figure 3.7- Effect of agitator speed on the size of the polymer particles at constant conversion.

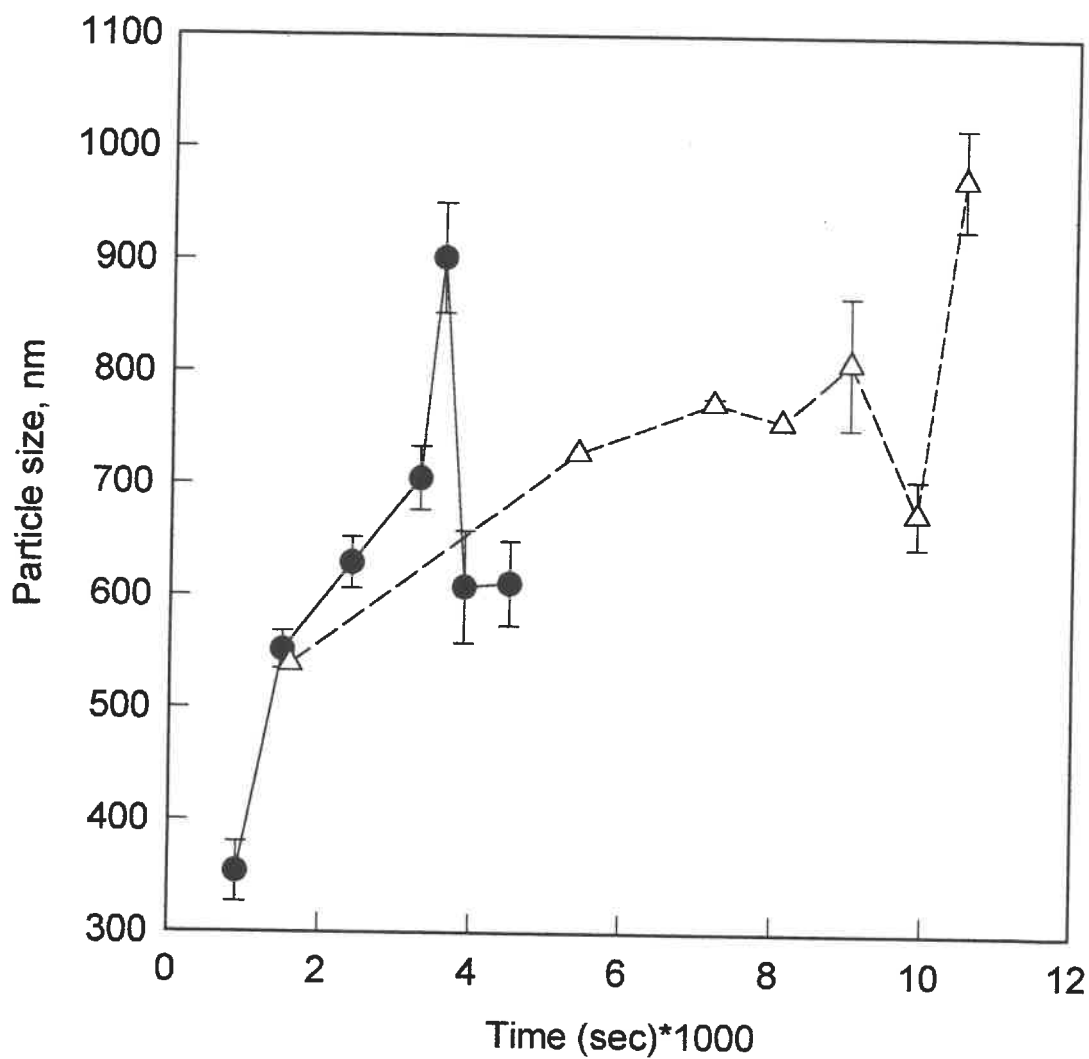


Figure 3.8.1- Variation of particle size for agitation speeds greater than 400rpm at 70°C and [I]= 3.8g.

● exp.J - 500 rpm;
—△— exp. L - 600 rpm.

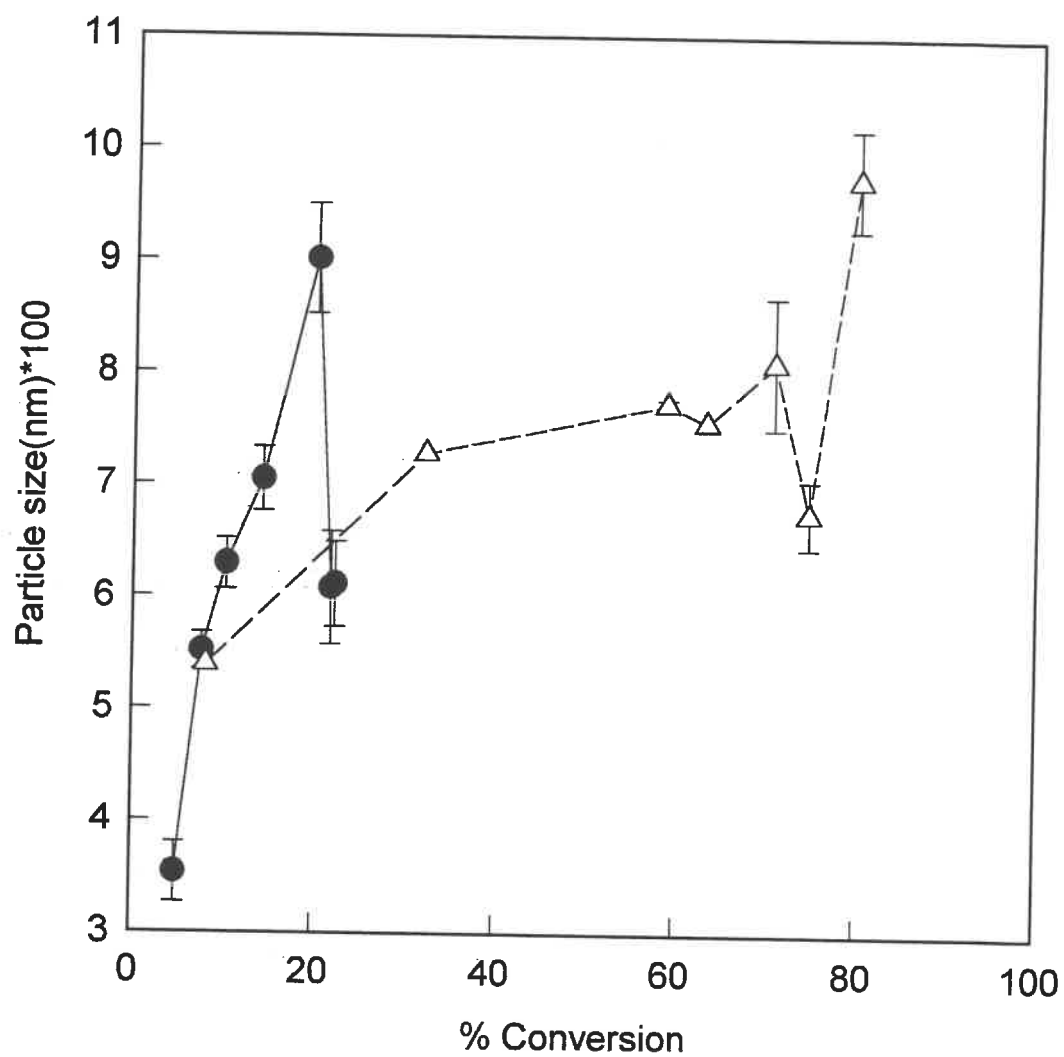


Figure 3.8.2- Variation of particle size for agitation speeds greater than 400rpm at 70°C and $[I] = 3.8g$.

—●— exp. J - 500 rpm;

—△— exp. L - 600 rpm.

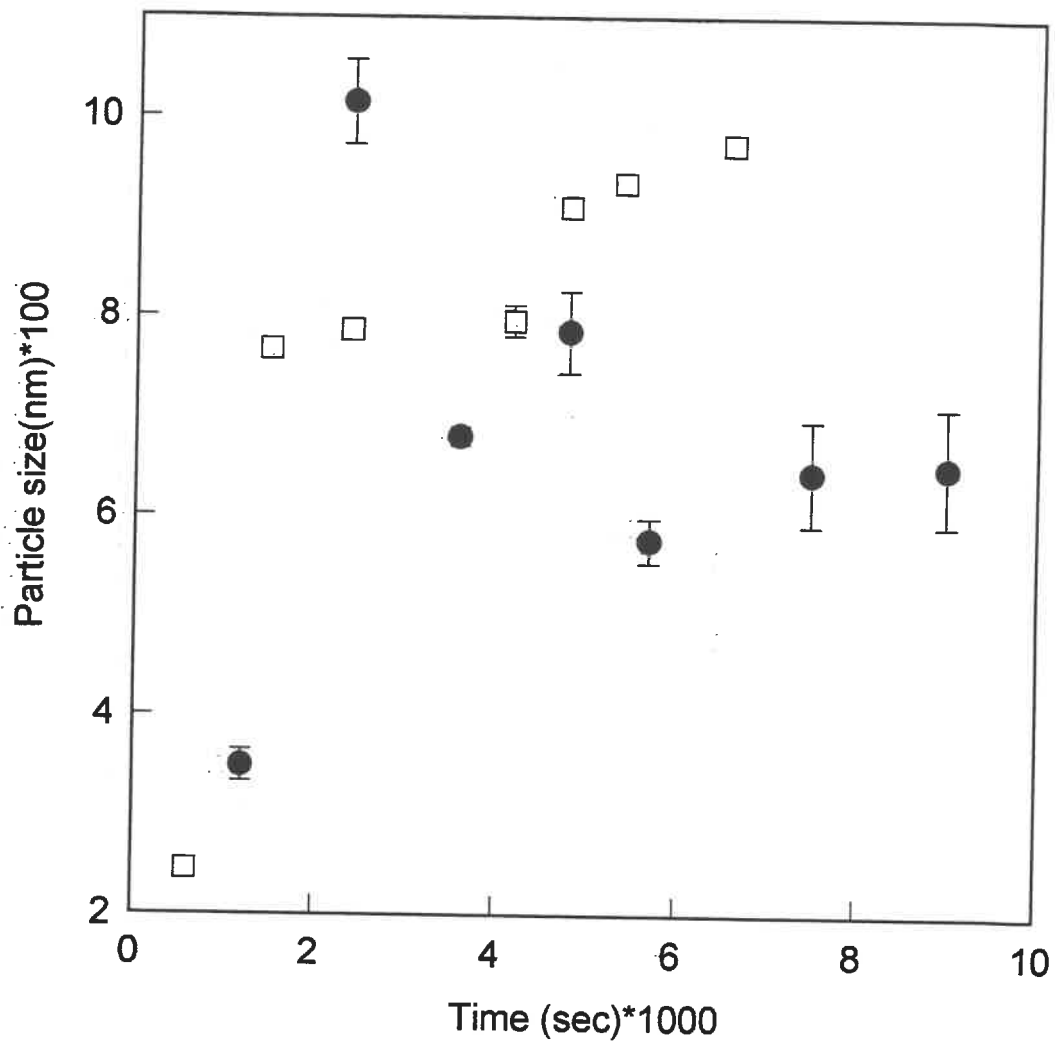


Figure 3.9.1 - Effect of speed on the particle size and the appearance of new particles for speeds greater than 400rpm at 70°C and $[I] = 3.0g$.

- exp. D - 400 rpm;
- exp. H - 500 rpm.

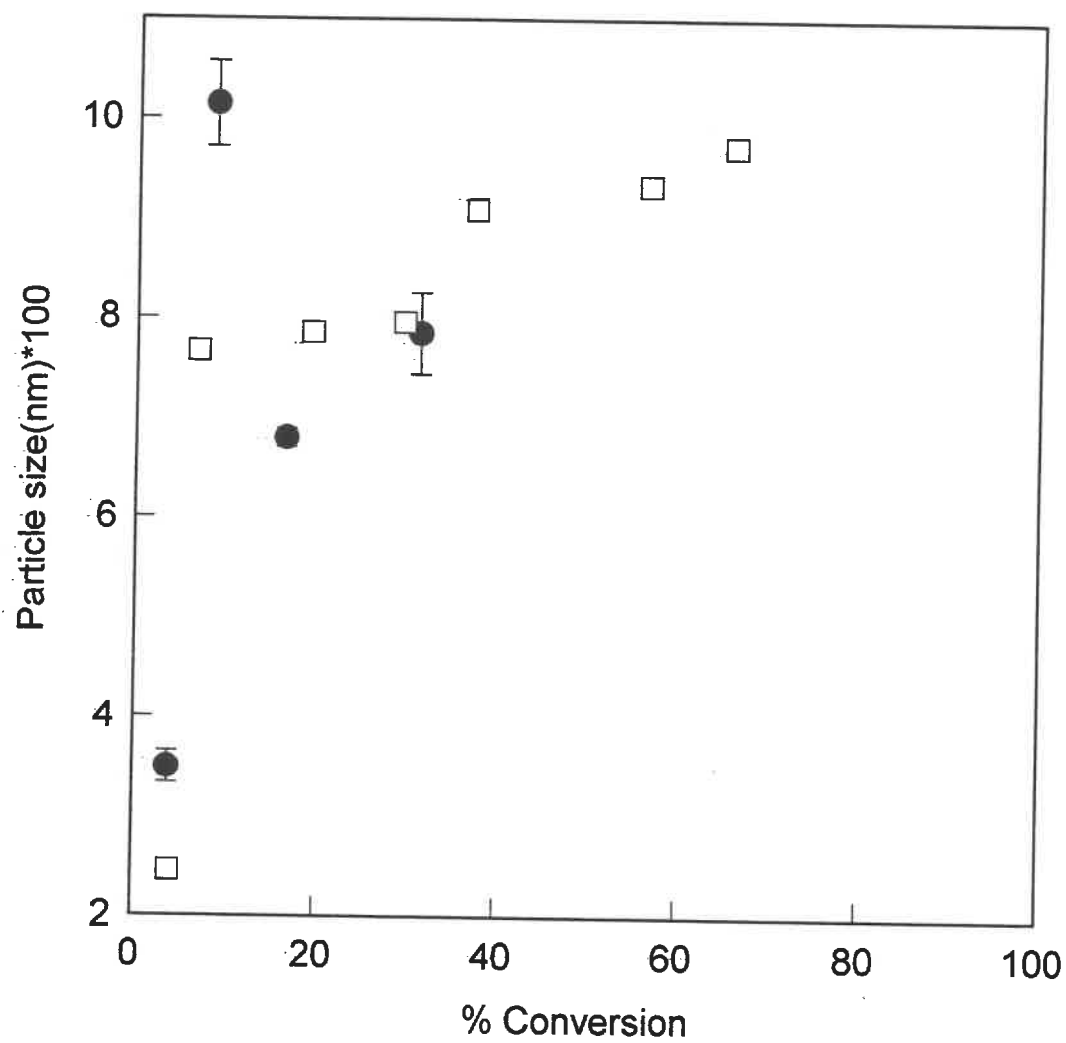


Figure 3.9.2 - Effect of speed on the particle size and the appearance of new particles for speeds greater than 400rpm at 70°C and $[I] = 3.0g$.

- exp. D - 400 rpm;
- exp. H - 500 rpm.

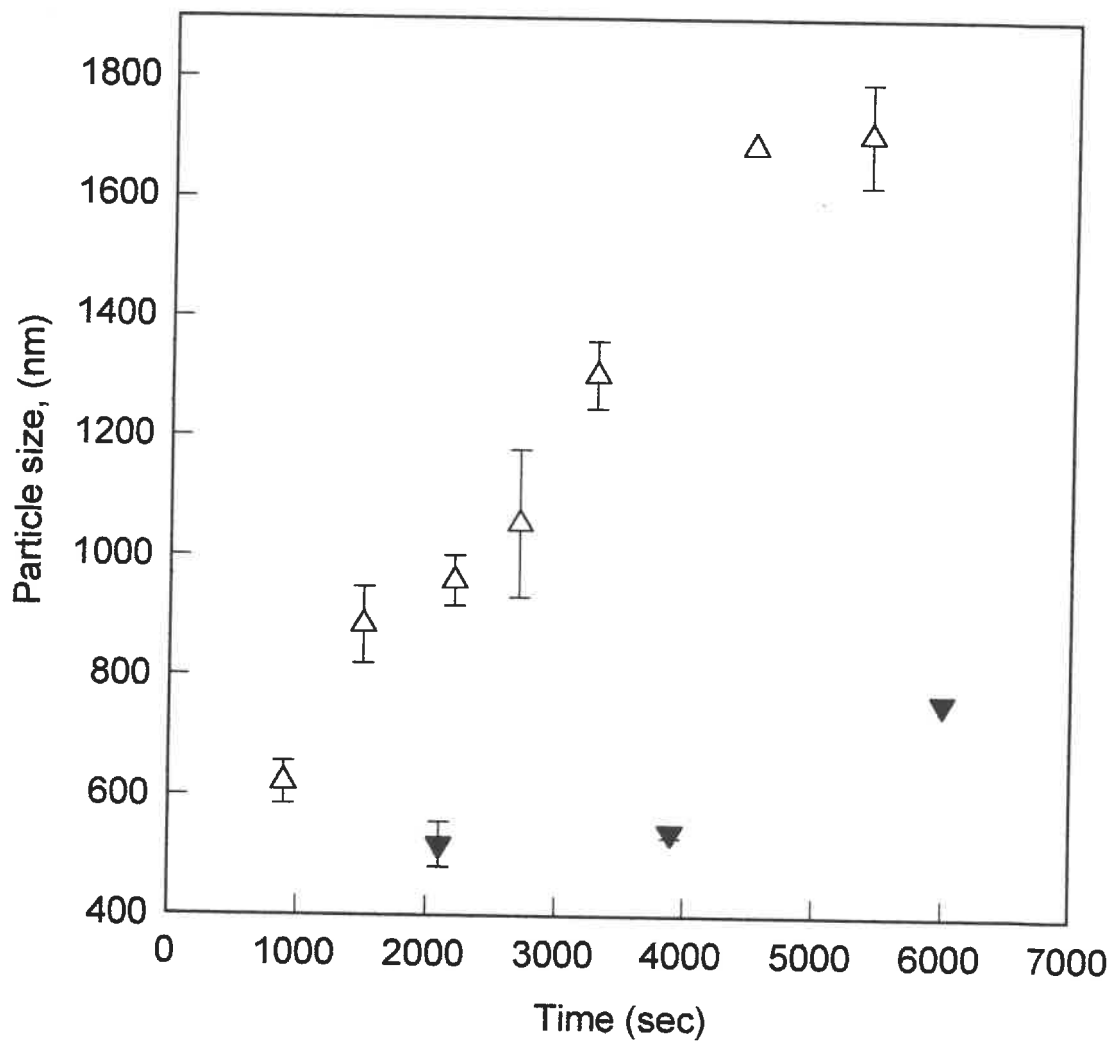


Figure 3.10.1 - Effect of agitator speed on particle size at 70°C and $[I] = 3.4\text{g}$.

- \triangle exp. A - 400 rpm;
- \blacktriangledown exp. K - 600 rpm.

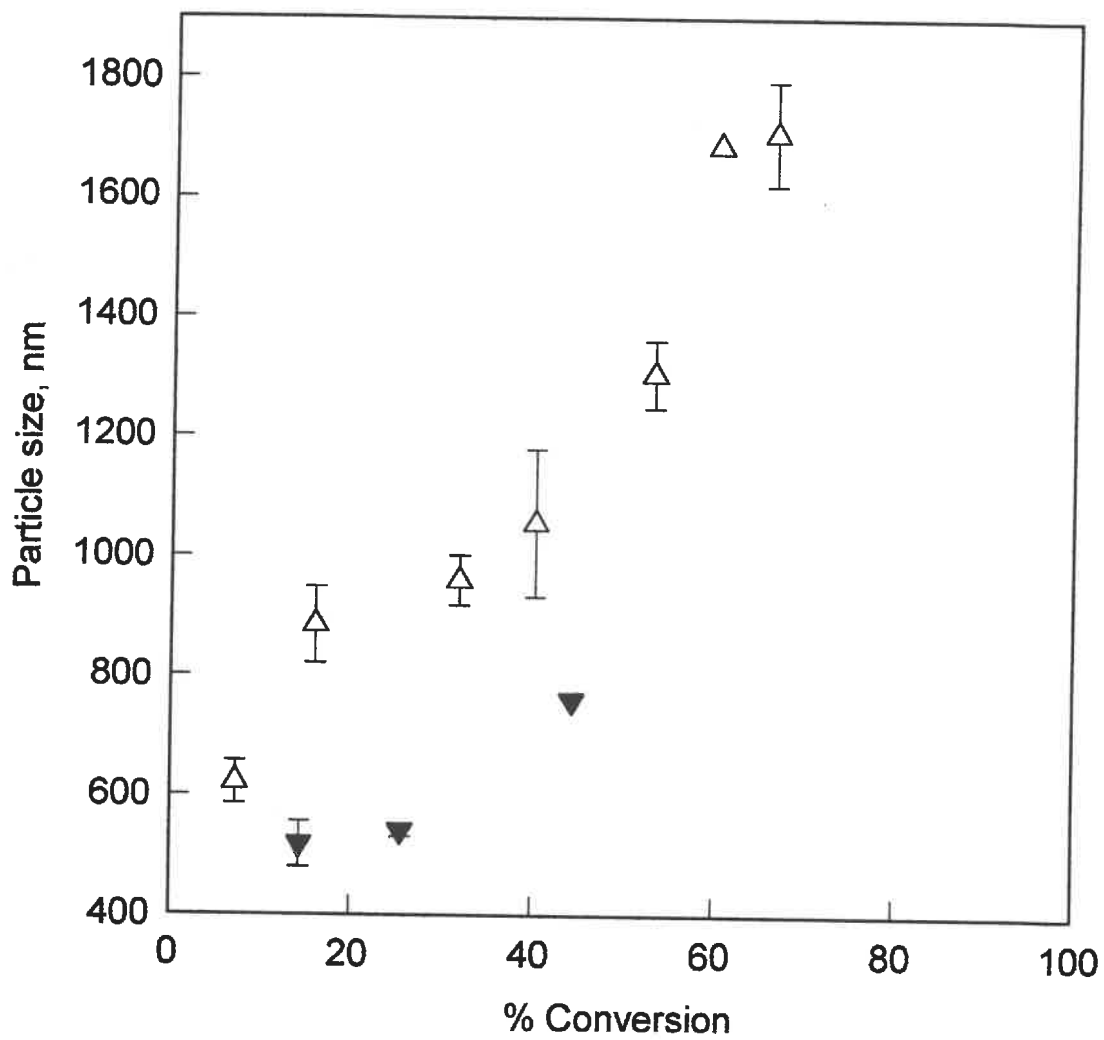


Figure 3.10.2 - Effect of agitator speed on particle size at 70⁰C and

[I] = 3.4g.

△ exp. A - 400 rpm

▼ exp. K - 600 rpm

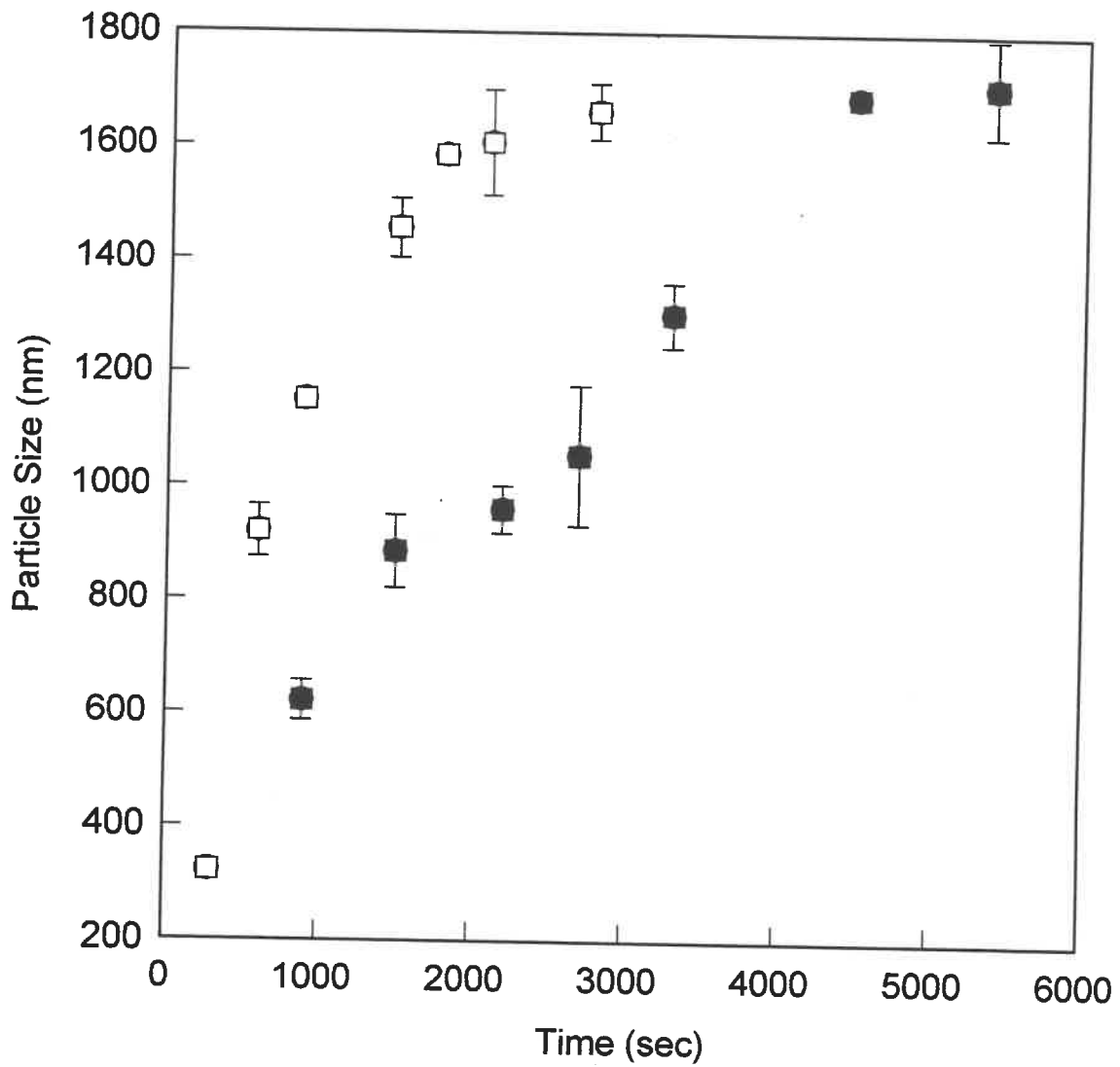


Figure 3.11.1- Effect of temperature on polymer particle size
at 400rpm and $[I] = 3.41\text{g}$.

- exp. A - 70°C
- exp. B - 80°C

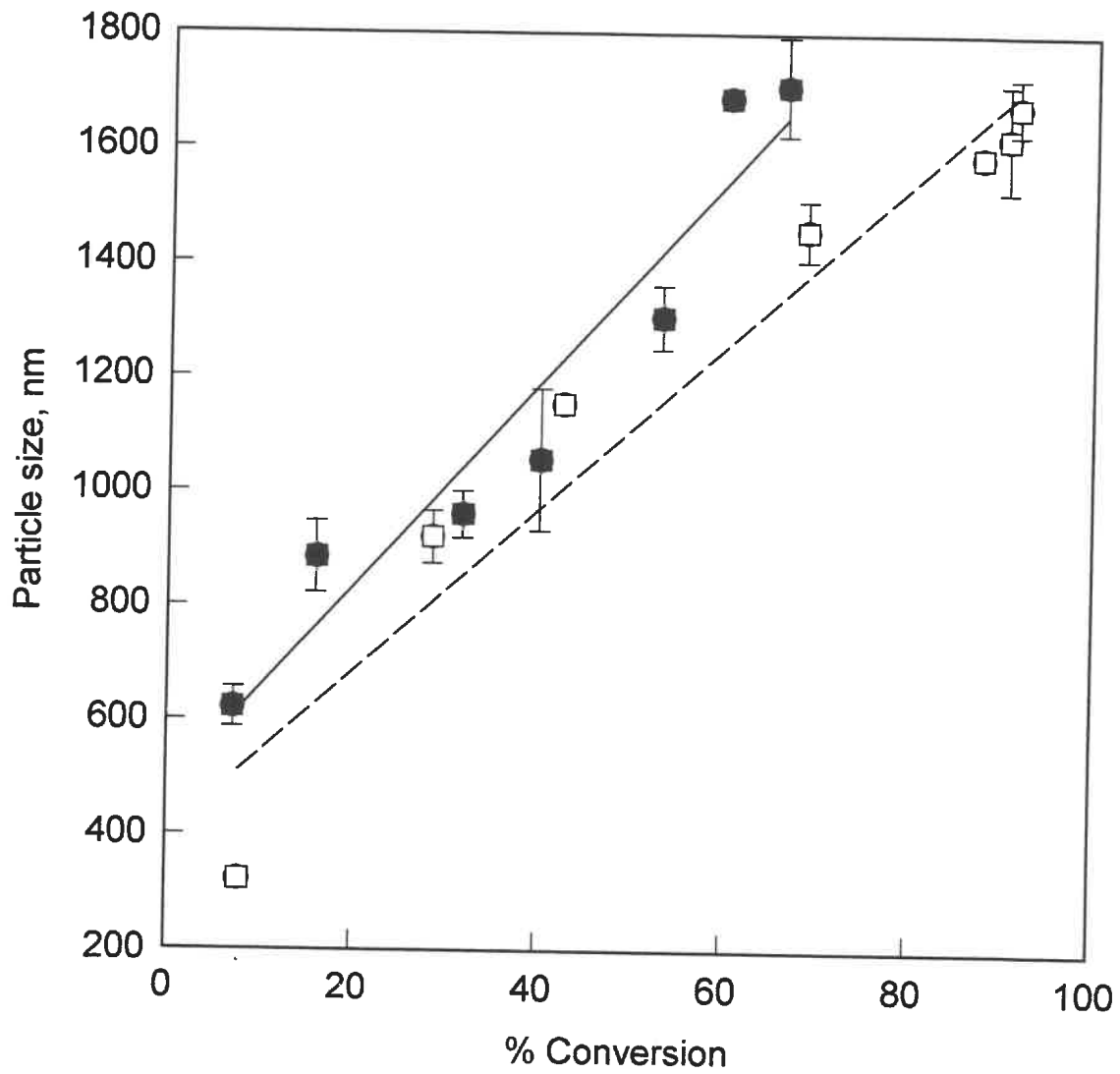


Figure 3.11.2 - Variation of particle size for different temperatures with respect to conversion at 400rpm and $[I] = 3.4g$.

- exp. A - 70°C
- exp. B - 80°C

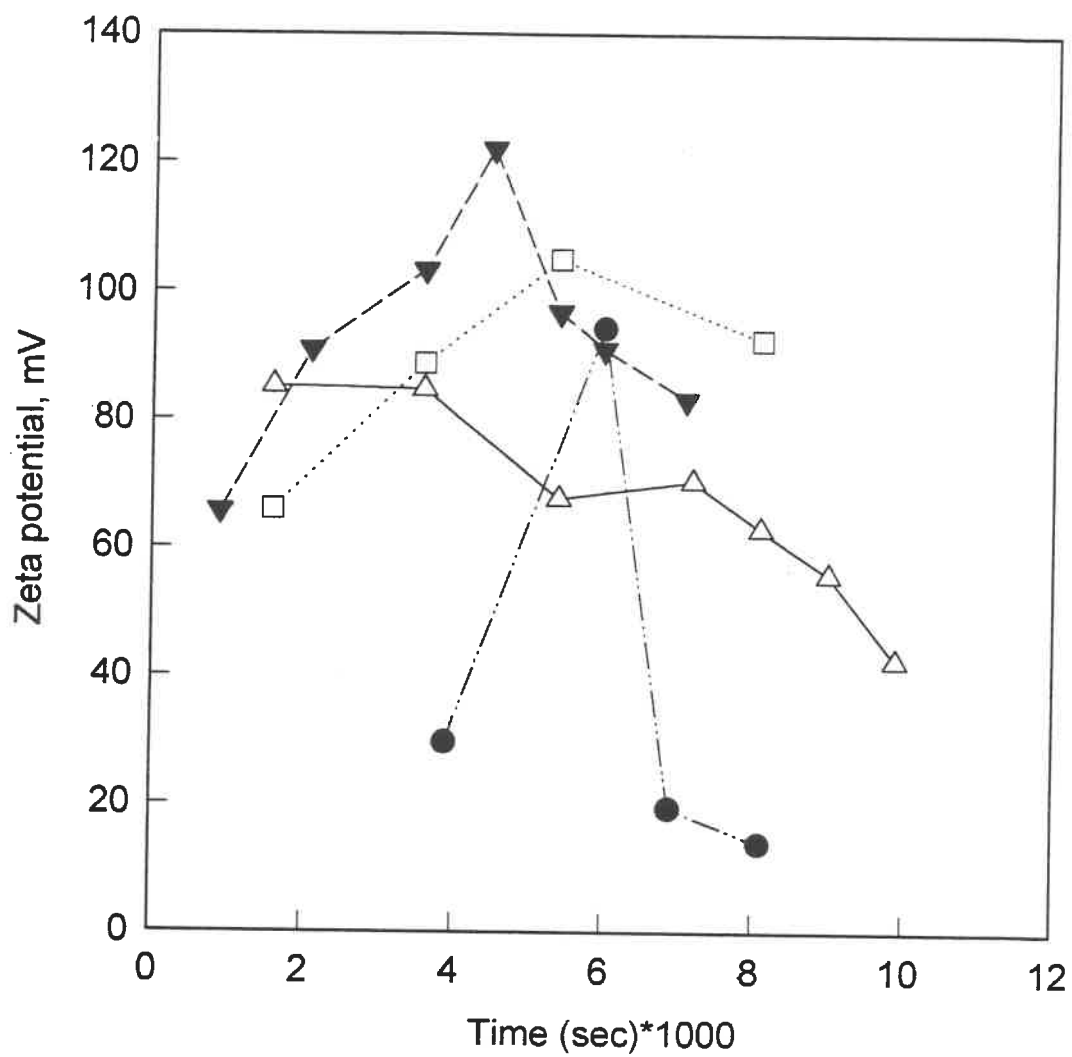


Figure 3.12.1 - Effect of initiator amount on the zeta potential at 600 rpm and 70⁰ C.

- exp. K - [I] = 3.5 g.;
- △ exp. N - [I] = 3.7 g.;
- exp. L - [I] = 3.8 g.;
- ▼ exp. M - [I] = 4.0 g.

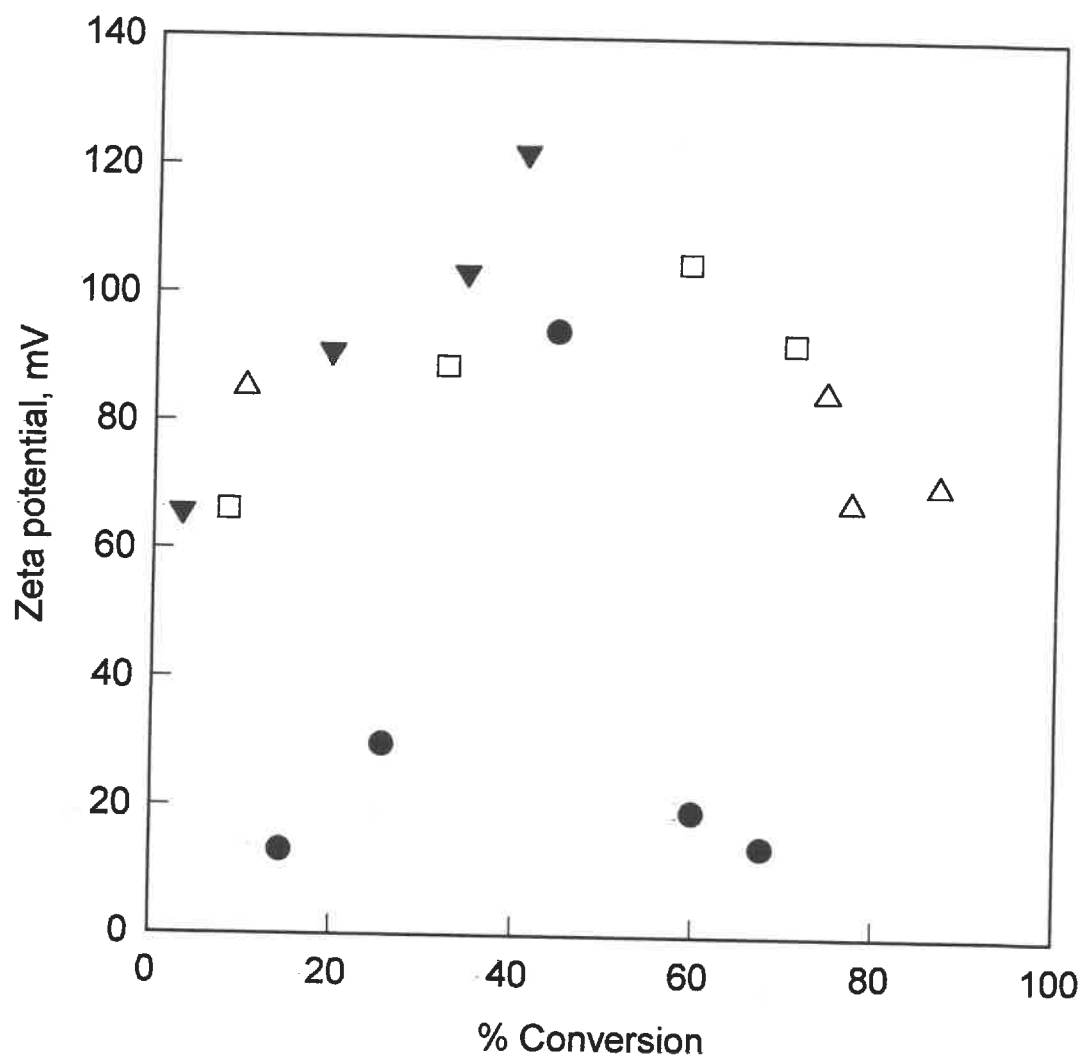


Figure 3.12.2 - Variation of zeta potential with conversion for different amounts of initiator at 600 rpm and 70°C.

- exp. K - [I] = 3.5g.;
- △ exp. N - [I] = 3.7g.;
- exp. L - [I] = 3.8g.;
- ▼ exp. M - [I] = 4.0g.

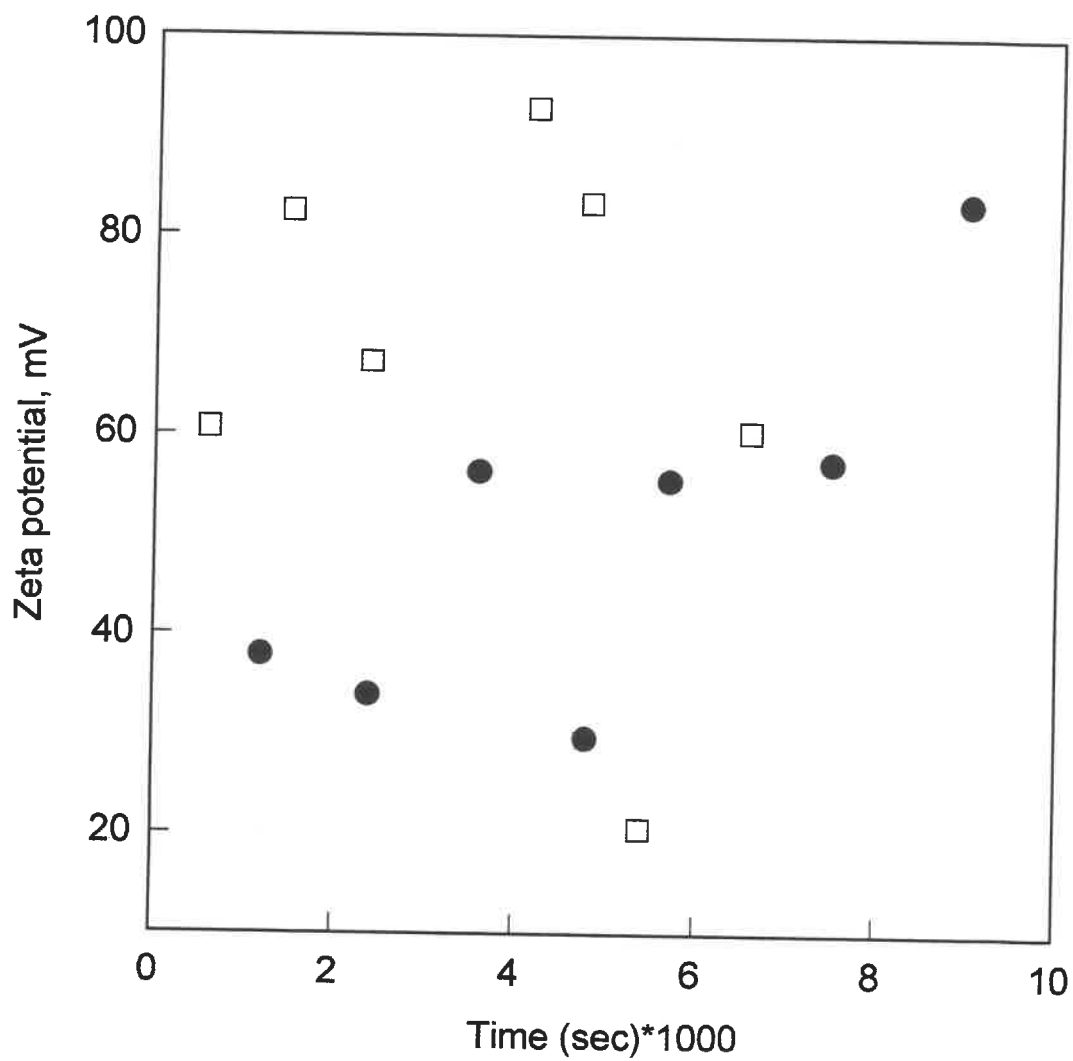


Figure 3.13.1 - Effect of speed on the zeta potential at 70°C and $[I] = 3.0\text{g}$.

□ exp. D - 400 rpm;

● exp. H - 500 rpm.

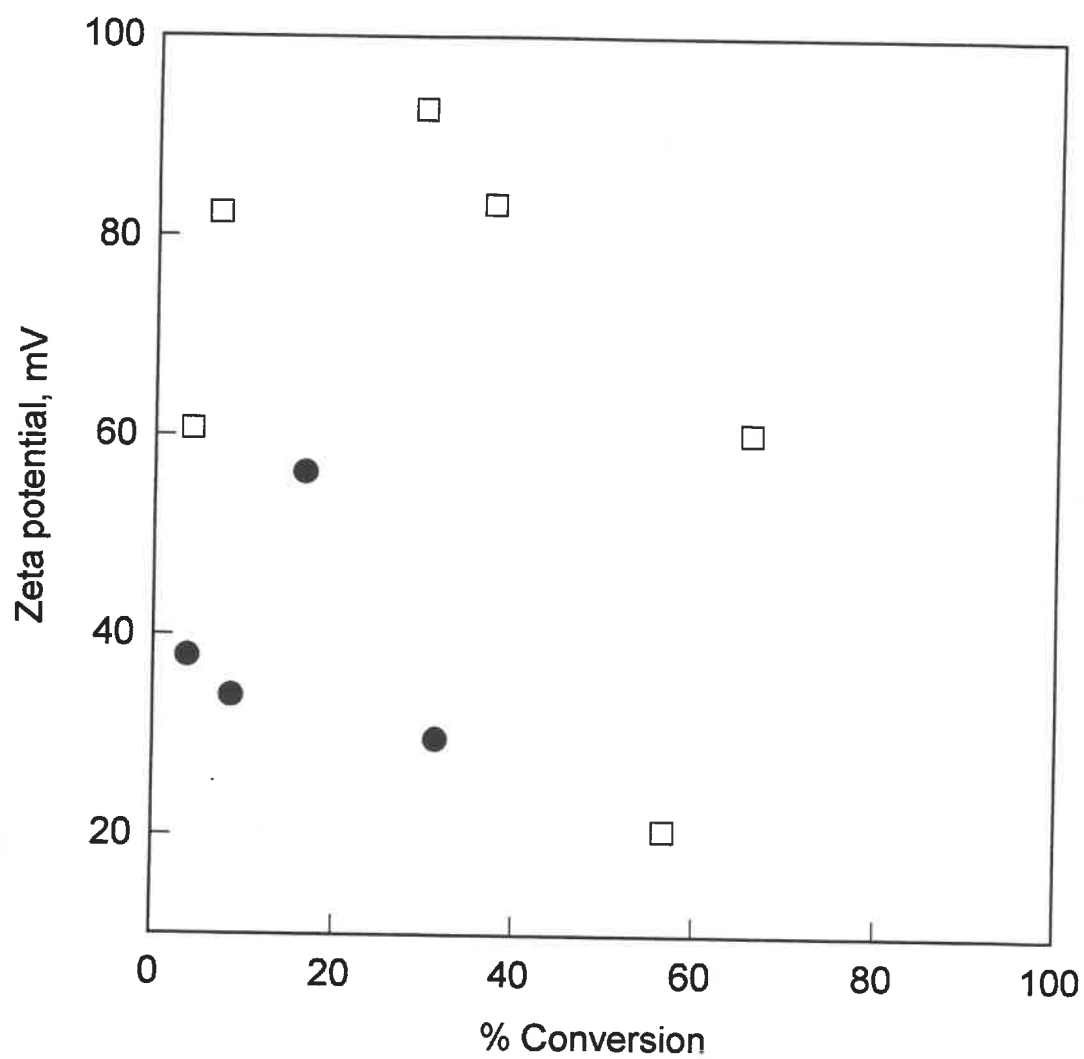


Figure 3.13.2 - Effect of speed on the zeta potential at 70°C and $[I] = 3.0\text{g}$.

- exp. D - 400 rpm;
- exp. H - 500 rpm.

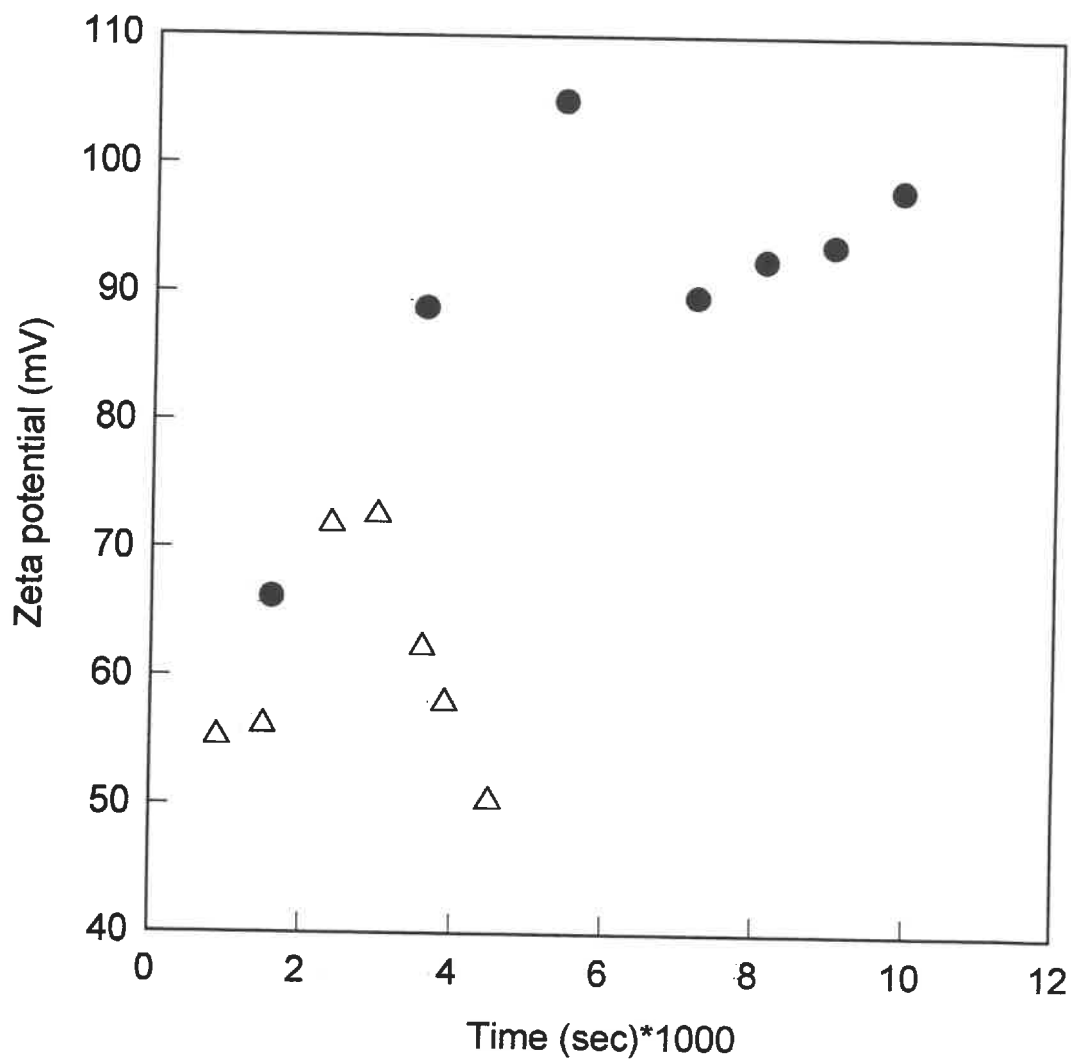


Figure 3.14.1 - Effect of agitator speed on the zeta potential at 70°C and $[I] = 3.8\text{g}$.

△ exp. J - 500 rpm;

● exp. L - 600 rpm

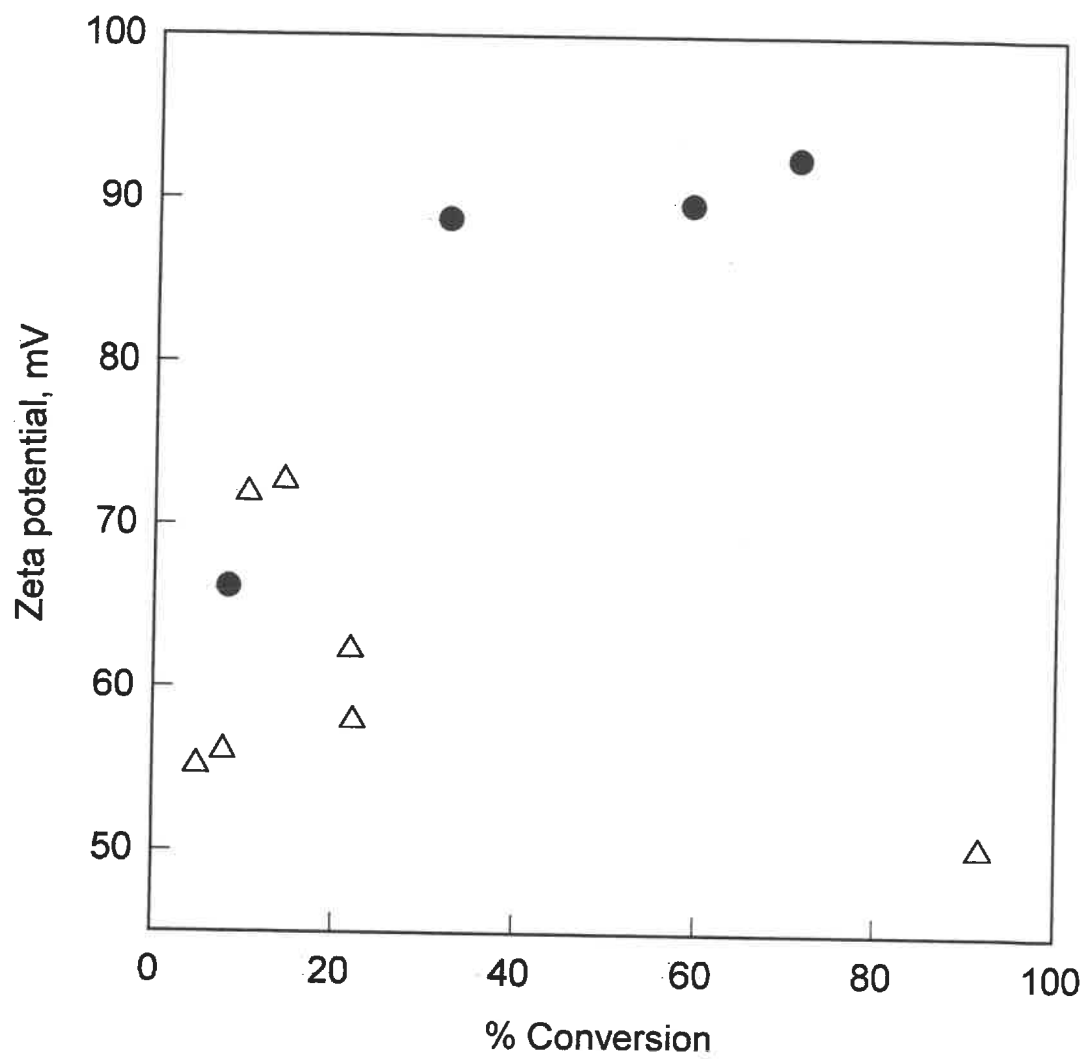


Figure 3.14.2 - Effect of agitator speed on the zeta potential at 70°C and $[I] = 3.8\text{g}$.

\triangle exp. J - 500 rpm;

\bullet exp. L - 600 rpm.

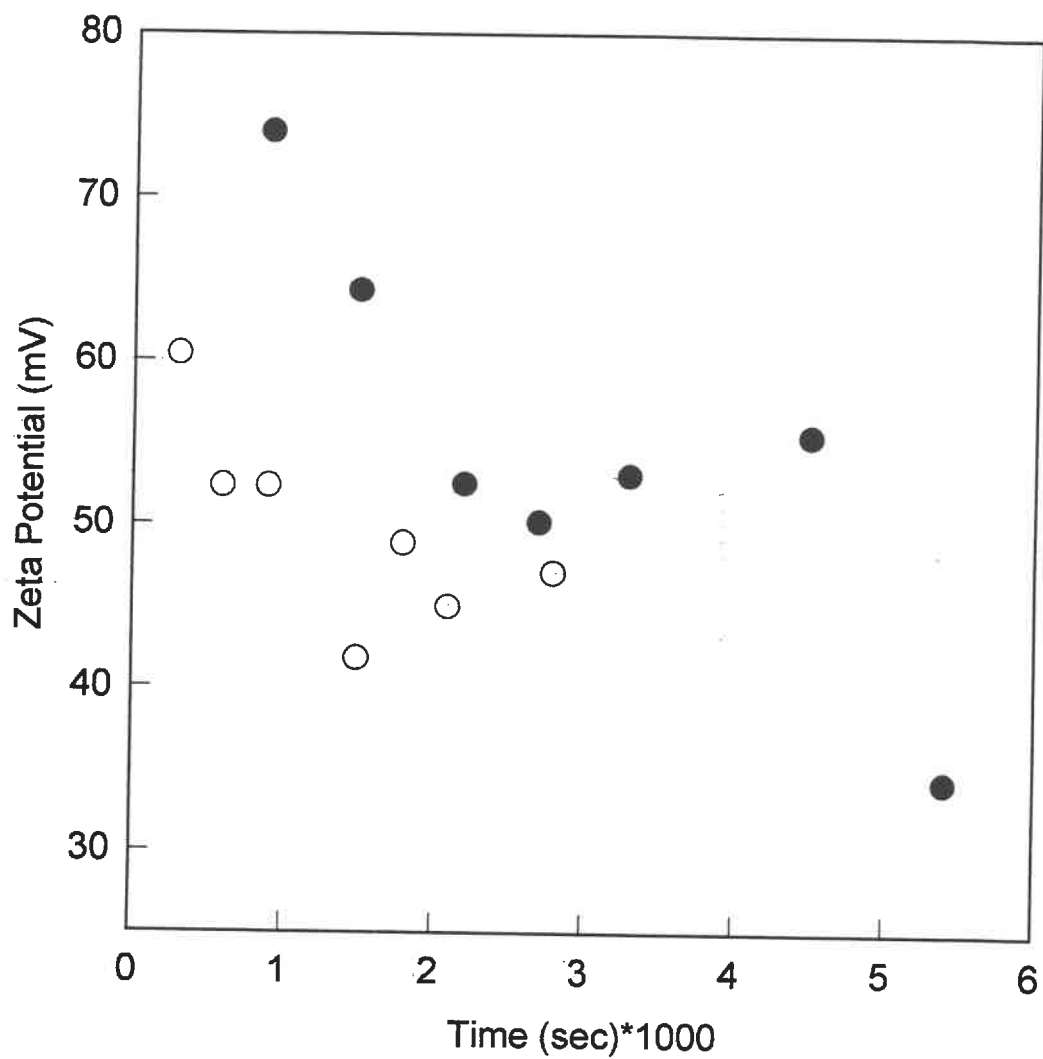


Figure 3.15.1 - Effect of temperature variation on the zeta potential

at 400 rpm and $[I] = 3.41\text{g}$.

- exp. A - 70°C
- exp. B - 80°C

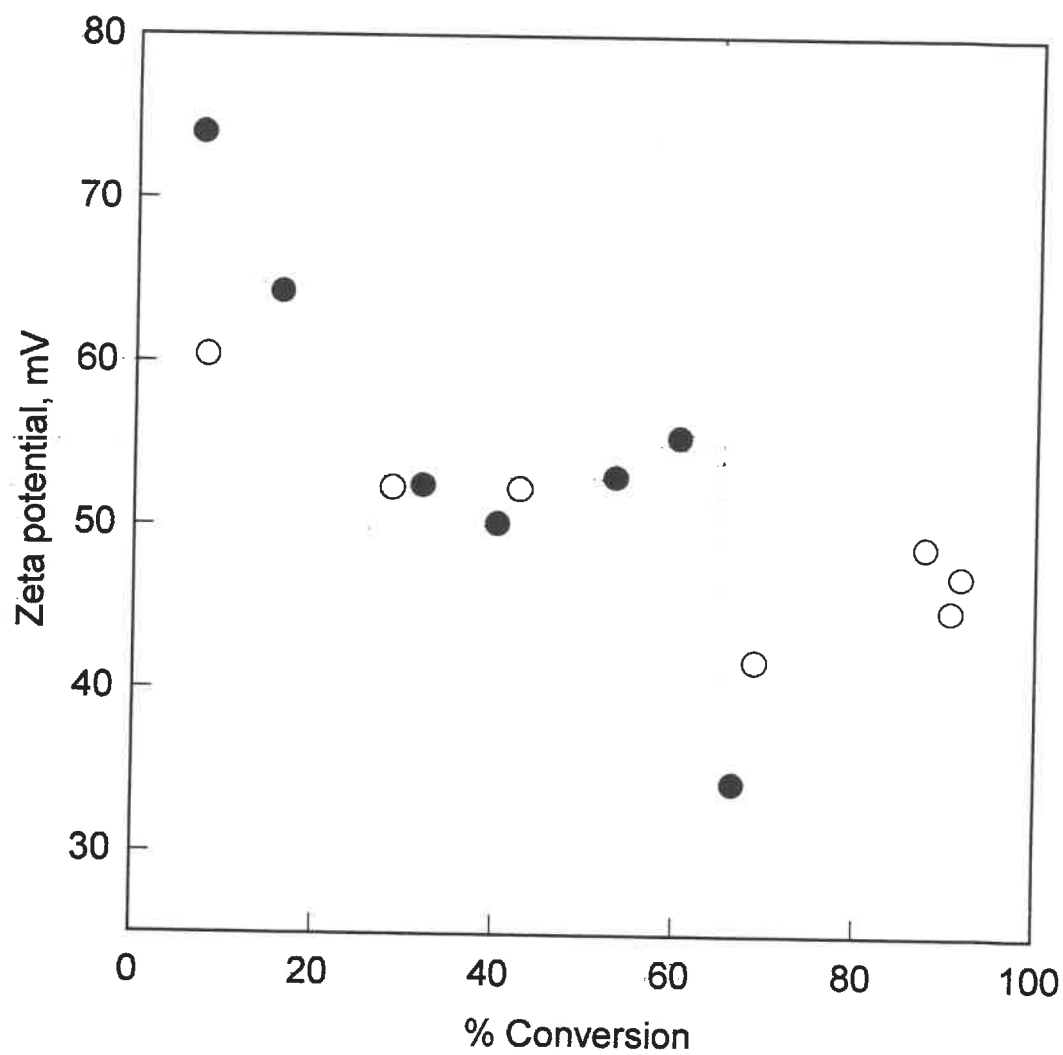


Figure 3.15.2 - Effect of temperature on the zeta potential at 400rpm and $[I] = 3.41\text{g}$.

- exp. A - 70°C
- exp. B - 80°C

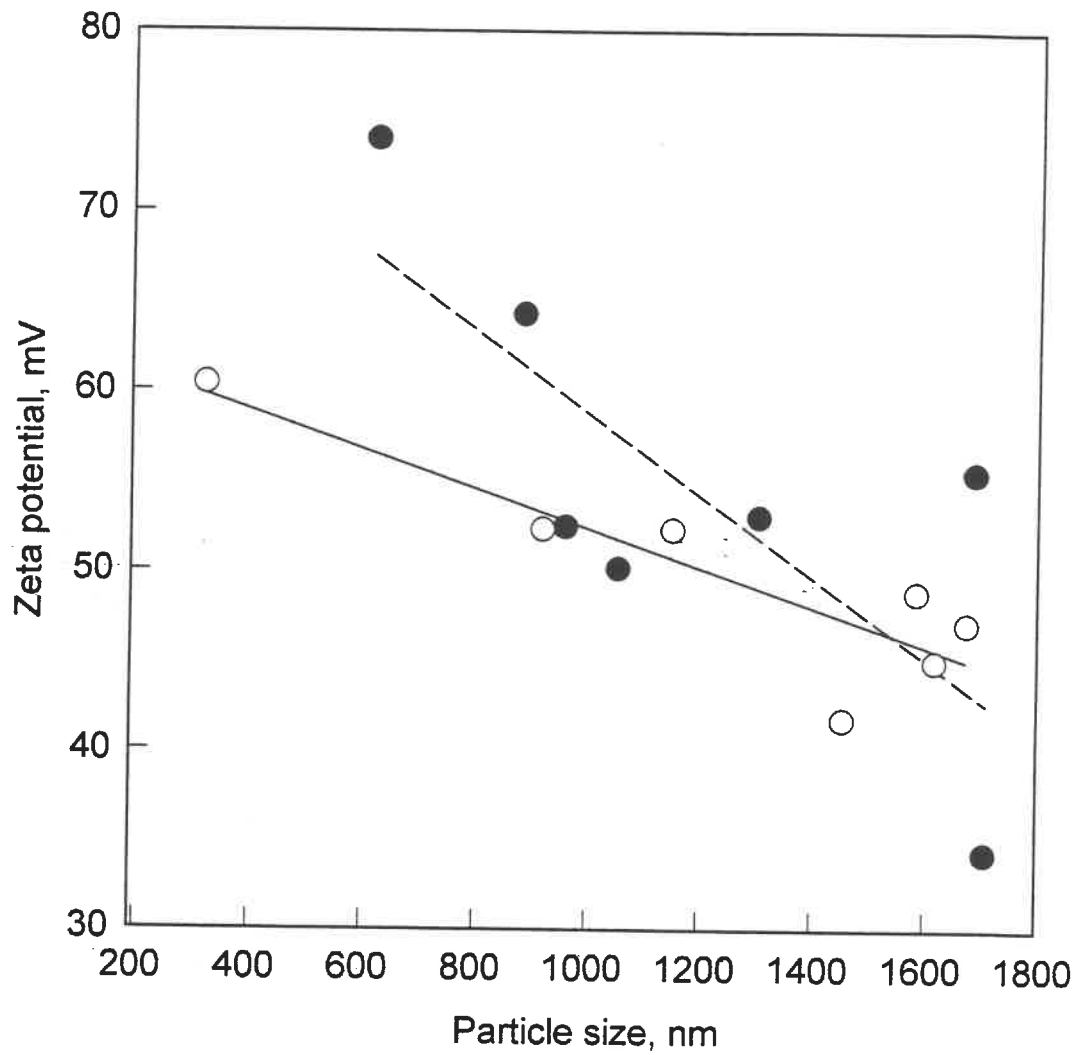


Figure 3.16 - Variation of particle size with zeta potential at 400rpm and $[I] = 3.41\text{g}$ for different temperatures.

- exp. A - 70°C
- exp. B - 80°C

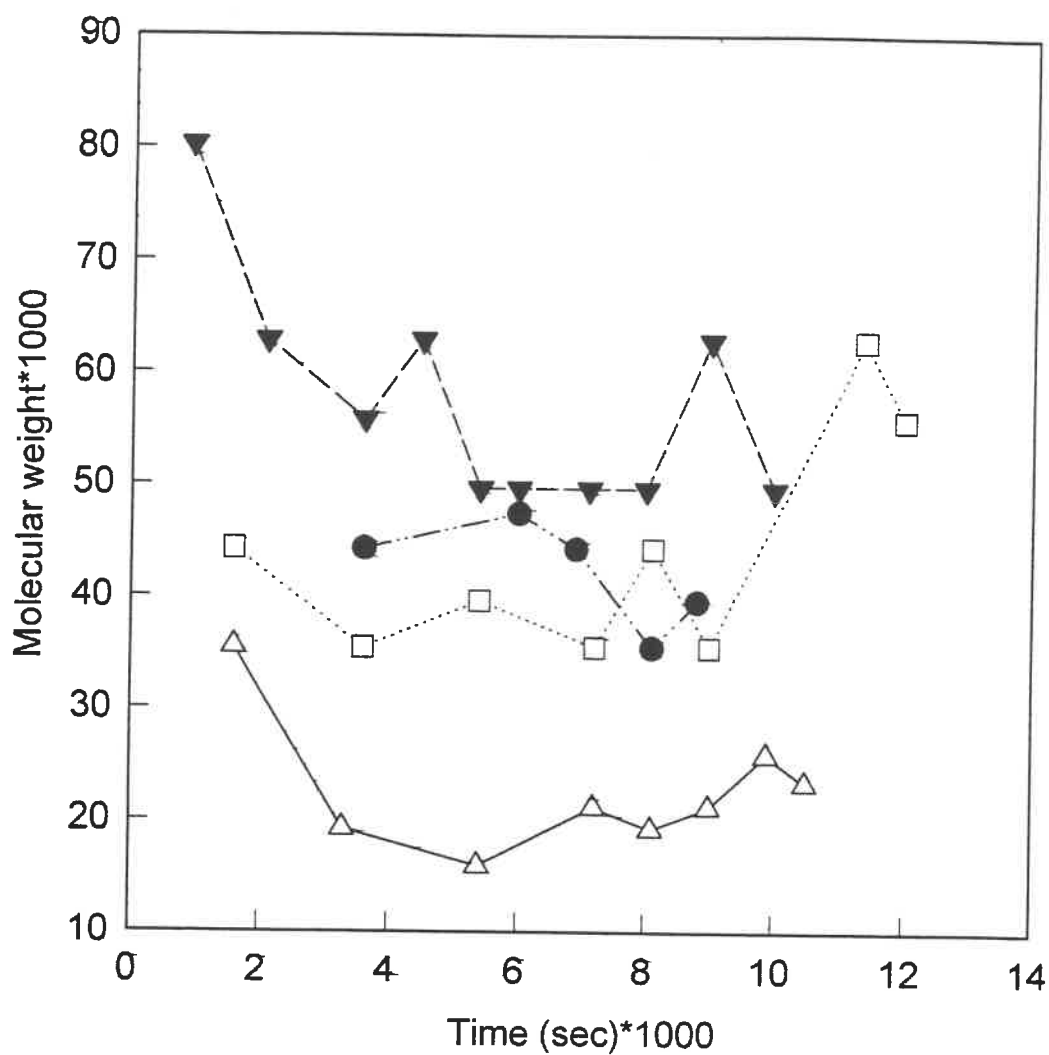


Figure 3.17.1 - Effect of amount of initiator on the molecular weight at 600 rpm and 70⁰C.

- exp. K - [I] = 3.5 g.;
- △ exp. N - [I] = 3.7 g.;
- exp. L - [I] = 3.8 g.;
- ▼ exp. M - [I] = 4.0 g.

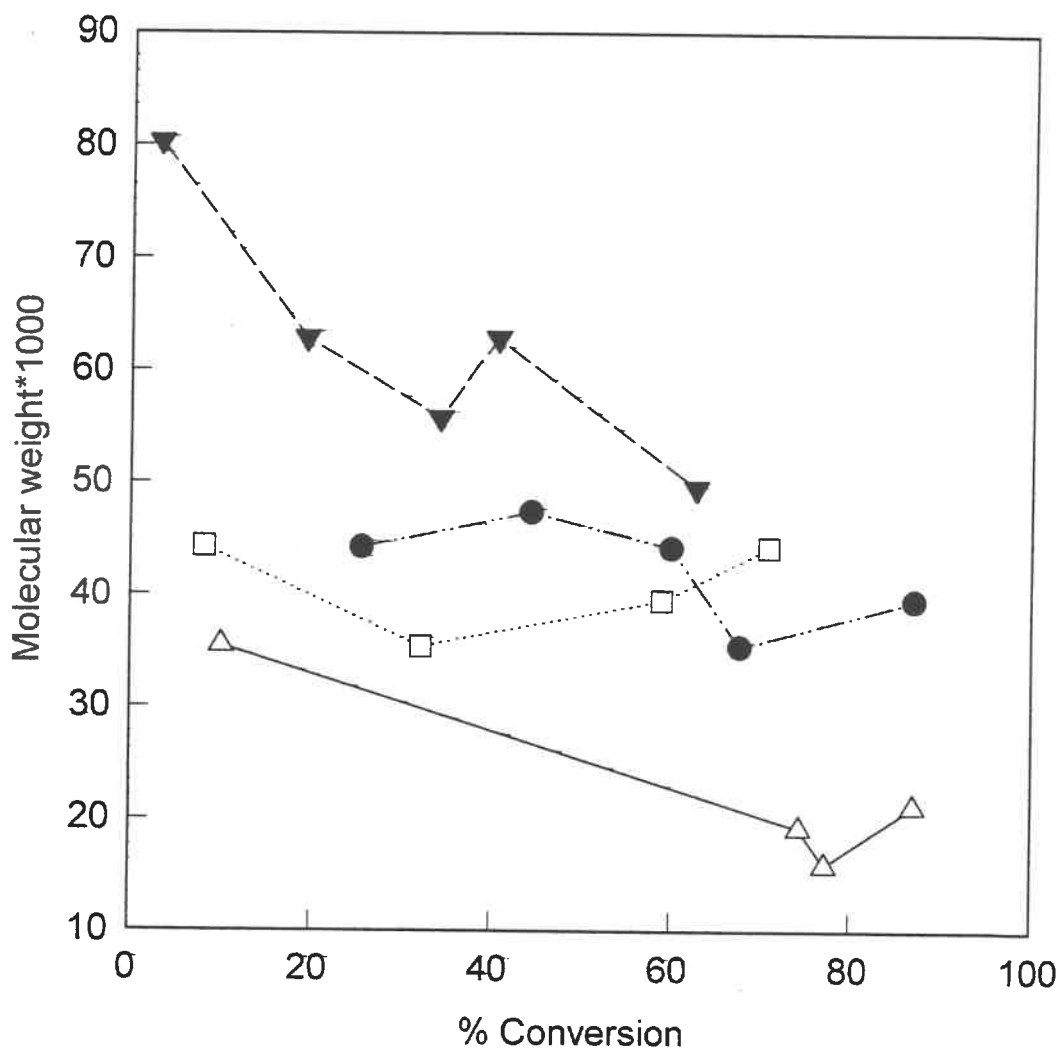


Figure 3.17.2 - Effect of amount of initiator on the molecular weight with respect to the conversion at 600rpm and 70°C.

- exp. K - [I] = 3.5 g.;
- △ exp. N - [I] = 3.7 g.;
- exp. L - [I] = 3.8 g.;
- ▼ exp. M - [I] = 4.0 g.

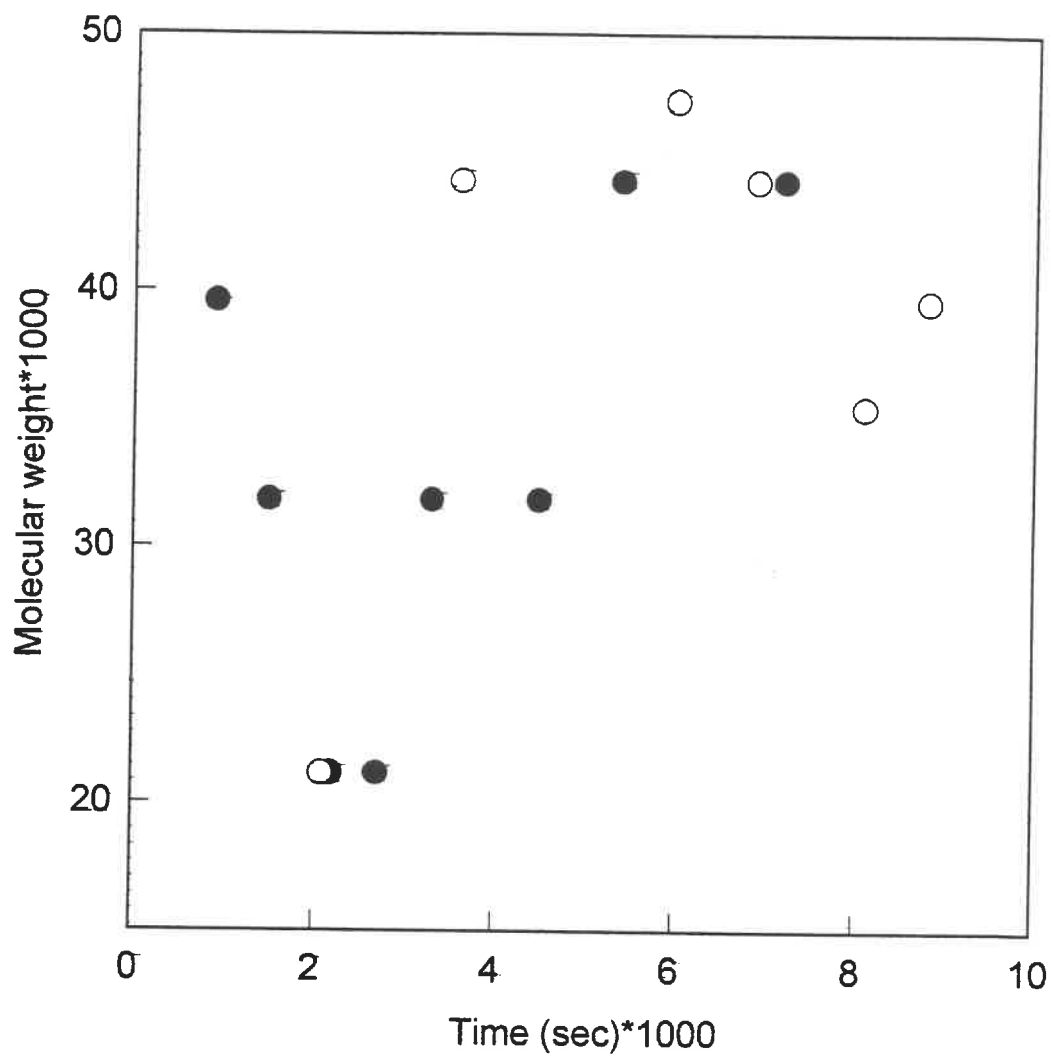


Figure 3.18.1- Effect of speed on the molecular weight at 70°C and $[I] = 3.4\text{g}$.

- exp. A - 400 rpm
- exp. K - 600 rpm

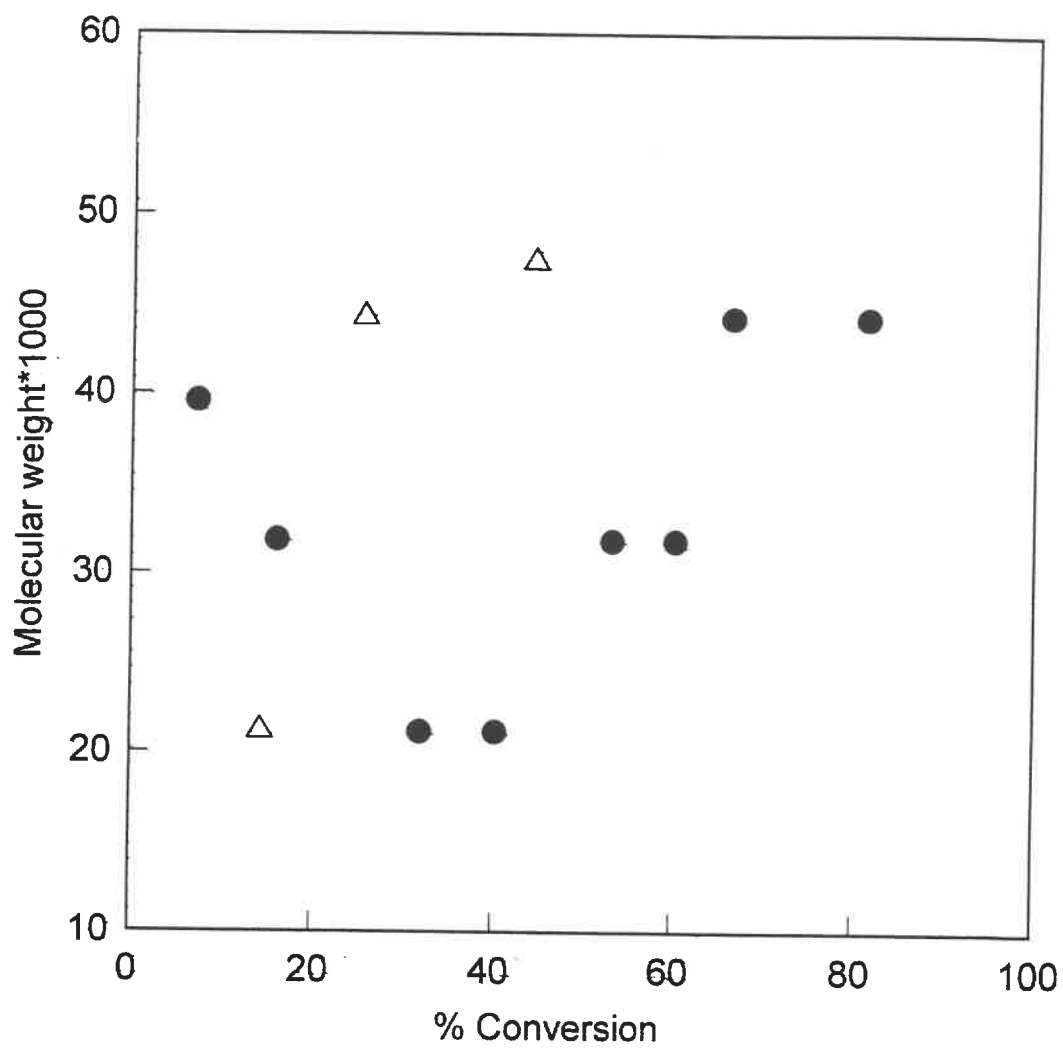


Figure 3.18.2 - Effect of speed on the molecular weight with respect to the polymerization conversion at 70°C and $[I] = 3.4\text{g}$.

- exp. A - 400 rpm
- △ exp. K - 600 rpm

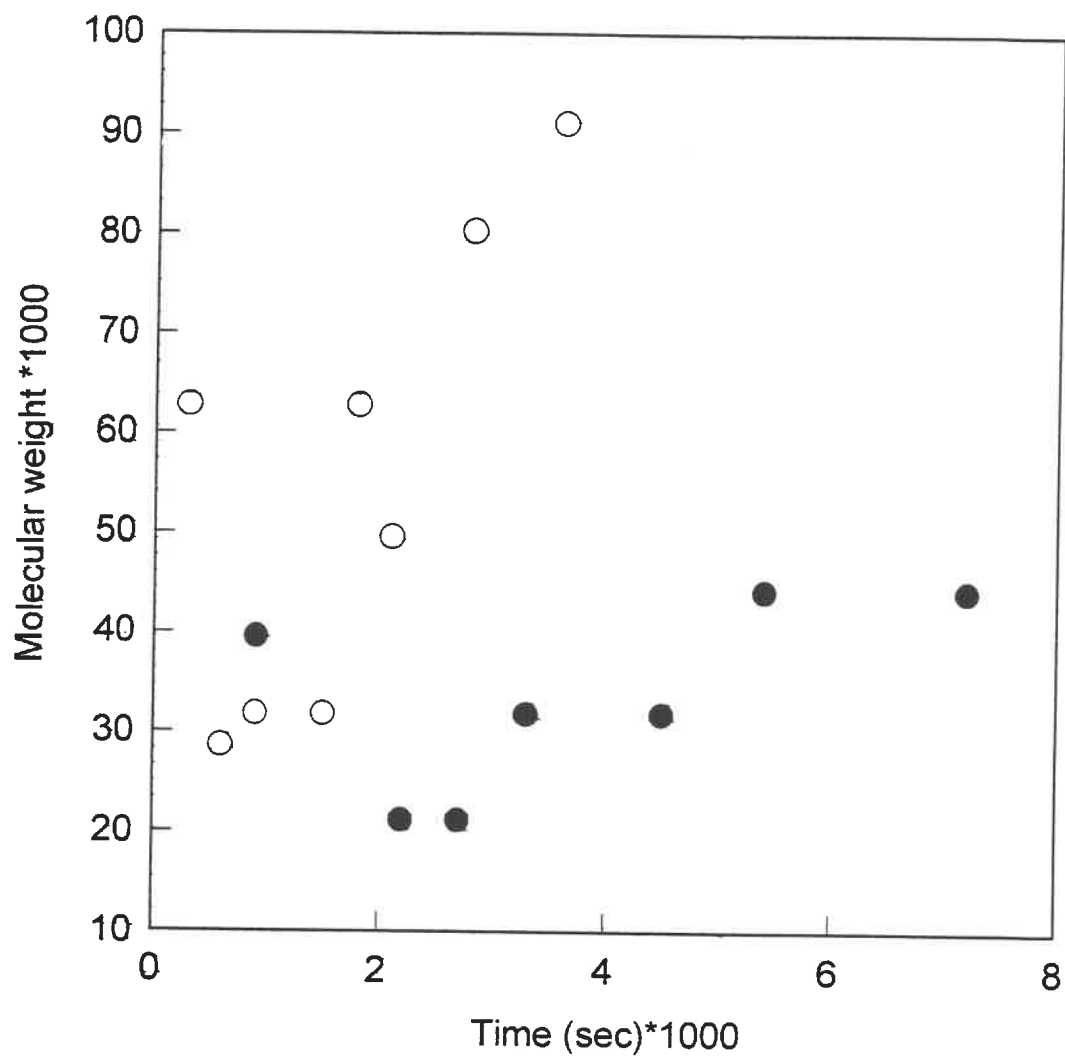


Figure 3.19.1 - Effect of temperature on the molecular weight at 400rpm and $[I]=3.41\text{g}$.

- exp. A - 70°C
- exp. B - 80°C

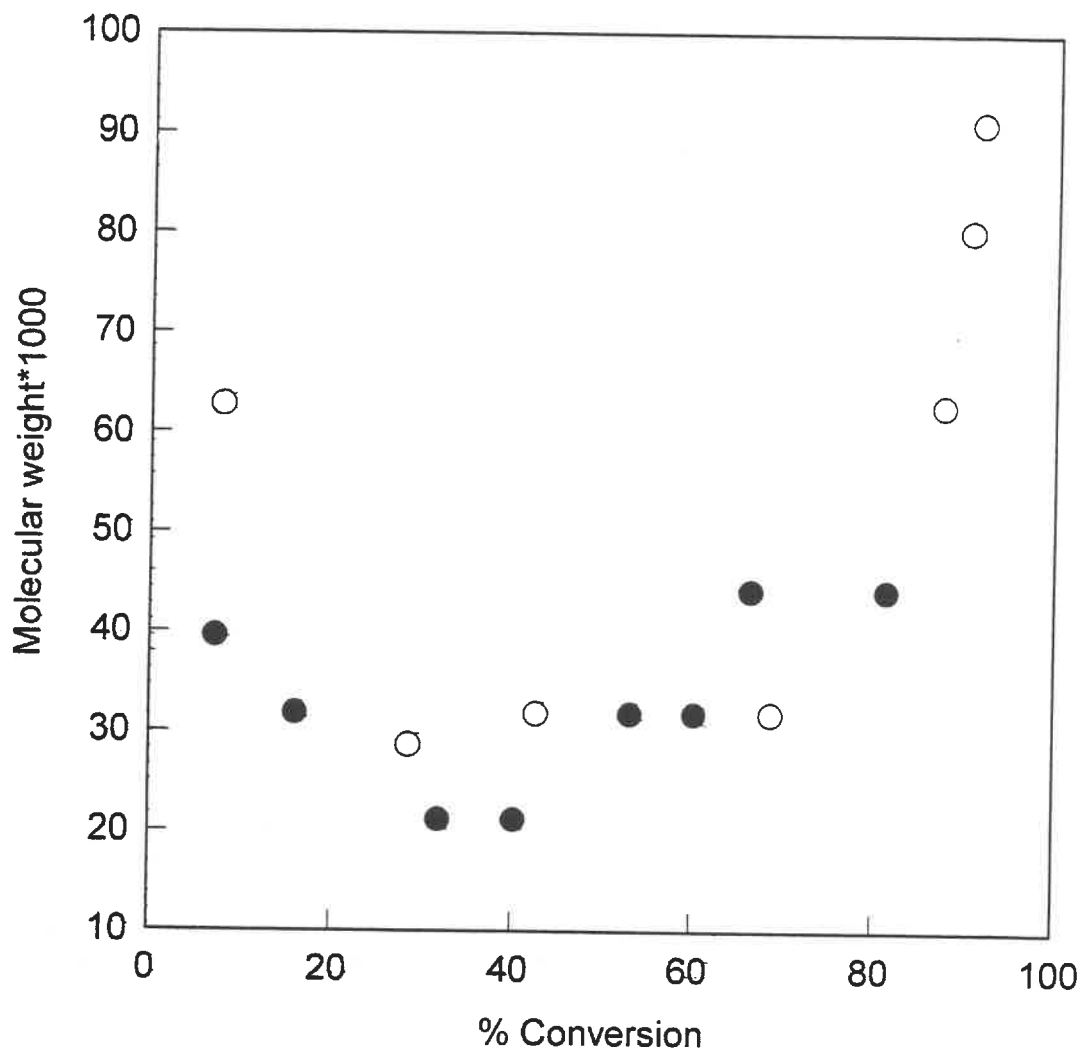
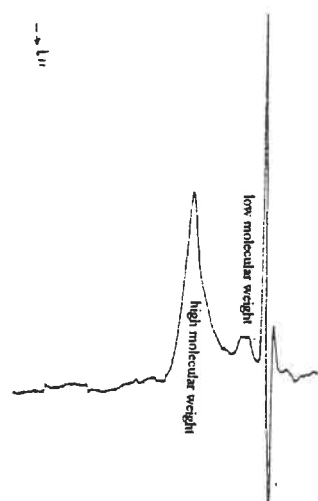
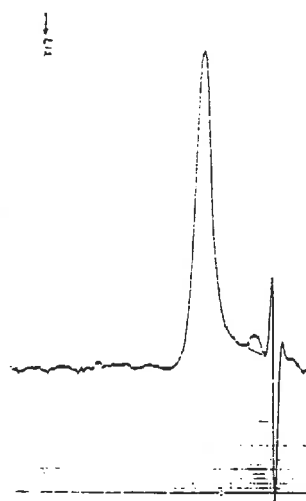


Figure 3.19.2 - Effect of temperature on molecular weight with respect to conversion at 400 rpm and $[I] = 3.4g$.

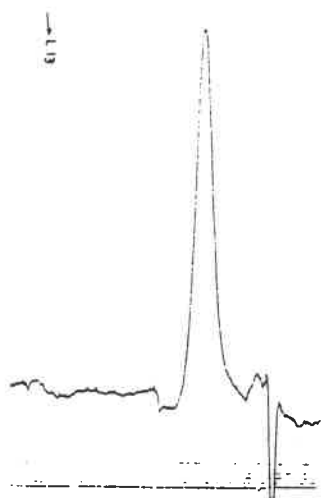
- exp. A - 70°C
- exp. B - 80°C



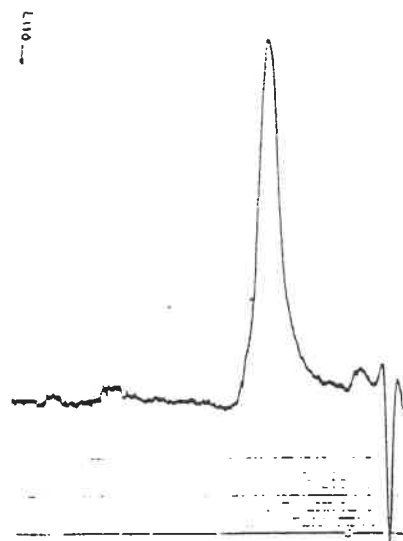
L11 - after 1600 sec



L12 - after 3600 sec



L13 - after 5400 sec



L110 - after 12,200 sec

Figure 3.20 - Typical GPC curves obtained from the emulsifier-free polymerization of n-butyl methacrylate at 600 rpm and $[I] = 3.8\text{g}$. in exp.L

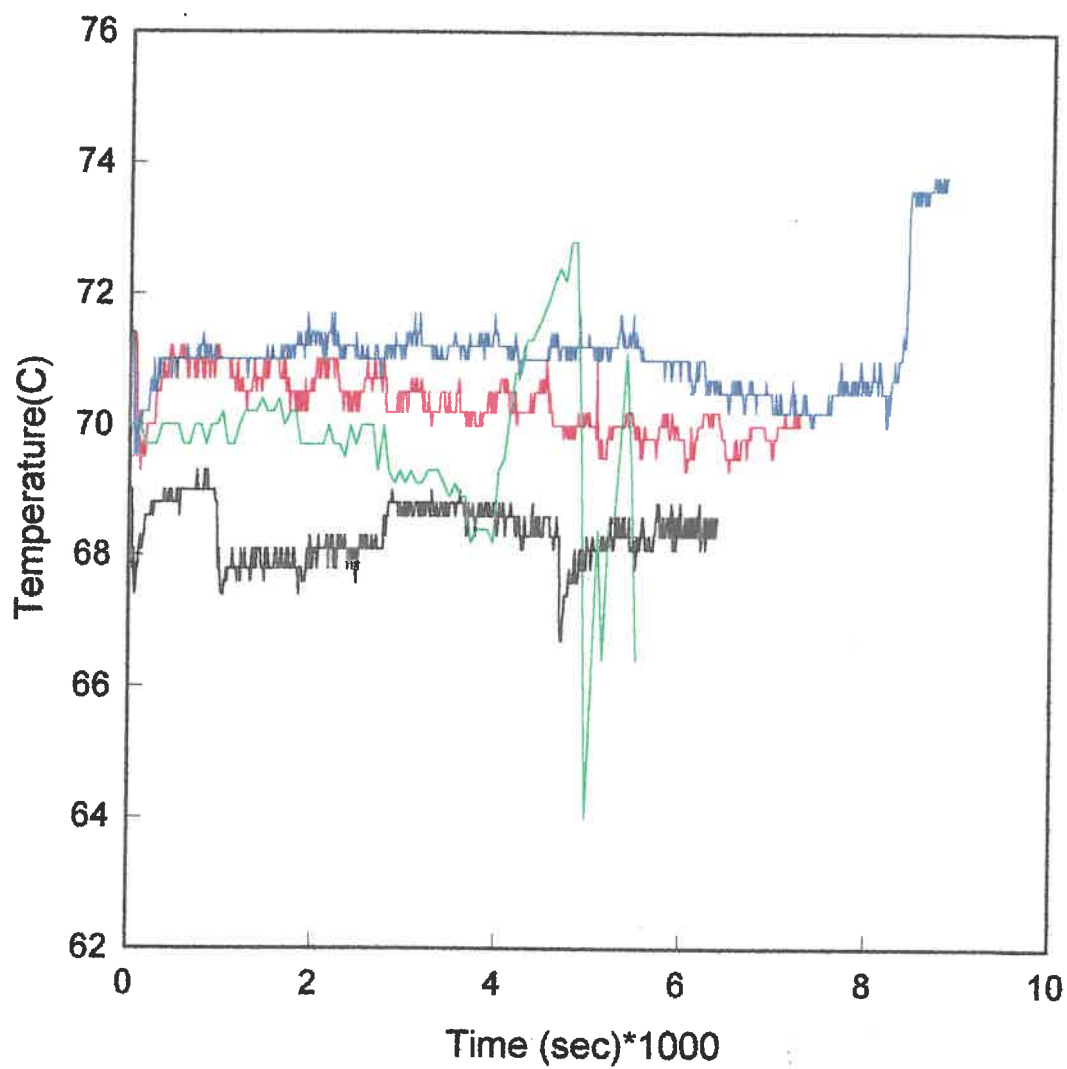


Figure 3.21- Effect of agitator speed on the reaction time and temperature distribution at 70°C for [I]=3.4g.

— 300 rpm — 500 rpm
— 400 rpm — 600 rpm

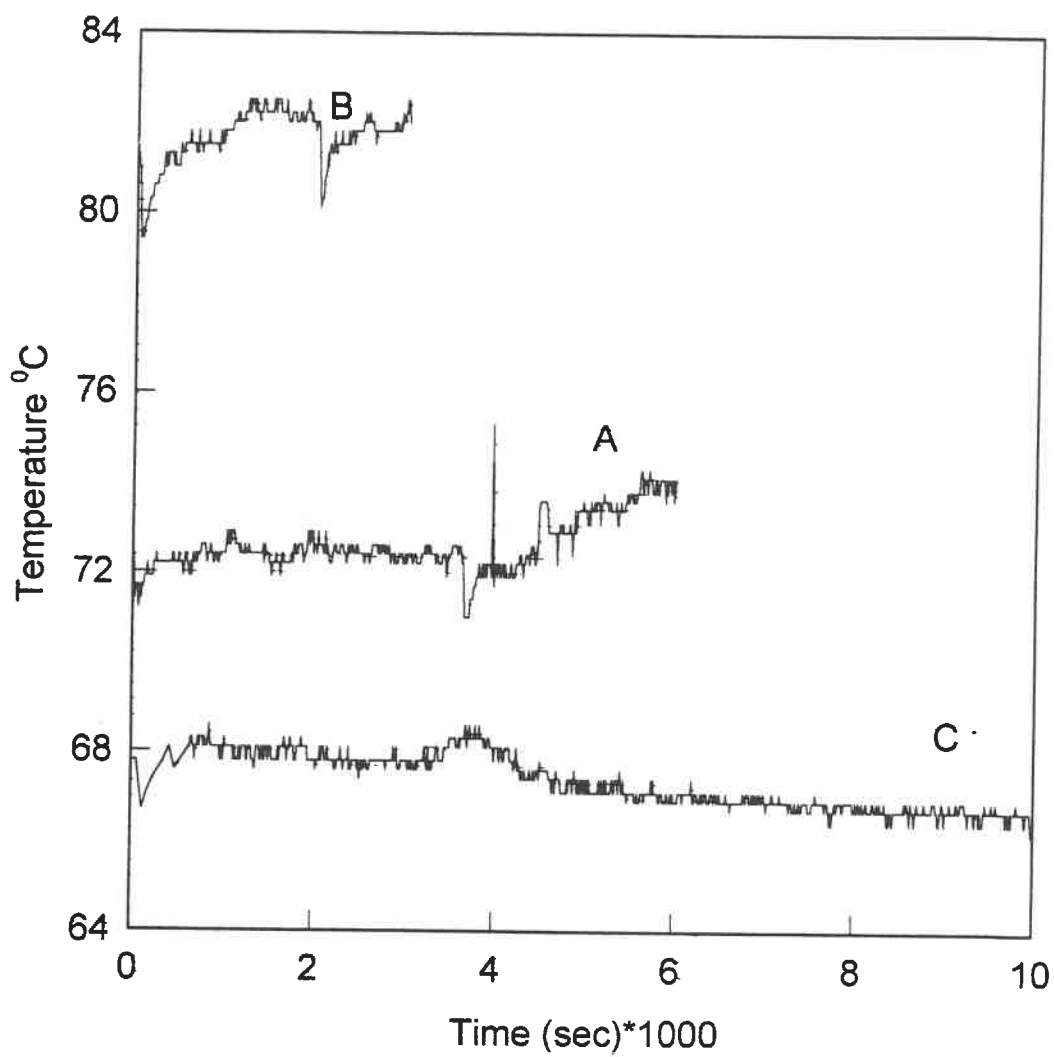


Figure 3.22- Effect of temperature on the reaction time at 400rpm and $[I] = 3.4 \text{ Ig}$.

exp. A - 70°C

exp. B - 80°C

exp. C - 60°C

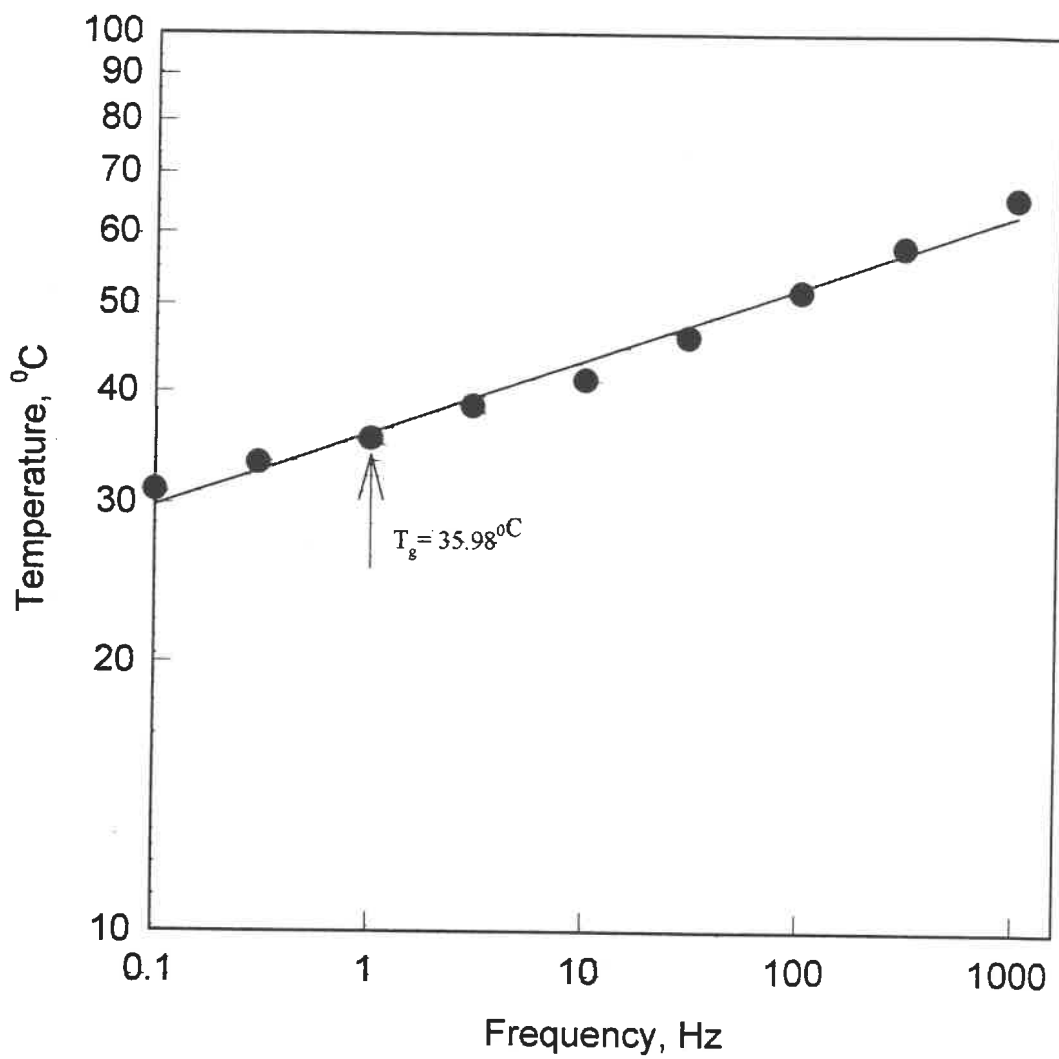


Figure 3.23 - Frequency and temperature data from the DEA instrument for measurement of the T_g of poly n-butylmethacrylate.

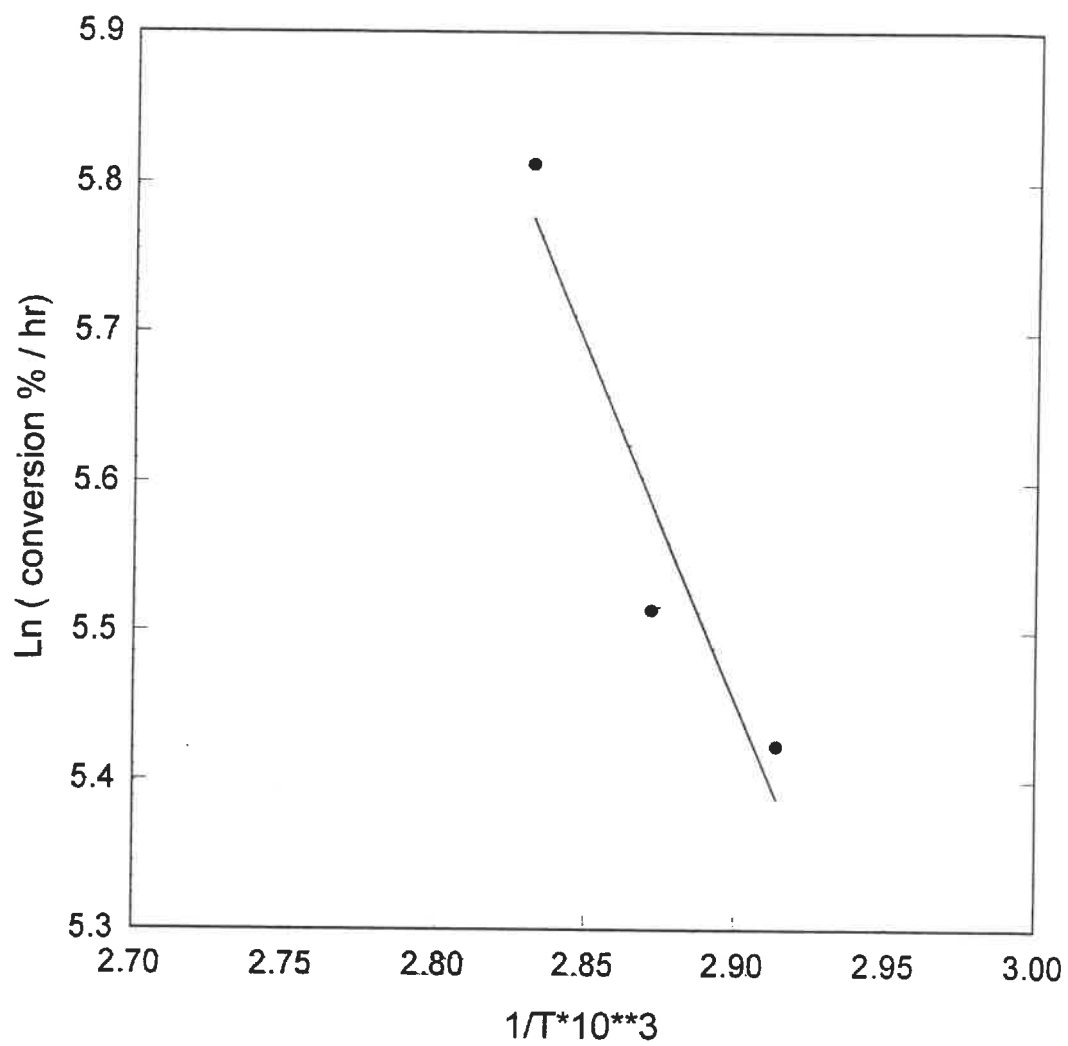


Figure 3.24 - Graph of $1/T$ versus $\ln(\% \text{ conversion/ hr})$

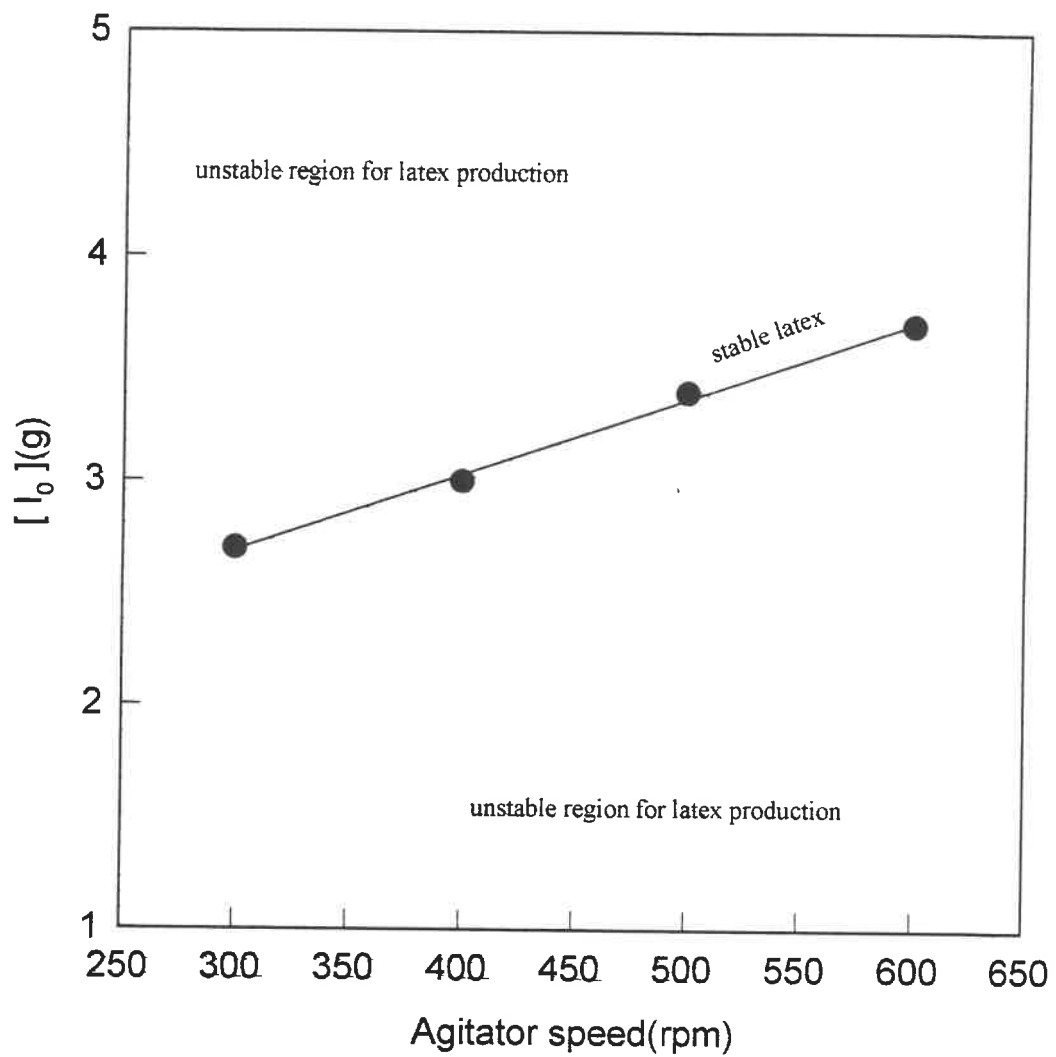


Figure 3.25 - The specified level for the initiator concentration at each speed.

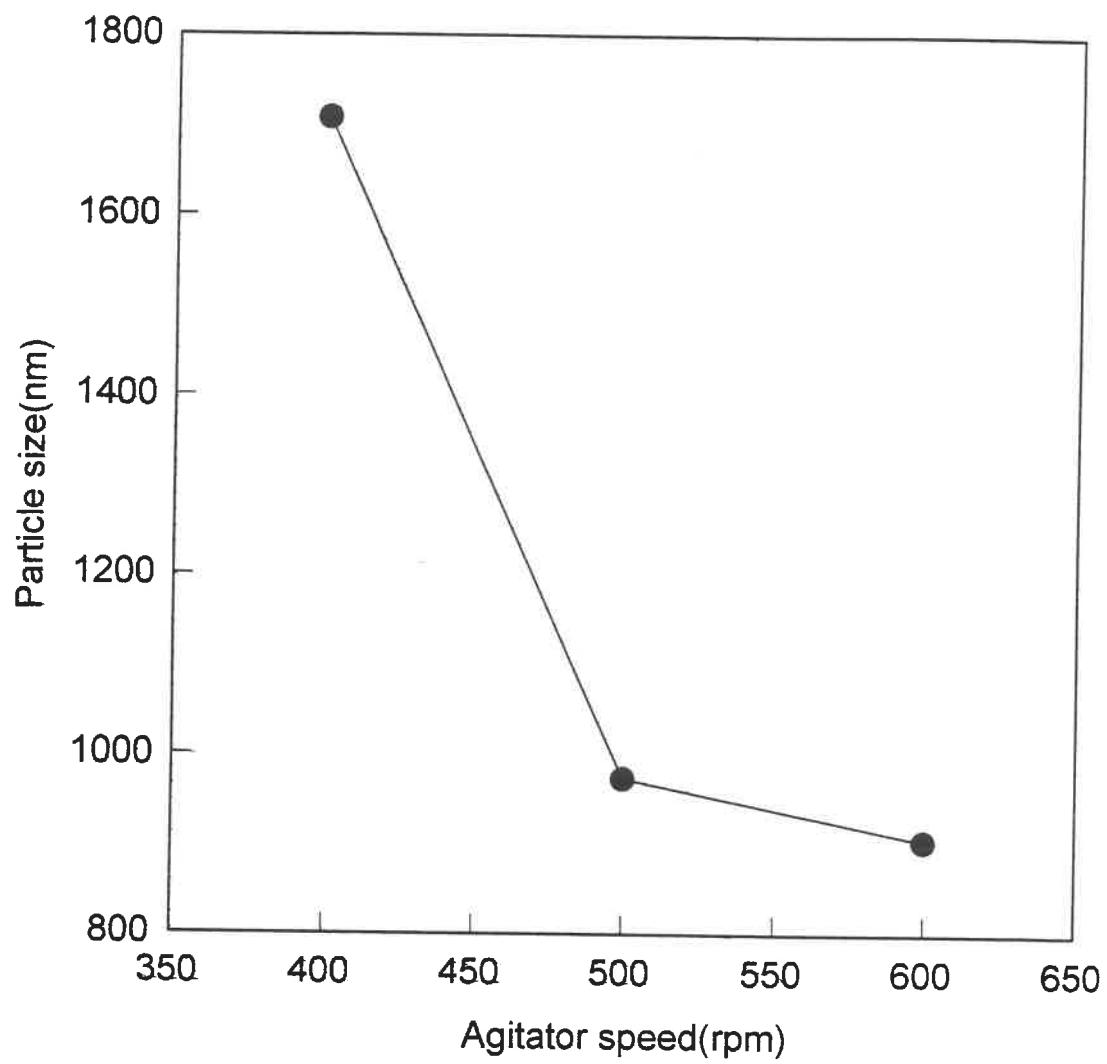


Figure 3.26 - Effect of agitator speed on the particle size of the stable latexes.

CHAPTER 4

DISCUSSION

4.1- INTRODUCTION

In this Chapter, the results obtained in the previous Chapter will be discussed. The results will be explained with respect to the theory given by Z. Song and G. W. Poehlein [1989, 1990], mentioned in Chapter 1.

From the mixing results obtained by the decoloration method, the anchor agitator with a speed of 300rpm was chosen for the initial polymerization reactions. The decoloration method does not represent an emulsion system, therefore the effect of speed is further investigated in the emulsifier-free polymerization of BMA.

4.2- REACTION KINETICS AND MECHANISM

In the previous Chapters, it was mentioned that the water solubility of a monomer can help predict the kinetics and the mechanism of the particle formation. The low water

solubility of BMA, which is similar to that of styrene, predicts that the mechanism follows the micellization nucleation given by Z. Song and G.W. Poehlein [1989, 1990]. This prediction is confirmed for BMA by the GPC diagrams. The results are shown in Figure 3.20 for experiment L. It can be seen that in the early stage of polymerization, low molecular weight oligomers are made and their concentration does not change during the reaction. In addition, results obtained from particle size analysis also show that there is a rapid growth in the particle size of the polymer at stage two of the reaction, where the polymerization continues inside the micellized particles (Figure 3.6.1). However, the rapid increase of zeta potential in the first half-hour of the reaction (Figures 3.14.1-2), which is the particle formation period, indicates that the particle formation takes place by micellization nucleation. This can not be observed in the homogeneous nucleation of particles [Song, 1989, 1990]. According to the GPC, particle size, and zeta potential results, the micellization nucleation proposed by Z. Song and G. W. Poehlein [1989] for styrene is found to be applicable for the emulsifier-free polymerization of n-butyl methacrylate.

From the initial reactions done in this work, it was observed that the temperature inside the reactor was not steady during the polymerization. In order to follow the reaction temperature, a thermocouple was placed inside the reaction medium. The obtained temperature records showed that there is an optimum concentration of initiator required for each speed. These results show that at this initiator level, the temperature inside the reactor stays steady during the reaction. Below this optimum initiator

concentration, the temperature decreases during the polymerization, while for amounts of initiator above this specific level, an increase is seen in the temperature at the end of the reaction. These results can be observed in Figures 3.1.1-3, and correspond to the two different types of coagulation [Chen, 1992] and termination in the polymerization system. Figure 3.25 shows the trend for the optimum initiator concentration at which stable latexes can be produced. At concentrations of initiator less than the one required for the optimum conditions at a certain speed, the formed particles grow in the propagation step to a point where the charge on the surface of the particles is insufficient to stabilize them. Coagulation begins, and the polymerization proceeds in the coagulated particles. Coagulation occurs again when the charge density decreases by growth of the particles. As a result, large particles (greater than 2000nm) are produced in the final product. This type of system is accompanied by a decrease in the temperature during the polymerization reaction. Since there was no sudden increase in the viscosity of the latex during the polymerization reaction, therefore, the termination should be a disproportionation versus coupling reaction.

At initiator concentration higher than this special limit, the number of free radicals in the reaction medium will be high in the first step of polymerization. The higher amount of initiator will result in smaller oligomers and therefore, the CMC for these oligomers is higher. More particles are made during the reaction and the particles will be stabilized in the polymerization system by the diffusion of small oligomers on the surface of the particles rather than coagulation. At the end of the reaction, when the almost all of the

oligomers have been used in precursor and mature particles, their concentration in the aqueous phase will decrease and the mature particles will tend to coagulate. In such system, the number of particles is higher than previous reactions and a coupling termination happens. This result manifests itself by the sudden increase in the reaction temperature and the increase in the viscosity of the latex which is related to the molecular weight of the polymer at the end of the reaction. If the initiator concentration increases to amounts greater than 0.5 to 0.75g, of the specific level at the particular speed, then, at the early stages of the reaction, large amounts of particles are formed. Since the number of free radicals is very high, therefore, the number of polymerization sites is increased, thus, the polymerization rate is fast in the early stages of reaction and coagulation starts in this stage. The coagulation is accompanied by the coupling termination, which can be observed in the molecular weight results(Figure 3.18.1) and will cause an increase in the viscosity. The temperature inside the reactor, also shows an increase, caused by the termination reaction. This is shown in the temperature records for the experiment G in Figure 3.1.1. In higher amounts of initiator than latter, the precursor particles will lose their stability and start to coagulate during the very early stages of polymerization. The density of the particles is higher than the previous reactions as the coagulation starts. All of the particles flocculate, and produce a solid-like material where the monomer molecules are trapped inside. Upon completion, this solid-like material has a conversion of 75% (exp. 23). This is confirmed by the sudden increase in the reaction temperature during the very early stages of polymerization procedure.

4.3-POLYMERIZATION RATE

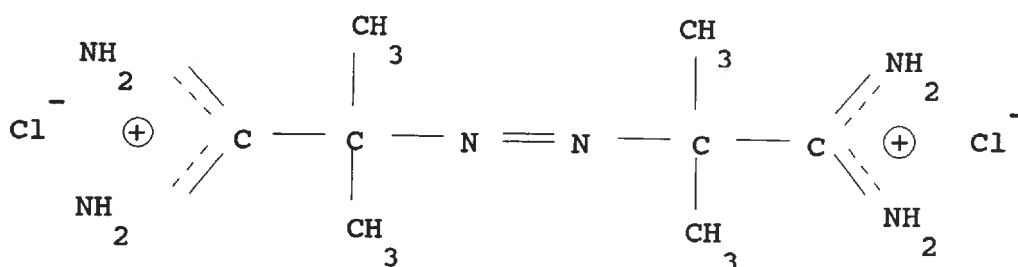
The amount of monomer added plays an important role in the polymerization process. Recent works in this area of research have used small amounts of monomer (less than 10% based on the water content). At higher monomer contents, it is very difficult to produce stable latices without coagulation. However, larger amounts of monomer will decrease the polymerization rate and increase the polymerization time, as shown in Figure 3.2. Therefore, a high monomer concentration will increase the large n^* (the number of monomer molecules in the primary chains before the nucleation takes place) concentration, resulting in a decrease in the CMC and thus higher amounts of particles with low charge density and high particle size are produced. Since the concentration of oligomers with high n^* is increased, thus, the diffusion of oligomers onto the surface of the growing particles decreases. Therefore, the probability of coagulation will increase in the early stage of reaction. The number of particles will decrease and thus the number of polymerization sites (active particles) will decrease and the polymerization rate shows a decrease during the reaction.

As expected, the polymerization rate increases as the amount of initiator increases, as shown in Figure 3.3. This is due to the greater amount of free radicals in the system, resulting in smaller oligomers with higher CMC. Therefore, the number of

particles will increase. This will increase the radical capture by the particles. Therefore the number of active particles will increase and obviously the polymerization rate increases.

It can be pointed out that, agitation speed has a great influence on the polymerization conversion. Since the particles produced during these reactions are larger than 500nm, therefore, the shearing effect on the particles will be greater by increasing the agitation speed. The shear rate in these systems is estimated to be between 66 to 100sec^{-1} , which can affect the particles in this size. As was mentioned by Nomura[1972], the stirring effect is not negligible as long as the concentration of emulsifier is lower than CMC. In this case, in the early stage of the reaction, the oligomers are formed which they act as the emulsifier in the polymerization system and their concentration is lower than CMC in stage 1. The firstly formed oligomers which usually have longer chain lengths, have lower CMC. The precursor particles will form rapidly. By increasing the speed, it was mentioned by Song[1990] that, the radical capture by micelles will increase. In addition, as was mentioned by Nomura[1972], the produced oligomers will tend to adsorb onto the surface of the premier mature particles, by increasing the agitation speed. Therefore, the rate of micelle formation will decrease as the speed increases. This will cause a decrease in the final number of particles which decrease the coagulation at very high speeds during the reaction. At very high conversions, by increase in the particle size at which the shear rate can have its own effect on these particles, the coagulation of these large particles will take place. Consequently, the rate of polymerization will show a decrease by increasing the speed of agitation. This result is shown in Figure 3.4.

The polymerization rate increases with an increase in the temperature (Figure 3.5). This has been verified at different temperatures, such as 60, 70, 75, and 80°C. 2,2'-Azobis isobutyramidine dihydrochloride (abbreviated as $\text{ABA}H_2^{++}2\text{Cl}^-$) has the following chemical formula:



Its thermal decomposition was studied by T. J. Dougherty [1961]. As a first step, $\text{ABA}H_2^{++}2\text{Cl}^-$ will decompose into two positively charged radicals, which happens with an azo-loss reaction (Figure 4.3.1). The half-life of these radicals at 60°C is 300 minutes, and is affected by temperature. For example, at 70°C the half-life is 39 minutes. There is no evidence of the disproportionation reaction of the two radicals, although small amounts may form and produce tetramethyl-succinamide.

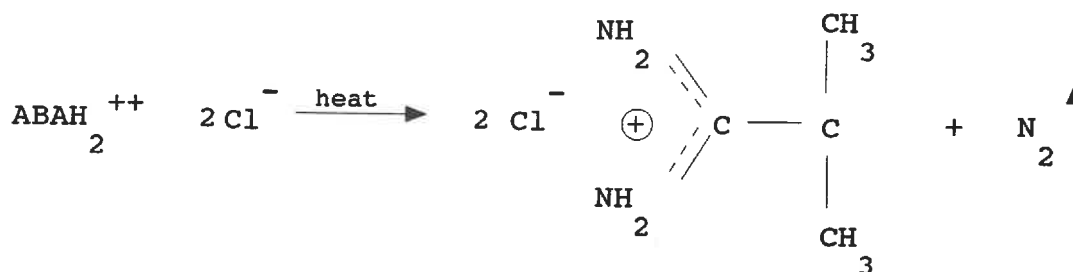


Figure 4.3.1- Thermal decomposition of $\text{ABA} \text{H}_2^{++} 2 \text{Cl}^-$

The rate constant for decomposition of $\text{ABA} \text{H}_2^{++} 2 \text{Cl}^-$ is reported to be equal to $k_d = 15.2 \pm 0.3 \cdot 10^{-5} \text{ sec}^{-1}$ at 70°C . Meanwhile, the decomposition rate for unsalted initiator at the same temperature is $0.2 \cdot 10^{-5} \text{ sec}^{-1}$. This shows the inefficiency in the free radical production by the unsalted initiator [Hammond, 1963]. The addition of a small amount of hydrochloric acid to the system will retard the amidine loss without affecting the rate of azo loss. For this reason, 20 drops of hydrochloric acid were added to the salted material. Therefore, in the polymerization system it is guaranteed that increasing the reaction temperature will increase the number of free radicals in the polymerization system. The number of micellar particles then increases with smaller critical oligomer chain. In addition, since the concentration of free radicals increase, therefore, the radical capture by the particles will also increase. In another words, there will be more reaction sites in the system at higher temperatures. Thus, higher polymerization rates with higher conversions are obtained at higher temperatures.

4.4-PARTICLE SIZE

In emulsion systems, the particle diameter increases as conversion increases. Figures 3.6.1-2 confirms that there is a specific level for the initiator used in these polymerization system. In lower amounts than this critical concentration, the particle size will increase by increasing the initiator level. The reason for this, in the early stage of reaction is that long chains of oligomers are produced. They have a low CMC, which they reach to it very fast. The micelles will form rapidly and capture the free radicals. Although the speed is high, but since the oligomer chain length is high, the mature particles can not retain their stability by oligomer adsorption and they tend to homocoagulation. As long as the oligomers can not absorb onto the particle surfaces, The number of micelles and the number of polymer sites will increase and the rate of coagulation will also increase during the first stage, as well as, polymerization procedure and larger particles are obtained.

In higher amounts of initiator than this critical concentration, the particle size will decrease by increasing the initiator concentration. This can be explained by the decrease in the critical chain length of oligomers. Therefore, the stereospecific hinderance for the oligomers to diffuse on the surface of the particles will decrease. The particles retain their stability through oligomer diffusion rather than mature particles coagulation. Consequently, up to end of the reaction, the effect of shear on the obtained large particles can be neglected and the particle size will decrease. Figure 3.26 shows the effect of speed on the particle size of the stable latexes obtained at each speed.

As was observed in the emulsifier-free emulsion polymerization of styrene by Song and Poehlein [1990], at agitation speeds greater than 450 rpm, new particles began to appear after the polymer particles have grown to a specific size (about 300 to 400nm for styrene). The same observation was made in this study from the results of the particle size for BMA particles. At agitation speeds of 500 and 600 rpm, there is a decrease in the particle size at about 800 to 900nm, as shown in Figures 3.8.1 and 3.8.2. These can be compared to the two particle size results in the reactions at 400 and 500 rpm (Figures 3.9.1 - 3.9.2), where, there is no new particle formation at 400 rpm. For the same percent of conversion and amount of initiator, the particle size changes with agitation speed as shown in Figure 3.7. This suggests that, in low agitation speed of 300rpm, in the early stage of polymerization, large number of oligomers are produced, which they reach their CMC and form the precursor particles. As was mentioned by Song[1990], k_c (the radical capture coefficient), by these micelles is decreased in low speeds. Therefore, the polymerization system tends to form more micelles. The particles which capture free radicals will retain their stability by their coagulation with the micelles. In addition, monomer separation from the emulsion phase in the course of reaction will happen, which will decrease the number of micelles, and the monomer concentration in the produced particles is decreased by speed. Therefore, their particle size is smaller. At the end of reaction, the homocoagulation happens.

By increasing the speed to 400rpm, the radical capture coefficient, k_c , is increased comparing to 300rpm. The monomer is better distributed. Larger number of oligomers

with higher chain length are produced. They reach their CMC and larger number of primary particles are formed. This large oligomer size will decrease the oligomer absorption onto the surface of these mature particles and the stability is maintained only through homocoagulation. During the polymerization in these particles, other oligomers with different chain lengths reach their CMC and the micelle formation is completed in the early steps of polymerization. In the rest of reaction, the particles will grow only by polymerization in the particles and homocoagulation happens in order to retain their stability. Therefore, larger particles than 300rpm are produced(Figures 3.7 to 3.11.2).

In 500, the monomer is very well distributed in the emulsion phase. The primary micelles are formed. The rate of radical capture is increased according to results obtained by Nomura[1972]. Therefore, the polymerization starts in the micelles, while the oligomers are getting formed in the reaction. these growing particles will loss their stability and in order to retain their condition they will absorb the oligomers onto their surfaces. This will cause a delay in micelle formation and reduce the number of micelles. Consequently, during the reaction, the obtained particles are smaller. At the end of reaction, the stability loss is retained only by coagulation of particles. Since the end particle number is decreased the coagulation is less pronounced and the particles are smaller.

In 600rpm, same conditions are obtained as 500rpm, except that the micelle formation has a longer retention time and the number of micelles and particles is decreased. Therefore coagulation is less noticeable than in 500rpm. Consequently, the final particle size is smaller than in 500 rpm.

Larger particles are produced at the same conversion at a lower temperature due to the fast initiator decomposition at higher temperatures, resulting in higher oligomer concentration and fast micelle formation in the early stage of the reaction(Figure 3.11.2). The oligomer critical chain length will decrease in higher temperature, because of the higher aqueous termination rate. As was mentioned by Song[1990], the radical capture rate increases by increasing the temperature. Thus the polymerization inside the micelles will start while oligomers and micelles are forming. The stability of the mature particles can be retained by oligomer adsorption or coagulation of newly formed and mature particles than mature particles coagulation.

4.5-ZETA POTENTIAL

An increase in the amount of initiator will increase the zeta potential, shown in Figures 3.12.1-2. Since the initiator used in this polymerization system is ionic and the system is stabilized by ionic end groups from the initiator, increasing the initiator concentration will cause an increase in the free radicals produced by the initiator, and thereby increasing the zeta potential of the particles. In addition, as was discussed previously with regards to the particle size, the particles are smaller at higher initiator concentrations, so the charge density will be spread on a smaller surface area and the zeta potential will be higher, as shown in Figures 3.12.1 and 3.12.2. Obviously, higher amounts of initiator will increase the amount of positive charge in the system, and will

help to create a more stable system. In addition, the zeta potential also has a sharp distribution for the specific amount of initiator which is about 3.7 to 3.8 at 600 rpm.

In two reactions which differ only in applied agitator speed, the zeta potential variation can be divided into two different groups:

In Figure 3.13.2, the zeta potential decreases with an increase in the agitation speed. This can be explained as, in 400rpm, the latex retains its stability only by coagulation of two mature particles. Therefore, the zeta potential is higher than 500rpm in which there is a particle formation during the reaction, which allows the oligomers to absorb onto the particle surface, during the particle growth.

There is an increase in the zeta potential with an increase in the agitation speed from 500 to 600rpm(Figures 3.14.1-2). This is due to the delay in the formation of micelles(stage 1) in the reaction medium, as well as reaching the constant n^* stage (stage 2) where particle growth by means of the polymerization reaction occurs inside the particles. The mature particles will retain their stability from the oligomer absorption onto the surface or by coagulation of newly formed and the mature particles. Therefore, there is a delay in the mature particles coagulation. It can be seen that using higher speeds of agitation decreases the coagulation and increases the uniformity of the polymerization system, and the produced latices are more stable.

As shown in figures 3.15.1&2, by increasing the temperature, the free radical concentration increases at the beginning of the reaction. Therefore, the concentration of oligomers will increase, they will reach their CMC very fast, and the rate of micelle

formation is high. In this high free radical concentration and high temperature as mentioned by Nomura[1972], the rate of radical capture by micelles is increased and the particle growth happens when the stage 1 is not completed and there is a high rate of oligomer formation. Therefore, in 80⁰C, the particles will retain their stability by coagulation of the mature and precursor particles or by adsorption of oligomers onto the particle surface. Thus, as it has been shown in figure 3.16, although the particle size is increasing, the zeta potential remains in a very small range.

4.6-MOLECULAR WEIGHT

The effect of initiator concentration on the molecular weight is shown in figures 3.17.1&2, and can be explained as follows:

Below the determined specific level, an increase in the initiator concentration will decrease the molecular weight. More free radicals are formed and, therefore, more precursor particles are produced. For the same amount of initiator concentration, a lower molecular weight polymer is produced.

Above the determined specific level of initiator, the molecular weight increases with an increase in the initiator concentration. At a constant agitation speed and in the early stages of the reaction, there will be a high concentration of free radicals and the amount of primary oligomers first formed will increase. In view of increasing the amount of free radicals, the rate of radical capture increases, and therefore the number of active particles will increase. This will increase the rate of coagulation. As was mentioned

previously coagulation in these systems is accompanied by coupling termination and thus the molecular weight increases.

The effect of agitation speed is shown in Figures 3.18.1-2. It should be noted that at 400rpm the utilized initiator concentration is greater than its specific level for this speed (approximately 3.00g), while at 600rpm the initiator concentration is less than its specific concentration, which is 3.7g. At 400rpm, the molecular weight shows a sudden increase. Particle coagulation in the early stage of the precursor particles which is accompanied by coupling termination.. Since the agitation speed is low, the number of micelles is high. The polymerization starts inside the micelles, and after particle coagulation, the coupling termination will take place. The reason for the decrease in the molecular weight is the creation of new chains in the same formed particles by radical transfer or radical diffusion to the particles. Therefore, low molecular weight polymers start to grow in the mature particles. At 600rpm, the molecular weight increases slowly until new particles start to form, after about 6000sec. At this point, the molecular weight drops and then increases as the reaction proceeds.

As a result of the higher yield for the polymerization at a higher rate, the molecular weight increases with an increase in the temperature, as shown in Figure 3.19.1-2. The sudden increase in the molecular weight at 80⁰C is due to the coupling termination of the chains existed in the particles.

4.7-REACTION TIME

The reaction time has been increased by increasing the amount of initiator in the polymerization system. At higher amounts of initiator, a greater concentration of particles is made during the reaction, therefore the polymerization rate will increase. Thus, the polymerization takes place in less time. This is shown in Figures 3.1.1-3.

By increasing the agitation speed, the polymerization time will increase. This is due to the shearing effect on the polymerization system, which includes the monomer molecules and droplets, as well as the polymer particles. Also since this reaction is diffusion controlled, increasing the agitation speed will increase the polymerization time. This can be seen in Figure 3.21.

The temperature will also affect the polymerization time. An increase in the temperature will decrease the half-life of the initiator from 300 minutes at 60°C to 39 minutes at 70°C. Therefore, the initiator decomposes to its surface active radicals faster at higher temperatures, which increases the polymerization rate and decreases the polymerization time. This is shown in Figure 3.22.

4.8-GLASS TRANSITION TEMPERATURE, T_g

The glass transition temperature has a significant influence on the latexes which are used in the paper industry. As indicated earlier, this temperature should be between

40 and 55°C for this application. The T_g of the BMA polymer is found to be between 15 and 30°C, depending on the polymerization method. In the type of system used in this work, in one case it was found to be 35.98°C, the T_g is near the desired temperature. Therefore, the cationic polymer produced here may be considered for certain application in the paper industry. However, further work will have to be done to measure the T_g to within the desired for this industry.

4.9-OVERALL ACTIVATION ENERGY

The activation energy obtained from these reactions at different temperatures ($E_R=9.37$ Kcal/ mol) is lower than the activation energies reported for this monomer in other different systems. No data is obtained through this point for the propagation and termination activation energies for this system.

CHAPTER 5

CONCLUSION AND FUTURE WORK

5.1-CONCLUSION

At high monomer concentrations, it has been found that polymerization is difficult in an emulsifier-free emulsion polymerization system. In these systems, the problem of coagulation is well noticeable. However, there are several ways to decrease the coagulation, such as increasing the agitation speed. It has been found in this work that at each speed of agitation, there exists a specific initiator concentration at which the reaction temperature stays steady during the reaction, resulting in higher conversion and sharp particle size and zeta potential. An increase in the speed of agitation increases the specific amount of the initiator used in the polymerization system. For example, the specific amount of initiator at 400rpm is 3.0g, while it is 3.8g at 600rpm. Since the initiator carries the positive charge in the system, the latices formed at higher speeds have better stability. In order to obtain small polymer particles, working with speeds greater than 400rpm is recommended.

The measured T_g of this polymer shows that this latex may be used as a sizing agent in the paper industry.

The polymerization mechanism of BMA without emulsifier was found to follow the one suggested by Song and Poehlein [1989, 1990]: the micellization nucleation which involves a three step polymerization mechanism. In both their works and in the present study, for speeds greater than 400rpm the new particle formation takes place. For BMA particle formation happens while the particles reach a certain size which is approximately 800 to 900nm. As was mentioned in chapter 4, this was due to the delay in the micelle formation in higher speeds.

By following the particle size during the polymerization at different speeds, it was found that the particle size decreases at speeds greater than 400rpm. Same particle size results were obtained for the stable latex produced in each speed.

An overall activation energy for this polymerization reaction was determined and found to be equal to $E_R = 9.37$ Kcal/mol, which shows that this is a low energy-consuming reaction.

5.2-FUTURE WORK

In this project, the most important criteria to be considered is the stability and the particle size of the latex. As was mentioned previously, in order to obtain the best results in the papermaking processes the particle size should be less than 100nm in diameter, so

that the particles can enter the free volumes in the fibrous network. To achieve this aim, it is necessary to use speeds greater than 400rpm, which also allows for the possibility of working at higher special amounts of initiator, thereby producing latices with higher stability. In addition, one can also increase the polymerization temperature. Working at 80°C can be recommended as a future work on this project to obtain stable latexes. Adding a small portion of cationic comonomer such as 2-diethyl-aminoethyl methacrylate [Alinec, 1995] can also be recommended in order to produce smaller particles in stable systems. This will decrease the potential for coagulation. The preferred glass transition temperature for a latex which can be used in the paper industry is between 40 and 55°C, while the obtained latexes produced in this project have a T_g of 35.98°C. Since the amount of initiator changes with the speed of agitation, the production of a stable latex is best achieved with a cationic comonomer in the polymerization system. Meanwhile, the low glass transition temperature of the n-butyl methacrylate latex can be increased by using comonomers.

Instead of using the emulsifier-free emulsion polymerization, a microemulsion process is another possibility for producing latices with small particles of less than 100nm size. This is particularly valid in cases where the surfactant is eliminated in the polymerization process, such as that mentioned by Pérez-Luna *et al* [1990], where a three component system of water-initiator-monomer is used and there is no further interference of emulsifier for the end use properties of latex in the paper industry.

REFERENCES

- "ALINCE, B. "; "INOUE, M. " and "ROBERTSON, A. A. " (1976), Latex-fiber interaction and paper reinforcement, *Journal of Applied Polymer Science*, vol. 20, p. 2209.
- "ALINCE, B. " (1977), Performance of cationic latex as a wet-end additive, *Tappi*, No. 12, vol. 60, p. 133.
- "ALINCE, B. " (1985), Interaction of cationic latex with pulp fibers, *Paperi ja Puu-Papper och Trä*, No. 3, p.118.
- "ARAI, M. "; "ARAI, K. "and "SAITO, S. "(1979), Polymer particle formation in soapless emulsion polymerization, *Journal of Polymer Science*, Polymer Chemistry Ed. , vol. 17, p.3655.
- ASTM STANDARDS (1995), E200-91.
- "BATAILLE, P. " (1994), *Chimie Physique des Polymeres Notes*, École Polytechnique de Montréal.
- "BRANDRUP, J. "and "IMMERGUT, E. H. " (1975), "Polymer Handbook", Wiley- Interscience, New York.
- "CANDAU, F. "; "BUCHERT, P. " and "KRIEGER, I. " (1990), Rheological studies on inverse macrolattices, *Journal of Colloid and Interface Science*, vol. 140, no. 2, p. 466.

"CHEN, C. Y. " and "PIIRMA, I. " (1980), Emulsion polymerization of Acenaphthylene. I. A study of particle nucleation in water phase and in aqueous emulsions, *Journal of Polymer Science*, Polymer Chemistry Ed., vol. 18, p. 1979.

"CHIU, W. Y. "; "LAI, S. M. "; "CHEN, L. W. " and "CHEN, C. C." (1991), Particle size distribution and molecular size distribution of polymers in soap-free emulsion polymerization of styrene , *Journal of Applied Polymer Science*, vol. 42, p. 2787.

"DOUGHERTY, T. J. " (1961), Chemistry of 2,2' - Azobisiso butyramidine hydrochloride in aqueous solution: A water-soluble azo initiator , *Journal of American Chemical Society*, vol. 83, p. 4849.

"FITCH, R. M. " (1969), The mechanism of particle formation in polymer hydrosols.I. Kinetics of aqueous polymerization of methyl methacrylate , *Journal of Polymer Science*, Part C, vol. 27, p. 95.

"FITCH, R. M. " and " TSAI, C. H. " (1970), Polymer colloids: Particle formation in nonmicellar systems , *Journal of Polymer Science*, Part B, vol. 8, no. 10, p.703.

"FITCH, R. M. " (1973), The homogeneous nucleation of polymer colloids, *British Polymer Journal*, No. 5, p. 467.

"GOODALL, A. R. "; "WILKINSON, M. C. " and "HEARN, J. "(1980), Characterization of particles during growth in emulsifier- free emulsion polymerization of styrene, *Polymer colloids II* (R. M. Fitch Ed.), p. 629, Plenum, New York.

- "GORDON, J. L. " (1968), Emulsion polymerization. I. Recalculation and extension of the Smith-Ewart theory , *Journal of Polymer Science*, A-1, vol. 6, p. 623.
- "HAMMOND, G. S. " and "NEUMAN, R. C. " (1963), Mechanism of decomposition of azo compounds (III) Cage effects with positively charged geminate radical pairs , *Journal of American Chemical Society*, vol.85, p. 1501.
- "HANSEN, F. K. " and "UGELSTAD, J. " (1978), Particle nucleation in emulsion polymerization. I. A theory for homogeneous nucleation, *Journal of Polymer Science*, Polymer Chemistry Ed., vol 16, p. 1953.
- "HARKINS, W. D. "(1947), A general theory of the mechanism of emulsion polymerization, *Journal of American Chemical Society*, vol. 69, p. 1428.
- "MUNRO, D. "; "GOODALL, A. R. "; "WILKINSON, M. C. "; "RANDLE, K. " and "HEARN, J. " (1979), Study of particle nucleation, flocculation, and growth in emulsifier-free polymerization of styrene in water by total intensity light scattering and photon correlation spectroscopy , *Journal of Colloid and Interface Science*, vol. 68, no. 1, p. 1.
- "NOMURA, M. "; "HARADA, M. "; "EGUCHI, W. "; and "NAGATA, S."(1972), Effect of stirring on the emulsion polymerization of styrene , *Journal of Applied Polymer Science*, vol. 16, p. 835.
- "PÉREZ-LUNA, V. H. "; "PUIG, J. E. "; "CASTAÑO, V. M. "; "RODRIGUEZ, B. E. "; "MURTHY, A. K. "; "KALER, E. W. " (1990), Styrene polymerization in three-component cationic microemulsion , *Langmuir*, vol. 6, p. 1040.

"RODRIGUEZ-GUADARRAMA, L. A. "; "MENDIZABAL, E. ";
"PUIG, J. E. " and "KALER, E. W. " (1993), Polymerization of methyl methacrylate in 3-component cationic microemulsion, *Journal of Applied Polymer Science*, vol. 48, p. 775.

"SHAO, Y. "; "INOUE, M. "; "ALINCE, B. " and "VAN DE VEN, T.G.M. " (1995), Factors affecting particle size in the synthesis of cationic polystyrene and poly(butyl methacrylate) latexes, Pulp and paper report, No.PPR 1135.

"SMITH, W. V. " and "EWART, R. H. " (1948), Kinetics of emulsion polymerization, *Journal of Chemical physics*, vol. 16, No. 6, p.592.

"SONG, Z. " and "POEHLEIN, G. W. " (1989), Particle nucleation in emulsifier-free aqueous- phase polymerization: Stage 1 , *Journal of Colloid and Interface Science*, vol. 128, No.2, p. 486.

"SONG, Z. " and "POEHLEIN, G. W. " (1989), Particle formation in emulsifier-free aqueous-phase polymerization of styrene, *Journal of Colloid and Interface Science*, vol. 128, No.2, p. 501.

"SONG, Z. " and "POEHLEIN, G. W. " (1990), Kinetics of emulsifier- free emulsion polymerization of styrene, *Journal of Polymer Science, Part A: Polymer Chemistry*, vol. 28, p. 2359.

"STOFFER, J. O. " and "BONE, T. " (1979), Polymerization in water-in-oil microemulsion systems containing methyl methacrylate, *Journal of Dispersion Science and Technology*, vol. 1, p. 37.

"STOFFER, J. O. " and "BONE, T. " (1980), Polymerization in water-in-oil microemulsion systems. I. . , *Journal of Polymer Science*, Polymer Chemistry Edition, vol. 18, p. 2641.

"SÜTTERLIN, N. " (1980), Influence of monomer polarity on particle formation in emulsion polymerization, Polymer Colloids II, proceedings of the symposium on the physical chemical properties of colloidal particles held in Miami, Florida, Sept. 1978, Plenum Press, Edited by R. M. Fitch, p. 583.

"WATERHOUSE, J. F. " (1983), Paper reinforcement by polymer addition, Pulp and Paper Chemistry and chemical technology, third ed., vol. IV, Wiley publication, p.2399.

"YAP, C. Y. " (1976), Mixing of viscoelastic fluids with helical-ribbon agitators, Thèse de Doctorat, École polytechnique de Montreal.

APPENDIX A

A.1-DECOLORATION METHOD

The fluid which is used in this method is initially colored, and by adding a small quantity of a reagent to the system turns colorless. Using this method, the final mixing patterns can be closely observed and the flow patterns can be clearly seen. The mixing time is usually taken as the disappearance of the last trace of color. The decoloration method used in this work is the iodide/potassium iodide system (I_2 -KI), which gives a deep blue color in the presence of a starch indicator. Reactions of this colored mixture will be decolorized by sodium thiosulphate ($Na_2S_2O_3$). The solutions of iodine, starch, and sodium thiosulphate were highly concentrated, and a maximum quantity of each was used in this decoloration method.

A.2-SOLUTION PREPARATION

A.2.1-2N IODINE-POTASSIUM IODIDE SOLUTION

The 2N iodine-potassium iodide solution was prepared according to the following procedure:

25.4g of iodine crystals and 80g of potassium iodide (I_2 -KI) were weighed and placed together in a beaker. 30ml of water was added and stirred until all of the materials were dissolved. The solution was then diluted to 100ml and filtered through a sintered

glass filter. The solution was stored in a cool place and allowed to stand over night before use [ASTM Standards, 1995].

A.2.2-1N SODIUM THIOSULPHATE SOLUTION

62.5g of $\text{Na}_2\text{S}_2\text{O}_3 \cdot 5\text{H}_2\text{O}$ crystals were weighed and dissolved in 125ml freshly boiled and cooled water. 0.275g sodium carbonate were then added. The solution was diluted to 250ml with freshly boiled and cooled water. The solution was stored for 24 hours in a tightly closed glass bottle before use [ASTM Standards, 1995].

A.2.3-STARCH INDICATOR

The starch solution must be freshly prepared each time as it is attacked by fungi and becomes unstable for use as an indicator.

The following procedure was used:

4g of starch were ground with a small amount of water until a smooth paste was formed. The paste was then poured slowly into 100ml of boiling water and the resulting suspension was boiled for approximately one minute. The solution was cooled and decanted into a bottle which was tightly closed [ASTM Standards, 1995].

A.3-MIXING TEST PROCEDURE

500ml of water are poured into the 1lit polymerization reactor, 3ml of starch indicator are then added, followed by the addition of 3ml of the iodine-potassium iodide

solution. Mixing in the reactor is started, after which the content is uniformly colored deep blue, then 2.7ml of sodium thiosulphate solution are added. The total mixing time is the time it takes to completely discolor the solution. This test was done for three types of agitators (propeller, turbine and anchor) and at three different speeds of 100, 200 and 300 rpm. The entire procedure was monitored by a video camera.

APPENDIX B

B.1- REACTION YIELD DETERMINATION

The results shown in the final chapters were determined as follows:

$$a = m_0 - m_1 \frac{m_{inhibitor}}{100} = \text{the weight of inhibitor in the sample}$$

$$b = m_2 - m_1 \frac{W_{monomer}}{W_{total}} = \text{the total weight of monomer in the sample}$$

$$c = m_3 - m_0 - a = \text{the polymer left in the sampling dish after drying}$$

$$\text{Reaction yield \%} = \frac{c}{b} \times 100$$

m_0 = weighing dish weight; g

m_1 = weighing dish weight + approximately 1ml of the inhibitor solution; g

m_2 = m_1 + weigh of the latex added into the dish; g

m_3 = weighing dish weight + dried latex; g

B.2- ZETA POTENTIAL (ζ) DETERMINATION

The zeta potential was determined using the following equations:

$$\zeta = u * 12.83$$

Using this equation and the following dimensions, the zeta potential is measured in mV.

$$u = \frac{V / L}{a / t}$$

V = constant voltage between the two electrodes; 50 volts.

L = inter-electrode distance, measured by using the standards for the cell; cm.

a = observation distance on the TV screen in which the traveling time of the particles has been measured, μm

t = traveling time of the particle between the two points on the screen (a); sec

$$L = kRA = 6.528 \text{ cm}$$

k = electrical conductivity for a standard KCl solution (7.419gKCl per 1000g solution);
 $1.286 * 10^{-2} \Omega^{-1}\text{cm}^{-1}$

R = resistance measured by an A.C. bridge to avoid polarization, measured by an external electrical device;

$$R = \frac{V}{I} = \frac{49.02}{10.12} = 4.844 \text{ K}\Omega$$

A = vertical cross section of the rectangular cell = $10 * 1.526 = 15.26 \text{ mm}^2$

Microelectrophoresis was used for the zeta potential measurements. Since in this instrument the particles should be seen by the naked eyes. Therefore, the obtained measurements and analysis is for the big, even coagulated particles. during the

measurements the voltage was considered to be 50v, although the real voltage is less than this voltage. Time was measured manually and therefore a delay error should be considered during all of the sample measurements. It should be noted that, there is no other way to measure the mobility and the zeta potential of the particles.

B.3 - MOLECULAR WEIGHT MEASUREMENTS

From Figure 3.20, it can be seen that the GPC diagrams contain two parts of high and low molecular weight. The curve from the GPC is divided into at least 30 to 50 equal parts. The distance between the injection point and each part is measured. Knowing the paper speed, the retention time can be determined for each portion. Each retention time is then placed in the calibration curve equation for the GPC and thus the molecular weight for each point (M_i) is then obtained. The area for each individual section is measured (A_i), and by using the following equations the number-average molecular weight, M_n , the weight-average molecular weight, M_w and the z-average molecular weight, M_z , can be evaluated for each sample.

$$M_n = \frac{\sum A_i}{\sum \frac{A_i}{M_i}}$$

$$M_w = \frac{\sum A_i M_i}{\sum A_i}$$

$$M_z = \frac{\sum (A_i M_i^2)}{\sum (A_i M_i)}$$

The polymer molecules obtained in these reactions are considered to be linear. According to the molecular weight measurements, the used columns for the partial fractional of the obtained latexes based on their chain lengths in the GPC are packed with styragel(crosslinked polymer of styrene with di-vinyl benzene). Thus, in order to obtain the molecular weight of the BMA polymer, a factor of ($M_{\text{BMA}}/ M_{\text{styrene}} = 142.19/104 = 1.367$) was used.

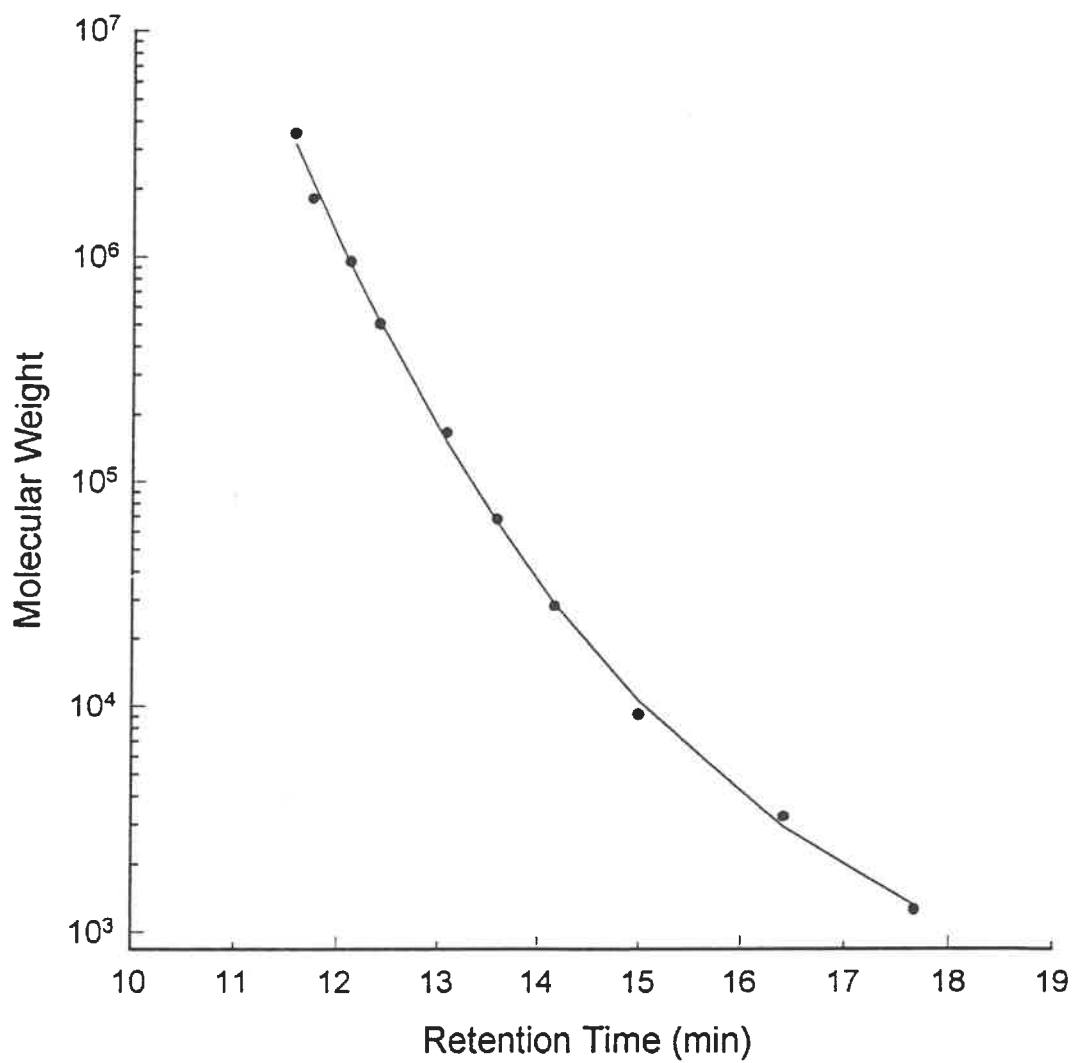


Figure B.1- Calibration curve for the GPC prepared from the standard solutions with the following curve equation:

$$\log Mw = 38.97 - 5.154 \cdot RT + 0.2526 \cdot RT^2 - 0.004287 \cdot RT^3$$

Table B.1- molecular weight determination from the obtained curve of the sample L.13.

RT (mm)	RT(min)	H (mm)	Ai	log Mi	Mi	Ai / Mi	Ai * Mi	Mi**2	Ai*Mi**2
108.0000	18.0000	0.0000	0.0000	3.0386	1092.9895	0.0000	0.0000	1.1946e+6	0.0000
110.0000	18.3333	4.0000	7.3333	2.9650	922.6009	7.9485e-3	6765.7402	851.19e+3	6.2421e+6
111.5000	18.5833	8.0000	14.6667	2.9123	817.1779	0.0179	11.985e+3	667.78e+3	9.7941e+6
113.0000	18.8333	8.0000	14.6667	2.8613	726.6399	0.0202	10.657e+3	528.01e+3	7.7441e+6
115.0000	19.1667	9.0000	16.5000	2.7953	624.1264	0.0264	10.298e+3	389.53e+3	6.4273e+6
116.5000	19.4167	3.0000	5.5000	2.7467	558.0574	9.8556e-3	3069.3157	311.43e+3	1.7129e+6
118.0000	19.6667	0.0000	0.0000	2.6984	499.3964	0.0000	0.0000	249.40e+3	0.0000
total			58.6667		5240.9885	0.0936	350.25e+3	27.468e+6	1.6434e+9

Mn Mw
 857.1104 8161.1561

APPENDIX C

The formulation and the polymerization conditions for each experiment is shown in this section.

Experiment A				
Formulation		Speed (rpm)	Temperature ($^{\circ}$ C)	Notes
BMA	105 g	400	70	The polymerization was completed in 2 hrs. The final conversion at the end of polymerization was 81.44%. At the end of the reaction, there was no coagulation around the agitator, thermocouple, or on the side walls of the reactor.
H ₂ O	245 g			
Hydrochloric acid	20 drops			
ABAH ₂ ⁺⁺ 2Cl ⁻	3.41 g			

Experiment B				
Formulation		Speed (rpm)	Temperature ($^{\circ}$ C)	Notes
BMA	105 g	400	80	The polymerization was completed in 50min. At the end of the reaction, large particles were attached to the agitator. The final conversion was 91.72%.
H ₂ O	245 g			
Hydrochloric acid	20 drops			
ABAH ₂ ⁺⁺ 2Cl ⁻	3.41 g			

Experiment C				
Formulation		Speed (rpm)	Temperature ($^{\circ}$ C)	Notes
BMA	105 g	400	60	The polymerization was stopped after 2 days. At the end of reaction, the final conversion was 6.2%.
H ₂ O	245 g			
Hydrochloric acid	20 drops			
ABAH ₂ ⁺⁺ 2Cl ⁻	3.41 g			

Experiment D				
Formulation		Speed (rpm)	Temperature ($^{\circ}$ C)	Notes
BMA	105 g	400	70	The polymerization was completed in 2 hr. Large particles were stuck to the agitator at the end of the reaction. The final conversion was 98%.
H ₂ O	245 g			
Hydrochloric acid	20 drops			
ABAH ₂ ⁺⁺ 2Cl ⁻	3.0 g			

Experiment E				
Formulation		Speed (rpm)	Temperature ($^{\circ}$ C)	Notes
BMA	105 g	400	70	The polymerization was stopped after 2.5hrs. At the end of the reaction, a latex with large particles was obtained. The final conversion was 84%.
H ₂ O	245 g			
Hydrochloric acid	20 drops			
ABAH ₂ ⁺⁺ 2Cl ⁻	2.75 g			

Experiment F				
Formulation		Speed (rpm)	Temperature ($^{\circ}$ C)	Notes
BMA	105 g	400	70	The polymerization was completed in 1.5hrs. At the end of the reaction, the obtained latex was very viscous but there was no sign of coagulation. The conversion for the final product was 71.73%.
H ₂ O	245 g			
Hydrochloric acid	20 drops			
ABAH ₂ ⁺⁺ 2Cl ⁻	3.50 g			

Experiment G				
Formulation		Speed (rpm)	Temperature ($^{\circ}$ C)	Notes
BMA	105 g	400	70	The polymerization was stopped after 1.5hrs. At the end of the reaction, the obtained latex had very large particles. The conversion for the final product was 86.2%.
H ₂ O	245 g			
Hydrochloric acid	20 drops			
ABAH ₂ ⁺⁺ 2Cl ⁻	3.70 g			

Experiment H				
Formulation		Speed (rpm)	Temperature ($^{\circ}$ C)	Notes
BMA	105 g	500	70	The polymerization was stopped after 2.8hrs. At the end of the reaction, the obtained latex was very viscous and all the latex was coagulated. The conversion for the final product was 87.3%.
H ₂ O	245 g			
Hydrochloric acid	20 drops			
ABAH ₂ ⁺⁺ 2Cl ⁻	3.0 g			

Experiment I				
Formulation		Speed (rpm)	Temperature ($^{\circ}$ C)	Notes
BMA	105 g	500	70	The polymerization was stopped after 2.2hrs. At the end of the reaction, the obtained latex did not have any large particles. The conversion for the final product was 72.05%.
H ₂ O	245 g			
Hydrochloric acid	20 drops			
ABAH ₂ ⁺⁺ 2Cl ⁻	3.41 g			

Experiment J				
Formulation		Speed (rpm)	Temperature ($^{\circ}$ C)	Notes
BMA	105 g	500	70	The polymerization was completed in 1.61hrs. At the end of the reaction, the latex was completely uniform and there was no sign of coagulation. The conversion for the final product was 91.71%.
H ₂ O	245 g			
Hydrochloric acid	20 drops			
ABAH ₂ ⁺⁺ 2Cl ⁻	3.80 g			

Experiment K				
Formulation		Speed (rpm)	Temperature ($^{\circ}$ C)	Notes
BMA	105 g	600	70	The polymerization was stopped after 8800sec (2.4hrs.). At the end of the reaction, the temperature started to increase and the obtained latex was very viscous. The conversion for the final product was 87.08%.
H ₂ O	245 g			
Hydrochloric acid	20 drops			
ABAH ₂ ⁺⁺ 2Cl ⁻	3.50 g			

Experiment L				
Formulation		Speed (rpm)	Temperature ($^{\circ}$ C)	Notes
BMA	105 g	600	70	The polymerization was stopped after 12,200sec (3.9 hrs). At this time, the obtained latex had no coagulum. No temperature decrease was seen during the reaction. The conversion for the final product was 97%.
H ₂ O	245 g			
Hydrochloric acid	20 drops			
ABAH ₂ ⁺⁺ 2Cl ⁻	3.80 g			

Experiment M				
Formulation		Speed (rpm)	Temperature ($^{\circ}$ C)	Notes
BMA	105 g	600	70	The polymerization was stopped after 10,000sec(2.8 hrs). At the end of the reaction, there was no sign of coagulation but the reaction yield results show coagulation of the latex during the polymerization. The conversion for the final product was 62.74%.
H ₂ O	245 g			
Hydrochloric acid	20 drops			
ABAH ₂ ⁺⁺ 2Cl ⁻	4.00 g			

Experiment N				
Formulation		Speed (rpm)	Temperature ($^{\circ}$ C)	Notes
BMA	105 g	600	70	The polymerization was stopped after 11400sec(3.17 hrs). The obtained latex had a conversion of 87% after 2hrs. After this, the reaction yield results show that coagulation occurred. At the end of the reaction, the obtained latex was very smooth without any sign of coagulates.
H ₂ O	245 g			
Hydrochloric acid	20 drops			
ABAH ₂ ⁺⁺ 2Cl ⁻	3.70 g			

Experiment 0				
Formulation		Speed (rpm)	Temperature (°C)	Notes
BMA	65g	400	75	The reaction was completed in 1hr. The final conversion at the end of the reaction was 89%. At the end of the reaction, there were no coagulum around the agitator, thermocouple, or on the side walls of the reactor.
H ₂ O	245g			
Hydrochloric acid	20 drops			
ABAH ₂ ⁺⁺ 2Cl ⁻	3.4g			

Experiment 23				
Formulation		Speed (rpm)	Temperature (°C)	Notes
BMA	65g	400	70	The reaction was very fast and the temperature increased very quickly during the first half hour. Even at the end of the reaction the temperature inside the reactor was 94°C. The final material was a complete coagulum with a final conversion of 75%.
H ₂ O	245g			
Hydrochloric acid	20 drops			
ABAH ₂ ⁺⁺ 2Cl ⁻	3.4g			

ÉCOLE POLYTECHNIQUE DE MONTRÉAL



3 9334 00171579 4